Univerzita Karlova
Přírodovědecká fakulta
Fyziologie živočichů

Mgr. Kolcheva Marharyta

Autoreferát dizertační práce

Funkční a farmakologické vlastnosti GluN1/GluN2 a GluN1/GluN3 podtypů NMDA receptorů

Školitel

Mgr. Martin Horák, Ph.D.

Praha 2022

Doktorské studijní programy v biomedicíně
Univerzita Karlova
a Akademie věd České republiky

Program: Fyziologie živočichů

Předseda oborové rady: doc. RNDr. Jiří Novotný, DSc.

Školicí pracoviště:

Fyziologický ústav AVČR
Oddělení buněčné
neurofyziologie

Ústav experimentální
medicíny AVČR
Oddělení neurochemie

Autor: Mgr. Marharyta Kolcheva
Vedoucí práce: Mgr. Martin Horák, Ph.D.

S dizertační prací je možno se seznámit v příslušných knihovnách Přírodovědecké fakulty Univerzity Karlovy.

Obsah

1. Abstract 4
2. Úvod 5
3. Hypotézy a cíle 8
4. Materiály a metody 10
5. Výsledky 16
    5.1. Tři patogenní mutace v doméně M3 podjednotky GluN1 regulují povrchovou expresi a farmakologickou citlivost NMDARs 16
    5.2. Přítomnost předpokládaných *N*-glykosylačních míst a jejich interakce se specifickými lektiny reguluje funkční vlastnosti receptorů GluN1/GluN3 32
6. Diskuse 38
    6.1. Tři patogenní mutace v doméně M3 podjednotky GluN1 regulují povrchovou expresi a farmakologickou citlivost NMDAR 38
    6.2. Přítomnost předpokládaných *N*-glykosylačních míst a jejich interakce se specifickými lektiny reguluje funkční vlastnosti receptorů GluN1/GluN3 42
7. Závěr 45
8. Použitá literatura 47
9. Seznam publikací 53
    9.1. Publikace *in extenso*, související s touto dizertační prací 53
    9.2. Publikace nesouvisející s touto dizertační prací 54
10. Životopis 55

1. Abstract

N-methyl-D-aspartátové (NMDA) receptory jsou ionotropní glutamátové receptory, které hrají klíčovou roli v excitačním synaptickém přenosu v centrálním nervovém systému savců (CNS). Hyperaktivita nebo hypoaktivita NMDAR může způsobit široké spektrum patologických stavů a psychiatrických poruch, jako například Alzheimerovu chorobu, Parkinsonovu chorobu, Huntingtonovu chorobu, epilepsii nebo schizofrenii. NMDAR tvoří heterotetramerní komplex složený z podjednotek GluN1, GluN2(A-D) a/nebo GluN3(A, B). Různé podtypy NMDAR by mohly mít různý vliv na patogenezi onemocnění, a proto je zásadní zkoumat specifickou roli jednotlivých podjednotek v regulaci normálního fungování NMDAR. Regulace NMDAR probíhá na různých úrovních, od ranného zpracování, včetně syntézy, sestavení, kontroly kvality v endoplazmatickém retikulu (ER), přesun na povrch buňky až po internalizaci, recyklaci a degradaci. V této disertační práci jsme se zaměřili především na určení role extracelulárních a transmembránových oblastí různých podtypů NMDAR v regulaci jejich funkce. Konkrétně jsme pomocí elektrofyziologických a mikroskopických metod na buňkách HEK293 a kultivovaných hipokampálních neuronech zkoumali: (i) vliv *N*-glykosylace a různých lektinů na regulaci funkčních vlastností receptorů GluN1/GluN3; (ii) vliv patogenních mutací v transmembránové doméně (TMD) podjednotky GluN1 na povrchové podání, funkční a farmakologické vlastnosti konvenčních a nekonvenčních di-heteromerních NMDAR; (iii) úloha integrity vazebného místa

glycinu podjednotek GluN1 a GluN3A v přenosu a funkčních vlastnostech NMDAR.

2. Úvod

N-methyl-D-aspartátové receptory (NMDAR) jsou ionotropní glutamátové receptory, které hrají klíčovou úlohu v centrálním nervovém systému (CNS) savců. Fyziologická funkce NMDAR je důležitá pro excitační synaptický přenos a tvorbu paměti. Zvýšení, nebo naopak snížení aktivity NMDAR však může vést k celé řadě patologických stavů a psychiatrických poruch, jako je Alzheimerova choroba, Parkinsonova choroba, Huntingtonova choroba, epilepsie nebo schizofrenie (Paoletti et al., 2013; Zhou and Duan, 2018).

NMDAR jsou heterotetramerní komplexy tvořené dvěma obligatorními podjednotkami GluN1 (která má osm sestřihových variant), podjednotkami GluN2 (GluN2A až GluN2D) a/nebo podjednotkami GluN3 (GluN3A a GluN3B). Všechny GluN podjednotky mají stejnou topologii, skládají se z extracelulární N-terminální domény (NTD) tvořené amino-terminální doménou (ATD) a ligand-vazebnou doménou (LBD), transmembránové domény (TMD) a intracelulární C-terminální domény (CTD).

ATD je definována prvními ~ 400 aminokyselinami, má "clamshell-like" strukturu tvořenou segmenty R1 a R2 a obsahuje vazebná místa pro alosterické modulátory, jako je ifenprodil, protony, Zn^{2+}, polyaminy (H. Furukawa a Gouaux, 2003; K. Furukawa, 2014). Existují také důkazy, že ATD

zprostředkovává sestavení úvodních dimerů podjednotek GluN v endoplazmatickém retikulu (ER) (Meddows et al., 2001). ATD je spojena s LBD prostřednictvím linkerů ATD-LBD. Podobně jako ATD se LBD skládá ze dvou segmentů – S1 a S2, které vytvářejí vazebnou kapsu pro ligandy (Amin et al., 2021; H. Furukawa a Gouaux, 2003; C. H. Lee et al., 2014; Paoletti et al., 2013). LBD podjednotek GluN1 a GluN3 obsahují vazebné místo pro glycin, zatímco LBD podjednotek GluN2 obsahuje vazebné místo pro glutamát (Traynelis et al., 2010).

Transmembránová doména (TMD) se skládá ze tří transmembránových α-helixů (M1, M3 a M4) a smyčky M2, přičemž smyčka M2 a segment M3 jsou hlavními doménami tvořícími póry (Wollmuth a Sobolevsky, 2004). Smyčka M2 tvoří nejužší část iontového kanálu a je selektivním filtrem pro ionty a také vazebným místem pro Mg^{2+} a blokátory otevřených kanálů (Hatton a Paoletti, 2005; Huettner, 2015). Helix M3 tvoří velmi těsné uspořádání kolem póru receptoru, zatímco zbývající helixy M1 a M4 se nacházejí spíše na periferii, kolem iontového kanálu (Karakas a Furukawa, 2014; Lee a kol., 2014). Helix M3 je také v kontaktu s krátkým helixem pre-M1, který je orientován rovnoběžně s membránou (Lee a kol., 2014; Sanz-Clemente a kol., 2013; Traynelis a kol., 2010). Helix M3 obsahuje konzervativní aminokyselinový motiv SYTANLAAF, který se vyskytuje u všech typů glutamátových receptorů. LBD a TMD jsou spojeny třemi krátkými linkery, které jsou označeny podle své

polohy a orientace: S1-M1, M3-S2 a S2-M4, kde S označuje segment LBD a M transmembránový helix. Linkery M3-S2 jsou centrální polypeptidové řetězce, které přímo spojují segmenty S2 z LBD s helixem M3 a vytvářejí tak iontový kanál. Linkery S1-M1 a S2-M4 se nacházejí spíše na periferii a podílejí se na regulaci otevření kanálu, jejich přesný podíl však zůstává neznámý (K. Furukawa, 2014; Johansen Amin et al., 2021).

CTD je nejvariabilnější částí NMDAR, její délka se mezi podjednotkami značně liší, od ~50 aminokyselinových zbytků u podjednotky GluN1 až po 660 zbytků u podjednotky GluN2B. CTD hraje důležitou roli při stabilizaci a fixaci NMDAR k buněčnému cytoskeletu, protože obsahuje vazebná místa pro mnoho regulačních molekul (Ataman et al., 2007; Warnet et al., 2020). Zajímavé je, že struktura CTD zůstává nedefinovaná, identifikovány byly jen některé krátké rozpoznávací motivy v komplexech s vazebnými partnery (např. krátká část vázající Ca^{2+}/kalmodulin) (Ataman et al., 2007). Nedostatečná znalost struktur je pravděpodobně způsobena tím, že CTD patří do třídy vnitřně neuspořádaných oblastí (v angl. intrinsically disordered regions, IDR), které neobsahují dostatek hydrofobních aminokyselin pro složení definované 3D struktury (Wright a Dyson, 2015)

Různé podtypy NMDAR by mohly mít různý vliv na patogenezi onemocnění, a proto je zásadní studovat specifickou roli jednotlivých podjednotek v regulaci fyziologického fungování NMDAR. Regulace NMDAR

probíhá na různých úrovních, od syntézy asbalení, přes kontrolu kvality v endoplazmatickém retikulu (ER), přesun na povrch buňky až po internalizaci, recyklaci a degradaci. V této disertační práci jsme se zaměřili především na určení role extracelulárních a transmembránových oblastí různých podtypů NMDAR v regulaci jejich funkce. Konkrétně jsme pomocí elektrofyziologických a mikroskopických metod na buňkách HEK293 i na kultivovaných hipokampálních neuronech zkoumali: (i) vliv N-glykosylace a různých lektinů na regulaci funkčních vlastností receptorů GluN1/GluN3; (ii) vliv patogenních mutací v transmembránové doméně (TMD) podjednotky GluN1 na povrchovouexpresi, funkční a farmakologické vlastnosti konvenčních a nekonvenčních di-heteromerních NMDAR; (iii) úlohu integrity vazebného místa glycinu podjednotek GluN1 a GluN3A ve funkčních vlastnostech NMDAR a jejich transportu na plazmatickou membránu.

3. Hypotézy a cíle

1) Předchozí studie zjistily, že receptory GluN1/GluN2 a NMDAR obsahující GluN3A jsou značně N-glykosylované. Bylo prokázáno, že několik typů rostlinných lektinů se váže na NMDAR a ovlivňuje funkční vlastnosti receptorů. Dále dřívější studie ukázaly, že funkční vlastnosti di-heteromerních receptorů GluN1/GluN2 a nativních NMDAR jsou méně citlivé na modulaci lektiny ve srovnání s receptorem α-amino-3-hydroxy-5-methyl-

isoxazolepropionové kyselin (AMPAR) a kainátovými receptory (Everts et al., 1997; M. L. Mayer a Vyklický, 1989), avšak specifický vliv lektinů na funkční vlastnosti receptorů GluN1/GluN3 nebyl dosud zcela objasněn.

Cíl: ověřit, jestli přítomnost specifických N-glykanů reguluje funkční vlastnosti receptorů GluN1/GluN3, a otestovat panel lektinů z pohledu jejich potenciálu modulovat funkční vlastnosti receptorů GluN1/GluN3.

2) Předchozí studie zjistily, že řada patogenních mutací identifikovaných v podjednotkách GluN - včetně mutací kolem vazebného místa pro blokátory otevřených kanálů - mění povrchovou expresi, glutamátovou a glycinovou účinnost, citlivost na Mg^{2+} a memantin (Chen et al., 2017; Fedele et al., 2018; Vyklicky et al., 2018). Memantin je látka, která se běžně používá k léčbě Alzheimerovy choroby s komplexním mechanismem účinku, včetně inhibice ve druhém vazebném místě (v angl. second site inhibition, SSI) (Glasgow et al., 2018), označované také jako inhibice kanálu přes membránu (v angl. membrane-to-channel inhibition, MCI) (Wilcox et al., 2022). fyziologické koncentrace Mg^{2+} (řádově 1 mM) mění inhibiční účinky memantinu na receptory GluN1/GluN2, a proto jsou důležitým faktorem při zvažování terapeutického využití memantinu (Johnson, 2006).

Cíl: ověřit, jestli tři dříve popsané patogenní mutace v dolní oblasti domény M3 v podjednotce GluN1 - M641I, A645S a Y647S - ovlivňují povrchovou expresi, funkční vlastnosti a/nebo farmakologické vlastnosti NMDAR

exprimovaných v buňkách HEK293 a kultivovaných potkaních hipokampálních neuronech.

4. Materiály a metody

Příprava primárních hipokampálních neuronů

Všechny postupy na zvířatech byly prováděny v souladu s pokyny ARRIVE a směrnicí Rady Evropské komise 2010/63/EU pro pokusy na zvířatech. Primární kultury hipokampálních neuronů byly připraveny z 18-denních embryí potkanů Wistar (Lichnerova et al., 2015). Ve zkratce: hipokampy byly vypreparovány ve studeném pitevním roztoku sestávajícím z Hanksova vyváženého solného roztoku doplněného o 10 mM HEPES (pH 7,4) a penicilin-streptomycin (Life Technologies) a následně inkubovány 20 minut při 37 °C v pitevním médiu. Poté byly buňky promyty, disociovány skleněnou pipetou a resuspendovány v médiu sestávajícím z minimálního esenciálního média (MEM) doplněného o 10% tepelně inaktivované koňské sérum, doplněk N2, 1 mM pyruvát sodný, 20 mM D-glukózu, 25 mM HEPES a 1% penicilin-streptomycin. Buňky byly naneseny v hustotě $2x10^4$ buněk na cm^2 na skleněná krycí sklíčka potažená poly-L-lysinem. Po 2 hodinách bylo médium nahrazeno médiem Neurobasal doplněným o B-27 a L-glutaminem (Thermo Fisher Scientific).

Příprava transfekovaných buněk HEK293

Buňky HEK293 byly kultivovány v Opti-MEM (Thermo Fisher Scientific) obsahujícím 5 % fetálního bovinního séra (Thermo Fisher Scientific) (Kaniakova et al., 2012; Lichnerova et al., 2015). Pro elektrofyziologii byly buňky HEK293 kultivovány na 24-jamkových destičkách a transfekovány celkem 0,9 μg konstruktů cDNA kódujících podjednotky GluN1/GluN2 nebo GluN1/GluN3 a GFP (pro identifikaci úspěšně transfekovaných buněk) smíchaných s 0,9 μl reagentu MATra-A (IBA) v 50 μl Opti-MEM I; buňky byly potom trypsinizovány a kultivovány při nižší hustotě na sklíčkách pokrytých poly-*L*-lysinem. Pro mikroskopii byly buňky HEK293 kultivovány na 12-jamkových destičkách a transfekovány celkem 0,45 μg konstruktů cDNA kódujících podjednotky GluN (v poměru 1:2 značené: neznačené podjednotky) smíchaných s 1 μl činidla Lipofectamine 2000 (Thermo Fisher Scientific) v 50 μl Opti-MEM I.

Imunofluorescenční mikroskopie

Povrchové NMDAR byly označeny podle předchozího popisu (Kaniakova et al., 2012; Lichnerova et al., 2015). Ve zkratce: buňky byly promyty ve fosfátem pufrovaném fyziologickém roztoku (PBS) ainkubovány v blokovacím roztoku – PBS s 10% normálním kozím sérem (NGS). Poté byly povrchové NMDAR označeny pomocí primární protilátky anti-GFP (15 min; 1:1000; Merck) a následně sekundární protilátkou konjugovanou s Alexa Fluor 647 (15

min; 1:1000; Thermo Fisher Scientific). Dále byly buňky fixovány ve 4% paraformaldehydu (PFA) v PBS, permeabilizovány 0,25% Tritonem X-100 v PBS a označeny primární protilátkou anti-GFP (30 min; 1:1000; Merck) následovanou kozí sekundární protilátkou konjugovanou s Alexa Fluor 488 (30 min; 1:1000; Thermo Fisher Scientific). Buňky byly potom upevněny na sklíčka pomocí reagentu ProLong Antifade (Thermo Fisher Scientific).

Snímky byly pořízeny při pokojové teplotě pomocí fluorescenčního mikroskopu (Olympus Scan) s objektivem 60x/1,35 s olejovou imerzí nebo konfokálního skenovacího mikroskopu (Leica TCS SP8) vybaveného pevnolátkovými lasery a apochromatickým objektivem pro olejovou imerzi 63x/1,30. Získané snímky byly analyzovány pomocí softwaru ImageJ (NIH). U hipokampálních neuronů byla analyzována povrchová a celková intenzita fluorescenčního signálu v 10 µm dlouhých segmentech sekundárních a terciárních dendritů (Lichnerova et al., 2015).

Elektrofyziologie

Záznamy získané metodou terčíkového zámku z celých buněk byly pořízeny na transfekovaných buňkách HEK293 pomocí zesilovače Axopatch 200B (Molecular Devices). Měřící mikropipety z borosilikátového skla (odpor hrotu 3-6 MΩ) byly připraveny pomocí tahovače P-97 (Sutter Instruments) a naplněny intracelulárním záznamovým roztokem obsahujícím (v mM): 125 kyseliny glukonové, 15

CsCl, 5 BAPTA, 10 HEPES, 3 MgCl2, 0,5 CaCl2 a 2 soli ATP-Mg (pH 7,2, upraveno CsOH). Standardní extracelulární roztok (ECS) obsahoval (v mM): 160 NaCl, 2,5 KCl, 10 HEPES, 10 D-glukózy, 0,2 EDTA a 0,7 $CaCl_2$ (pH 7,3, upraveno NaOH). Pro měření hodnot IC_{50} pro Mg^{2+} a měření proudů v přítomnosti 1 mM $MgCl_2$ byla EDTA z ECS vynechána. Pro aplikaci extracelulárních roztoků byl použit rychlý perfuzní systém s časovou konstantou výměny roztoku kolem buňky přibližně 20 ms. Pokud není uvedeno jinak, obsahovaly všechny ECS 50 µM glycin. Pro záznam měření v hipokampálních neuronech obsahoval ECS 1 µM tetrodotoxin (TTX) a 10 µM bikukulin. Všechna elektrofyziologická měření byla prováděna při pokojové teplotě a uváděné hodnoty udržovacího potenciálu byly korigovány na vypočtený potenciál tekutého spoje přibližně 14 mV (Vyklicky et al., 2018). Aktivační křivky NMDAR pro glutamát a glycin byly získány pomocí následující rovnice:

Rovnice (1):

$$I = I_{max}/(1 + (EC_{50}/[agonist])^{h}),$$

kde I_{max} je maximální odpověď, EC_{50} je koncentrace vyvolávající polomaximální odpověď, [agonista] je koncentrace glutamátu nebo glycinu a *h* je Hillův koeficient. Křivky inhibice NMDAR byly získány pomocí následující rovnice:

Rovnice (2):

$$I = 1/(1 + ([antagonist]/IC_{50})^{h}),$$

kde IC_{50} je koncentrace Mg^{2+} nebo memantinu, která způsobila 50% inhibici agonistou vyvolaného proudu, [antagonista] je koncentrace Mg^{2+} nebo memantinu a *h* je Hillův koeficient. Časový průběh inhibice MK-801 nebo memantinu byl analyzován pomocí jedno nebo dvojnásobné exponenciální funkce, vážené časové konstanty (τ_w) byly získány pomocí následující rovnice:

Rovnice (3):

$$\tau_w = (\tau_{fast} * A_{fast} + \tau_{slow} * A_{slow})/(A_{fast} + A_{slow}),$$

kde τ_{fast} a A_{fast} jsou časová konstanta a plocha rychlé komponenty, a τ_{slow} a A_{slow} jsou časová konstanta a plocha pomalejší komponenty; normalizované hodnoty A_{fast} byly získány vydělením každé hodnoty hodnotou ($A_{fast} + A_{slow}$).

SSI byl měřen podle předchozího popisu (Glasgow et al., 2018). Ve zkratce, minimální frakční odpověď po SSI (minimální $I_{SSI}/I_{control}$) byla vypočtena jako průměrná hodnota $I_{SSI}/I_{control}$ měřená v časovém okně 200 ms se středem na minimální hodnotu poměru; $I_{control}$ byla vypočtena jako průměr $I_{control1}$ a $I_{control2}$; odpovědi, u nichž byla hodnota $I_{control2}/I < 0,8$, byly z analýzy vyloučeny.

NMDA-indukovaná excitotoxicita

Pro vyvolání excitotoxicity byly DIV14 neurony umístěny přes noc do minimálního definovaného média obsahujícího 10 % MEM (Invitrogen) a 90 % média Salt-Glucose (SG) obsahujícího (v mM): 114 NaCl, 0,219 % NaHCO3, 5,292 KCl, 1 $MgCl_2$, 2 $CaCl_2$, 10 HEPES, 30

glukózy, 0,5 pyruvátu sodného a 0,1 % fenolové červeně (McQueen et al., 2017; Skrenkova et al., 2020). Následující den byly neurony umístěny do 100% SG média obsahujícího glycin, NMDA a memantin (Hello Bio) v uvedených koncentracích. Po 1 h bylo médium změněno na 10% MEM a 90% SG médium a po dalších 22-23 h byly neurony označeny 5 μM Hoechst 33342 (Molecular Probes) po dobu 30 min a poté fixovány ve 4% PFA v PBS. Po permeabilizaci neuronů pomocí Tritonu X-100 byly podjednotky YFP-GluN1 označeny pomocí primární protilátky anti-GFP a následně sekundární protilátkou konjugovanou s Alexa Fluor 488, jak je popsáno výše. Snímky (1024 × 1024 pixelů s velikostí pixelu 1,243 μm × 1,243 μm, tedy zorné pole o velikosti 1272 μm × 1272 μm) byly pořízeny pomocí konfokálního mikroskopu Olympus FV10i vybaveného superapochromatickým objektivem 10x/0,4 NA. Pro každé zorné pole byly získány tři snímky: signál YFP (pro označení infikovaných buněk), Hoechst (pro barvení jader) a snímek DIC. Jaderná plocha byla měřena pomocí softwaru ImageJ (NIH) a k automatickému měření jaderné plochy výhradně u infikovaných buněk identifikovaných podle exprese YFP byl použit vlastní makroskript. Počet buněk pro každou podmínku byl 519-1407, v každém experimentu bylo shromážděno 17446-24758 buněk (všechny podmínky byly sečteny). Program MATLAB (2019b) byl použit ke klasifikaci buněk jako pyknotických nebo nepyknotických na základě jaderné plochy naměřené u každé buňky.

5. Výsledky

5.1. Tři patogenní mutace v doméně M3 podjednotky GluN1 regulují povrchovou expresi a farmakologickou citlivost NMDARs

Nejprve jsme zkoumali, jestli tři patogenní mutace v doméně M3 podjednotky GluN1 (Lemke et al., 2016) mění povrchovou expresi receptorů GluN1/GluN2A, GluN1/GluN2B a GluN1/GluN3A exprimovaných v buňkách HEK293; tyto mutace jsou schematicky znázorněny na obr. 1A. Za tímto účelem jsme vytvořili podjednotky GluN1-1a označené YFP obsahující patogenní mutace M641I, A645S nebo Y647S; tyto podjednotky jsme pak exprimovali společně s podjednotkami GluN2A, GluN2B a GluN3A a měřili jsme jejich povrchové a celkové hladiny exprese pomocí imunobarvení protilátkou anti-GFP; příklady snímků transfekovaných buněk jsou uvedeny na obr. 1B. Zjistili jsme, že buňky exprimující receptory GluN1-1a-M641I/GluN2A, GluN1-Y647S/GluN2A a GluN1-1a-Y647S/GluN2B měly výrazně sníženou povrchovou expresi; všechny ostatní studované kombinace NMDAR byly na povrchu buněk exprimovány ve stejné míře jako odpovídající receptory WT (obr. 1C). Tyto výsledky naznačují, že specifické patogenní mutace v doméně M3 podjednotky GluN1-1a odlišně mění povrchovou expresi s různými podtypy podjednotek NMDAR. Podobně jako u našich výsledků získaných se sestřihovou variantou GluN1-1a jsme zjistili, že receptory GluN1-4a-

M641I/GluN2A, GluN1-4a-Y647S/GluN2A a GluN1-4a-Y647S/GluN2B - ale žádná jiná z testovaných kombinací NMDAR - měly ve srovnání s receptory WT významně sníženou povrchovou expresi (obr. 1D). Celkově tato data potvrzují, že specifické patogenní mutace v doméně M3 podjednotky GluN1 ovlivňují povrchovou expresi NMDAR a tento účinek je zřejmě nezávislý na sestřihové variantě GluN1.

Dále jsme zkoumali, zda tyto patogenní mutace v doméně M3 podjednotky GluN1 ovlivňují povrchovou expresi NMDAR v neuronech. Deset dní po virové infekci jsme provedli imunobarvení pomocí protilátky anti-GFP a měřili povrchové a celkové hladiny exprese podjednotek GluN1-1a pomocí konfokální mikroskopie (obr. 1E). Naše analýza ukázala, že podjednotka GluN1-1a-A645S byla na povrchu exprimována ve stejné míře jako podjednotka WT, zatímco podjednotky GluN1-1a-M641I a GluN1-1a-Y647S byly na povrchu buněk výrazně sníženy (obr. 1F). Tato zjištění jsou v souladu s našimi údaji získanými z buněk HEK293 a potvrzují, že specifické patogenní mutace v doméně M3 podjednotky GluN1 ovlivňují povrchovou expresi NMDAR.

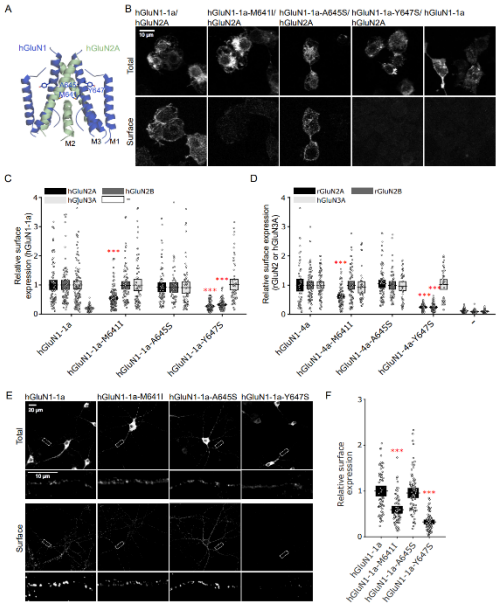

Obrázek 1. Patogenní mutace v podjednotce GluN1 odlišně mění povrchovou expresi NMDAR v závislosti na podjednotce. (A) Strukturní model domén M1, M2 a M3 v heterotetrameru GluN1/GluN2A (kód PDB: 6IRA); zde jsou označeny tři studované aminokyselinové zbytky. (B) Reprezentativní snímky buněk HEK293 transfekovaných podjednotkou GluN2A a uvedenými nemutovanými podjednotkami nebo mutovanými podjednotkami YFP-GluN1-1a (GluN1-1a); celkový a povrchový signál

podjednotek GluN1-1a byly označeny 24 h po transfekci pomocí protilátky anti-GFP. (C-D) Souhrn relativní povrchové exprese mutovaných a nemutovaných podjednotek GluN1-1a GluN1-1a (C) nebo GluN1-4a (D), které byly ko-transfekovány s uvedenými neznačenými podjednotkami GluN2 nebo GluN3A (C) nebo GFP-GluN2 (GluN2) a GFP-GluN3A (GluN3A) (D), měřeno pomocí fluorescenční mikroskopie ($n \geq 70/49$ buněk na skupinu); ***$p < 0.001$ vs. odpovídající WT NMDAR, (jednosměrná ANOVA). (E) Reprezentativní snímky kultivovaných potkaních hipokampálních neuronů infikovaných lentiviry kódujícími uvedené podjednotky YFP-GluN1-1a (GluN1-1a); celkový a povrchový signál podjednotek GluN1-1a byly označeny pomocí protilátky anti-GFP. (F) Souhrn relativní povrchové exprese uvedených podjednotek GluN1-1a měřený v 10 µm segmentech sekundárních nebo terciárních dendritů ($n \geq 30$ segmentů v ≥ 6 různých buňkách na skupinu); ***$p < 0,001$ vs. GluN1- 1a, (jednocestná ANOVA).

Dále jsme měřili závislost míry inhibice na koncentraci Mg^{2+} pro nemutované a mutované receptory GluN1-4a/GluN2A a GluN1-4a/GluN2B v přítomnosti saturující koncentrace (1 mM) glutamátu (obr. 2A, C). Zjistili jsme, že mutace M641I ani mutace A645S v podjednotce GluN1-4a neovlivnily hodnotu IC_{50} pro Mg^{2+} bez ohledu na podjednotku GluN2 koexprimovanou v buňkách HEK293 (obr. 2B, D). Ani jedna z těchto patogenních mutací tedy neovlivňuje citlivost receptorů GluN1-4a/GluN2 na Mg^{2+}.

Dále jsme měřili citlivost NMDAR na memantin stejným postupem jako výše; pro tyto experimenty obsahoval ECS 0 mM Mg^{2+} (obr. 2E-H). Naše analýza odhalila, že

memantin inhibuje receptory GluN1-4a/GluN2A i GluN1-4a/GluN2B s hodnotou IC_{50} přibližně 1 μM (obr. 2F, H), což je v souladu s dříve publikovanými údaji (Kotermanski a Johnson, 2009). Na rozdíl od našich experimentů s Mg^{2+} jsme zjistili, že hodnota IC_{50} pro memantin byla významně zvýšena u receptorů obsahujících podjednotku GluN1-4a-A645S (2 E-H), ale nebyla ovlivněna u receptorů obsahujících podjednotku GluN1-4a-M641I (obr. 2F, H). Dvě patogenní mutace v podjednotce GluN1 tedy neovlivňují citlivost NMDAR na Mg^{2+}, ale rozdílně ovlivňují citlivost NMDAR na memantin.

Dřívější studie ukázala, že fyziologické hladiny extracelulárního Mg^{2+} (přibližně 1 mM) ovlivňují selektivitu NMDAR vůči memantinu (Kotermanski a Johnson, 2009). Zkoumali jsme proto, zda patogenní mutace v doméně M3 podjednotky GluN1 ovlivňují citlivost NMDAR k memantinu v přítomnosti 1 mM Mg^{2+} měřením celobuněčných proudů vyvolaných 1 mM glutamátem při membránovém potenciálu -60 mV a zvyšujících se koncentracích memantinu (obr. 2I). Při těchto experimentech jsme se zaměřili na NMDAR obsahující GluN2A, protože v buňkách HEK293 obecně poskytují větší proudy ve srovnání s NMDAR obsahujícími GluN2B, což nám umožnilo snadněji zkoumat účinek memantinu na proudy indukované glutamátem v přítomnosti 1 mM Mg^{2+}. V přítomnosti 1 mM Mg^{2+} jsme pozorovali, že hodnota IC_{50} pro memantin byla u receptorů GluN1-4a/GluN2A WT přibližně 14 μM (obr. 2J a K), což odpovídá dříve publikovaným údajům (Kotermanski a Johnson, 2009). Zajímavé je, že jsme zjistili,

že receptory GluN1-4a-M641I/GluN2A měly výrazně sníženou hodnotu IC_{50} (~2 μM), zatímco receptory GluN1-4a-A645S/GluN2A měly výrazně zvýšenou hodnotu IC_{50} (~32 μM) pro memantin v přítomnosti 1 mM Mg^{2+} ve srovnání s receptory GluN1-4a/GluN2A WT; hodnoty IC_{50} pro memantin v nepřítomnosti a přítomnosti 1 mM Mg^{2+} pro různé receptory GluN1-4a/GluN2A jsou shrnuty na obr. 2K.

Kromě toho jsme zkoumali citlivost NMDAR na memantin v buňkách HEK293 měřených při membránových potenciálech -20 mV a +40 mV a zjistili jsme, že hodnoty IC_{50} pro memantin byly významně sníženy u receptorů GluN1-4a-M641I/GluN2A a významně zvýšeny u receptorů GluN1-4a-A645S/GluN2A ve srovnání s receptory GluN1-4a/GluN2A WT při obou membránových potenciálech (obr. 2L-N). Souhrnně tato data naznačují, že mutace M641I a A645S v doméně M3 podjednotky GluN1 zvyšují, respektive snižují citlivost receptoru GluN1/GluN2 na memantin při fyziologicky relevantních hladinách extracelulárního Mg^{2+} a membránových potenciálech.

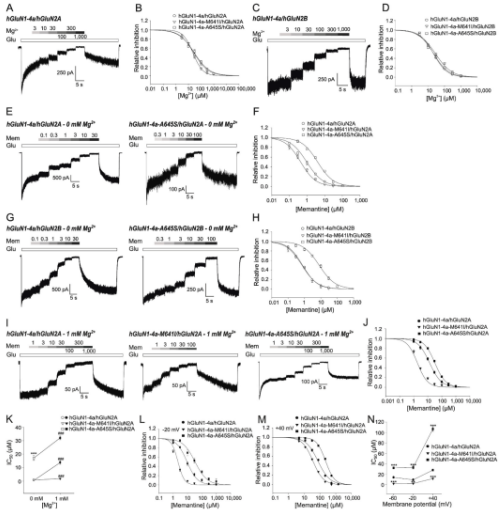

Obrázek 2 Specifické patogenní mutace v doméně M3 podjednotky GluN1 odlišně ovlivňují citlivost receptorů GluN1/GluN2 na memantin, ale nikoli na Mg^{2+}. (A, C) Reprezentativní záznamy měření v HEK293 buňkách, které byly transfekovány receptory GluN1-4a/GluN2A (A) nebo GluN1-4a/GluN2B (C) a měřeny při membránovém potenciálu -60 mV. Uvedené koncentrace Mg^{2+} (v μM) byly aplikovány za kontinuální přítomnosti 1 mM glutamátu (Glu). (B, D) Normalizované závislosti míry inhibice na koncentraci Mg^{2+} získané fitováním dat pomocí rovnice (2) (viz Metody). Každý datový bod představuje průměrný normalizovaný proud získaný z ≥ 5 buněk ± SEM. (E, G) Reprezentativní záznamy

měření v HEK293 buňkách, které byly transfekovány receptory GluN1-4a/GluN2A (E) nebo GluN1-4a/GluN2B (G) a měřených při membránovém potenciálu -60 mV. Uvedené koncentrace memantinu (Mem, v μM) byly aplikovány za kontinuální přítomnosti 1 mM Glu. (F, H) Normalizované závislosti míry inhibice na koncentraci memantinu (měřeno v 0 mM Mg^{2+}) byly získány fitováním dat pomocí rovnice (2). Každý datový bod představuje průměrný normalizovaný proud získaný z ≥5 buněk ± SEM. (I) Reprezentativní záznamy měření v HEK293 buňkách, které byly transfekovány receptory GluN1-4a/GluN2A a měřenýchpři membránovém potenciálu -60 mV, měřeno v přítomnosti 1 mM Mg^{2+}. Uvedené koncentrace Mem (v μM) byly aplikovány v kontinuální přítomnosti Glu a 1 mM Mg^{2+}. (J) Normalizované závislosti míry inhibice na koncentraci memantinu měřené v prostředí 1 mM Mg^{2+} byly získány fitováním experimentálních dat pomocí rovnice (2). Každý datový bod představuje průměrný normalizovaný proud získaný z ≥4 buněk ± SEM. (K) Hodnoty IC_{50} pro memantin vynesené v závislosti na extracelulární koncentraci Mg^{2+} pro uvedené receptory GluN1-4a/GluN2A. ***p < 0,001 oproti receptorům GluN1-4a/GluN2A (jednosměrná ANOVA s Tukeyho post hoc testem); ###p < 0,001 oproti 0 mM Mg^{2+} (Studentův t-test). (L, M) Normalizované závislosti míry inhibice na koncentraci memantinu měřené v buňkách HEK293 při udržovacím membránovém potenciálu -20 mV (L) nebo +40 mV (M). (N) Hodnoty IC_{50} pro memantin měřené v 1 mM Mg^{2+} vynesené proti membránovým potenciálům pro uvedené receptory GluN1-4a/GluN2A. **p < 0,010 a ***p < 0,001 oproti receptorům GluN1-4a/GluN2A divokého typu (jednosměrná ANOVA).

Důležité je, že memantin může působit na receptory GluN1/GluN2 také prostřednictvím druhého vazebného místa,

které je přístupné v nepřítomnosti agonistů, což je jev známý jako inhibice druhého místa (z angl. second site inhibition, SSI) (Glasgow et al., 2018), nebo nově jako inhibice kanálu přes membránu (z angl. membrane-to-channel inhibition, MCI) (Wilcox et al., 2022). Pro vyvolání SSI byl na buňky HEK293 aplikován ECS obsahující 100 μM memantin; po odstranění memantinu byl ihned přidán ECS obsahující 1 mM glutamát. Proud vyvolaný glutamátem po aplikaci memantinu byl posléze porovnán s kontrolními proudy, které byly naměřeny před a po aplikaci memantinu (obr. 3A). Pro kvantifikaci těchto údajů jsme vypočítali minimální poměr mezi SSI proudy a kontrolními proudy ("minimum $I_{SSI}/I_{control}$"); tyto výsledky jsou shrnuty na obr. 3B. V souladu s předchozími studiemi (Blanpied a kol., 1997; Glasgow a kol, 2018; Kotermanski a Johnson, 2009) jsme pozorovali, že za kontrolních podmínek je hodnota minimálního $I_{SSI}/I_{control}$ pro receptory GluN1-4a/GluN2A exprimovaných v buňkách HEK293 přibližně 0,5. Podobné hodnoty jsme pozorovali i v případě, kdy jsme aplikovali memantin společně s D-APV (kompetitivní antagonista pro glutamátové vazebné místo v podjednotce GluN2) nebo 1 mM Mg^{2+}. V případě, kdy byl 1 mM Mg^{2+} přítomem po celou dobu měření, hodnota minimálního $I_{SSI}/I_{control}$ se zvýšila přibližně na 0,9 (obr. 3B).

Kromě toho jsme také zjišťovali časovou konstantu zotavení z SSI ($\tau_{recovery}$), která byla za kontrolních podmínek u receptorů GluN1-4a/GluN2A přibližně 6 s (obr. 3C). Následně jsme zkoumali NMDAR obsahující patogenní mutace v

podjednotce GluN1 a zjistili jsme, že hodnota minimálního $I_{SSI}/I_{control}$ pro receptory GluN1-4a-M641I/GluN2A je za všech podmínek podobná jako u receptorů GluN1-4a/GluN2A, s výjimkou významného poklesu hodnoty minimálního $I_{SSI}/I_{control}$ v kontinuální přítomnosti 1 mM Mg^{2+} (obr. 3B); $\tau_{recovery}$ pro receptory GluN1-4a-M641I/GluN2A bylo rovněž podobné jako u receptorů GluN1-4a/GluN2A (obr. 3C). Naproti tomu jsme zjistili, že hodnota minimálního $I_{SSI}/I_{control}$ pro receptory GluN1-4a-A645S/GluN2A byla ve srovnání s receptory GluN1-4a/GluN2A WT výrazně zvýšená (~0. 8) za všech podmínek a nelišila se od receptorů GluN1-4a/GluN2A WT při měření v kontinuální přítomnosti 1 mM Mg^{2+} (obr. 3B); $\tau_{recovery}$ pro receptory GluN1-4a-A645S/GluN2A jsme nemohli vypočítat kvůli relativně slabé memantinem vyvolané SSI. Glasgow a kol. uvádějí, že SSI vyžaduje tranzit memantinu z druhého vazebného místa do tzv. hlubokého místa (Glasgow a kol., 2018). V souladu s předchozími údaji (Glasgow et al., 2018) jsme zjistili, že udržování membránového potenciálu při +40 mV (namísto -60 mV) eliminovalo memantinem indukovanou SSI (tj. $I_{SSI}/I_{control}$ byl přibližně 1) jak pro receptory GluN1-4a/GluN2A WT, tak pro mutantní receptory (obr. 3D, F). Naproti tomu jsme zjistili, že skokové zvýšení (tj. "přeskočení") membránového potenciálu z -60 mV na +40 mV pouze při aplikaci memantinu nemělo na memantinem indukovanou SSI žádný vliv ve srovnání s udržováním membránového potenciálu na -60 mV po celou dobu záznamu (obr. 3E a F). Souhrnně tato data naznačují, že

mutace M641I a A645S v podjednotce GluN1 rozdílně ovlivňují schopnost memantinu vyvolat SSI u NMDAR.

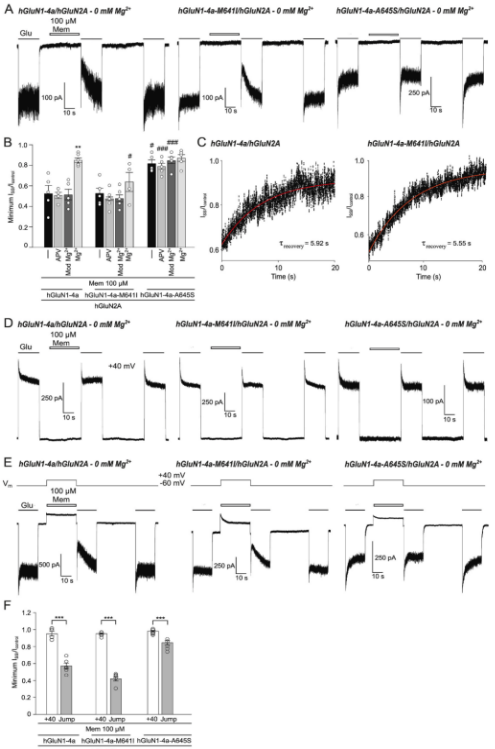

Obrázek 3. Specifické patogenní mutace v doméně M3 podjednotky GluN1 odlišně ovlivňují memantinem zprostředkovanou SSI receptorů GluN1/GluN2A. (A) Reprezentativní záznamy měření v HEK293 buňkách, které byly transfekovány receptory GluN1-4a/GluN2A a měřené při membránovém potenciálu -60 mV. Tam, kde je uvedeno, byl aplikován 1 mM glutamát (Glu) a 100 μM memantin (Mem). (B) Souhrn hodnot minimálních $I_{SSI}/I_{control}$ vypočtených pro uvedené receptory GluN1-4a/GluN2A (viz Metody). "-", kontrolní stav; "APV", 50 μM D-APV bylo aplikováno společně s Mem; "Mod Mg_{2+}", 1 mM Mg^{2+} byl aplikován společně s Mem; "Mg^{2+}", 1 mM Mg^{2+} byl přítomen po celou dobu záznamu (další podrobnosti viz text); $n \geq 5$ buněk pro každý stav. **p < 0,001 oproti kontrolnímu stavu (jednosměrná ANOVA); #p < 0,050 a ###p < 0,001 oproti divokému typu receptorů GluN1-4a/GluN2A (jednosměrná ANOVA). (C) $I_{SSI}/I_{control}$ je vykresleno z příkladových stop uvedených v panelu A, přičemž je zobrazena odpovídající časová konstanta zotavení z SSI ($\tau_{recovery}$). Průměrné hodnoty τrecovery byly 6,25 ± 0,72 s a 6,83 ± 0,66 s pro buňky exprimující receptory GluN1-4a/GluN2A a GluN1-4a-M641I/GluN2A ($n \geq 5$ buněk pro každou skupinu; $p > 0,05$; Studentův t-test). (D, E) Reprezentativní záznamy měření v HEK293 buňkách, které byly transfekovány receptory GluN1-4a/GluN2A a měřené při fixním membránovém potenciálu +40 mV (D) nebo při -60 mV se skokem ("jump") na +40 mV během aplikace Mem (E). (F) Souhrn t minimálních $I_{SSI}/I_{control}$ vypočtených pro uvedené receptory GluN1-4a/GluN2A zaznamenané způsobem uvedeným v panelech D (+40; šedé sloupce) a E (Skok, černé sloupce); $n \geq 5$ buněk v každé skupině. ***p < 0,001 vs. +40 mV (Student t-test).

Dále jsme provedli elektrofyziologická měření na kultivovaných hipokampálních neuronech exprimujících podjednotky GluN1-1a nemutovaného a mutovaného typu, abychom analyzovali citlivost na memantin v přítomnosti 1

mM Mg^{2+} při membránovém potenciálu -60 mV; při těchto experimentech jsme místo glutamátu použili k aktivaci NMDAR 300 μM NMDA a během měření byl přítomen TTX i bikukulin. Podobně jako u záznamů získaných z HEK293 buněk jsme zjistili, že hodnota IC_{50} pro memantin byla u neuronů exprimujících YFP-GluN1-1a-M641I významně snížena, zatímco u neuronů exprimujících YFP-GluN1-1a-A645S významně zvýšena ve srovnání s neurony exprimujícími YFP-GluN1-1a WT (obr. 4 A-B). Dále jsme během záznamu při membránových potenciálech od -80 mV do +80 mV (v krocích po 20 mV) pozorovali, že 30 μM memantin účinněji inhibuje NMDAR v neuronech exprimujících YFP-GluN1-1a-M641I, ale méně účinně NMDAR v neuronech exprimujících YFP-GluN1-1a-A645S, obojí ve srovnání s neurony exprimujícími YFP-GluN1-1a (s výjimkou neuronů exprimujících YFP-GluN1-1a-A645S měřených při membránových potenciálech -20 mV a 0 mV; Obr. 4C-D). Stejně jako u buněk HEK293 tedy dvě různé mutace v doméně M3 podjednotky GluN1 rozdílně ovlivňují citlivost NMDAR na memantin při expresi v hipokampálních neuronech.

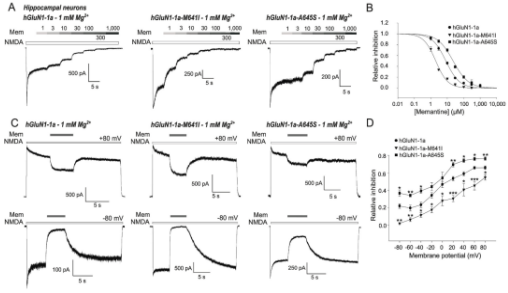

Obrázek 4. Specifické patogenní mutace v doméně M3 podjednotky GluN1 odlišně ovlivňují citlivost neuronálních NMDAR na memantin. (A) Reprezentativní záznamy měření v hipokampálních neuronech infikovaných lentiviry exprimujícími uvedené podjednotky GluN1-1a značené YFP (GluN1-1a); membránový potenciál byl měřen při -60 mV. Endogenní podjednotky GluN1 byly vyřazeny expresí shRNA-GluN1. Uvedené koncentrace memantinu (Mem; v μM) byly aplikovány v kontinuální přítomnosti 300 μM NMDA, 50 μM glycinu, 1 μM TTX, 10 μM bikukulinu a 1 mM Mg^{2+}. (B) Normalizované závislosti míry inhibice na koncentracimemantinu v kontinuální přítomnosti 1 mM Mg^{2+} byly získány fitováním dat pomocí rovnice (2). Každý datový bod představuje průměrný normalizovaný proud získaný z ≥4 buněk ± SEM. (C) Reprezentativní záznamy měření v infikovaných hipokampálních neuronech měřených při membránovém napětí -80 mV nebo +80 mV. NMDAR byly aktivovány přesně podle popisu v (A), pro všechny podmínky byl použit 30 μM memantin. (D) Graf shrnující relativní inhibici vyvolanou 30 μM memantinem, měřenou v hipokampálních neuronech exprimujících GluN1-1a, GluN1-1a-M641I a GluN1-1a-A645S při uvedených membránových potenciálech. n ≥ 5 buněk pro každou podmínku; ANOVA); *p < 0,050, **p < 0,010 a ***p < 0,001 vs. GluN1-1a.

Nakonec jsme zkoumali, zda mutace v podjednotce GluN1 ovlivňují NMDA indukovanou excitotoxicitu v kultivovaných hipokampálních neuronech. Proto jsme v neuronech exprimovali nemutované a mutované podjednotky YFP-GluN1-1a; potom jsme neurony kultivovali v médiu obsahujícím 1 mM Mg^{2+} spolu s 10 μM glycinem a 0, 30 nebo 100 μM NMDA a také v různých koncentracích memantinu po

dobu 1 h, po níž následovala další kultivace po dobu 22-23 h. Procento mrtvých buněk jsme poté stanovili barvením jader Hoechstem 33342 a měřením jaderné plochy (obr. 5A). Pomocí tohoto protokolu jsme zjistili, že neurony exprimující podjednotku YFP-GluN1-1a WT prodělaly významnou excitotoxicitu (~ 80 %) po působení 30 μM nebo 100 μM NMDA a memantin významně snížil excitotoxicitu v závislosti na dávce (obr. 5B-E). Neurony exprimující podjednotky YFP-GluN1-1a-M641I nebo YFP-GluN1-1a-A645S byly rovněž citlivé na excitotoxicitu vyvolanou NMDA, přičemž procento odumřelých buněk bylo podobné jako u neuronů exprimujících YFP-GluN1-1a WT. V souladu s našimi elektrofyziologickými daty jsme zjistili, že memantin odlišně ovlivňuje NMDA indukovanou excitotoxicitu u neuronů exprimujících mutantní podjednotky GluN1. Konkrétně memantin významně snížil excitotoxicitu u neuronů exprimujících podjednotku YFP-GluN1-1a-M641I, ale byl významně méně neuroprotektivní u neuronů exprimujících podjednotku YFP-GluN1-1a-A645S ve srovnání s neurony exprimujícími podjednotku YFP-GluN1-1a WT (obr. 5D a E). Tato data naznačují, že specifické patogenní mutace v doméně M3 podjednotky GluN1 odlišně ovlivňují farmakologickou citlivost NMDAR v hipokampálních neuronech.

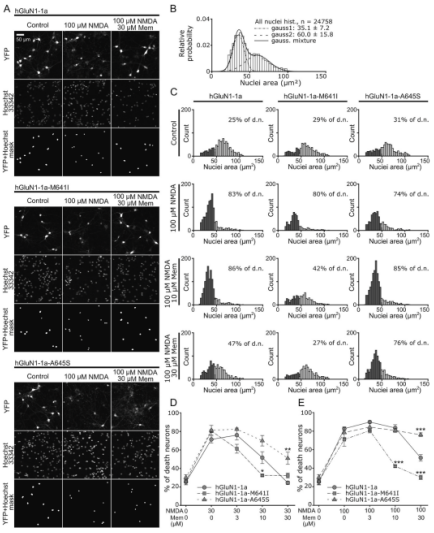

Obrázek 5. Memantin odlišně ovlivňuje NMDA indukovanou excitotoxicitu v hipokampálních neuronech exprimujících mutované podjednotky GluN1. (A) Reprezentativní fluorescenční snímky barvení YFP a Hoechst 33342 v hipokampálních neuronech exprimujících podjednotky YFP-GluN1-1a (GluN1-1a), YFP-GluN1-1a-M641I (GluN1-1a-M641I) nebo YFP-GluN1-1a-A645S (GluN1-1a- A645S). V levém sloupci jsou kontrolní neurony, v prostředním po aplikaci10 µM glycinu a 100 µM NMDA , a v pravém sloupci po aplikaci 10 µM glycinu, 100 µM NMDA a 30 µM memantinu (Mem). Horní řádky: signal YFP; prostřední řádky: signal Hoechst 33342; a spodní řádky: maska pro výběr pouze jader buněk exprimujících YFP. (B) Histogram

zobrazující rozložení velikosti jader naměřené u všech neuronů, který odhaluje dvě jasně odlišitelné skupiny představující pyknotické (tj. mrtvé) a nepyknotické neurony. Data byla vybavena směsí dvou Gaussových modelů rozdělení (plná čára) a pro každé rozdělení byly odhadnuty Gaussovy parametry (střední hodnota a hodnoty sigma), které jsou zobrazeny. Odhadnutá jednotlivá Gaussova rozdělení jsou znázorněna jako tečkovaná čára (pyknotické buňky) a přerušovaná čára (nepyknotické buňky). (C) Histogramy zobrazující distribuce jaderné plochy pro neurony v uvedených podmínkách. Pro každou podmínku byly neurony klasifikovány na základě pravděpodobnosti, že jsou pyknotické (tmavě šedé sloupce) nebo nepyknotické (bílé sloupce). Procenta v histogramech odpovídají množství pyknotických neuronů (d. n. z angl. dead neurons). (D-E) Souhrn výsledků zahrnujících procenta pyknotickýchneuronů exprimujících uvedené podjednotky GluN1-1a a po aplikaci uvedených koncentrací memantinu (Mem) v přítomnosti 30 μM (D) nebo 100 μM (E) NMDA; klasifikovaná jádra byla počítána pro každou podmínku a počet pyknotických buněk je vyjádřen jako procento z celkového počtu analyzovaných buněk. Chybové úsečky označují SEM; $n \geq 5214$ buněk pro každou podmínku získaných z 5 nezávislých experimentů. *$p < 0,050$, **$p < 0,010$ a ***$p < 0,001$ oproti podjednotce GluN1-1a WT (jednosměrná ANOVA; $p < 0,05$).

5.2. Přítomnost předpokládaných *N*-glykosylačních míst a jejich interakce se specifickými lektiny reguluje funkční vlastnosti receptorů GluN1/GluN3

Jak je znázorněno na obr. 6A a 6B, podjednotky GluN1 a GluN3A obsahují každá 12 předpokládaných *N*-glykosylačních konsenzuálních míst (*N*-X-S/T) (Skrenkova et

al., 2018); naproti tomu podjednotka GluN3B obsahuje 6 předpokládaných *N*-glykosylačních konsenzuálních míst (obr. 6B). V rámci těchto experimentů jsme kombinovali elektrofyziologii se systémem rychlé výměny roztoků, v němž jsme aplikovali široké rozmezí koncentrací glycinu (od 10 μM do 10 mM) na buňky HEK293 transfekované nemutovanou nebo mutovanou (N→Q) formou receptorů GluN1/GluN3. Nezaznamenali jsme žádný rozdíl mezi nemutovanými a mutovanými receptory GluN1/GluN3A, pokud jde o normalizovanou amplitudu vrcholového proudu nebo τ_w desenzitizace měřenou v reakci na různé koncentrace glycinu, avšak pozorovali jsme rozdíly ve funkčních vlastnostech mezi nemutovanými a mutovanými receptory GluN1/GluN3B. Vzhledem k tomu, že receptory GluN1/GluN3B produkují na konci aplikace glycinu velký chvostový proud (Smothers a Woodward, 2009), měřili jsme poměr amplitudy proudu v ustáleném stavu k amplitudě vrcholového proudu (ss/p) a také poměr amplitudy vrcholového chvostového proudu k proudu v ustáleném stavu (t/ss) GluN1/GluN3B WT a GluN1/GluN3B, které postrádají sady tripletů i jednotlivá předpokládaná *N*-glykosylační místa. Naše analýza odhalila, že poměr t/ss se zvýšil u receptorů GluN1-N440Q/GluN3B, GluN1-4/4N→Q/GluN3B a GluN1-N674Q/GluN3B, ale u ostatních testovaných receptorů GluN1/GluN3B se nezměnil (obr. 6C).

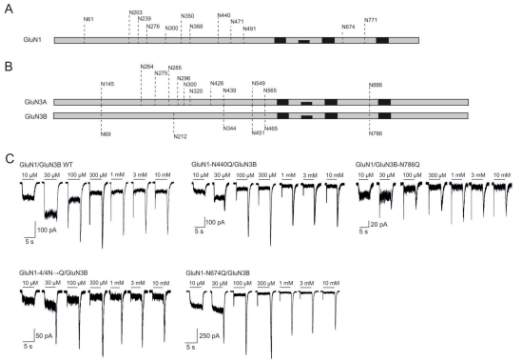

Obrázek 6. Přehled předpokládaných *N*-glykosylačních míst v podjednotkách GluN1, GluN3A a GluN3B. (A-B) Schéma znázorňující přibližnou polohu 12 předpokládaných *N*-glykosylačních konsenzuálních míst (*N*-X-S/T) v podjednotkách GluN1 (A) a GluN3A (B) a 6 předpokládaných *N*-glykosylačních konsenzuálních míst v podjednotce GluN3B (B); čtyři plná černá pole v každé podjednotce označují transmembránové domény. (C) Reprezentativní záznamy měření v HEK293 buňkách transfekovaných uvedenými receptory GluN1/GluN3B. Proudy byly vyvolány aplikací uvedených koncentrací glycinu (vyznačeno vodorovnými černými čarami).

Dále jsme zkoumali vliv lektinů na funkční vlastnosti receptorů GluN1/GluN3B. Buňky HEK293 exprimující receptory GluN1/GluN3B jsme inkubovali po dobu 8 min každým lektinem v koncentraci 200 µg/ml a poté jsme měřili

vlastnosti glycinem indukovaných proudů (obr. 7A). Naše analýza ukázala, že 14 z 19 testovaných lektinů významně snížilo poměr t/ss měřený u receptorů GluN1/GluN3B (obr. 7B). Poté jsme se zaměřili na analýzu concanavalin A ConA, WGA a AAL a zjistili jsme, že všechny tři lektiny významně zvýšily jak poměr ss/p (obr. 7C), tak i 10-90% dobu náběhu glycinem indukovaných proudů (obr. 7D) receptorů GluN1/GluN3B. Zjistili jsme také, že 20 µg/ml ConA, WGA a AAL stačí ke snížení poměru t/ss ve stejné míře jako 200 µg/ml (obr. 7E; k porovnání s obr. 7B).

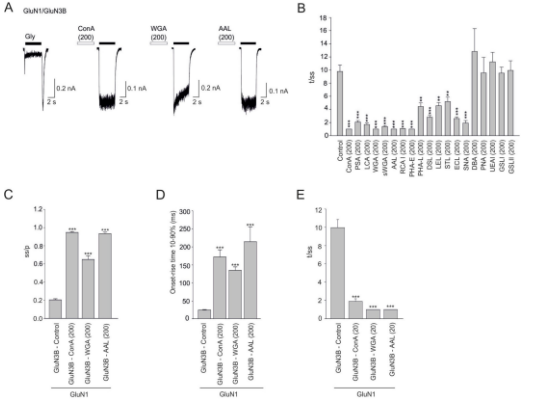

Obrázek 7. Receptory GluN1/GluN3B jsou modulovány specifickými lektiny. (A) Reprezentativní záznamy měření v HEK293 buňkách exprimujících receptory GluN1/GluN3B, aktivovaných 5 sekundovou aplikací 500 µM glycinu (vyznačeno černým pruhem). Tam, kde je uvedeno, byly

buňky předem inkubovány s 200 μg/ml ConA, WGA nebo AAL po dobu 8 min (označeno bílými sloupci, bez měřítka). (B) Souhrn poměru t/ss měřeného pro receptory GluN1/GluN3B; kde je uvedeno, byly buňky předem inkubovány s 200 μg/ml uvedených lektinů (n≥5 buněk/skupina). (C-E) Poměr ss/p, doba náběhu 10-90 % a poměr t/ss byly měřeny během 5 sekundové aplikace 500 μM glycinu v buňkách exprimujících receptory GluN1/GluN3B; kde je uvedeno, byly buňky předem inkubovány s 200 μg/ml (C a D) nebo 20 μg/ml (E) ConA, WGA nebo AAL (n ≥ 5 buněk/skupina). **p < 0,01, ***p < 0,001 oproti buňkám inkubovaným s kontrolní látkou (jednosměrná ANOVA).

Dále jsme zkoumali, zda je účinek lektinů na receptory GluN1/GluN3B závislý na konformaci. Měřili jsme proto proudy indukované glycinem před a po 1 minutové aplikaci 20 μg/ml ConA, WGA nebo AAL a analyzovali poměr p_2/p_1 receptorů GluN1/GluN3B (obr. 8A-B). Naše analýza ukázala, že všechny tři lektiny významně zvýšily poměr p_2/p_1 receptorů GluN1/GluN3B (obr. 8B). Zajímavé je, že ve srovnání s WT receptory jsme pozorovali výrazně nižší účinek AAL u receptorů obsahujících podjednotku GluN3B-N465Q (obr. 8A, B), což podporuje domněnku, že N465 v podjednotce GluN3B hraje roli ve schopnosti AAL modulovat funkční vlastnosti receptorů GluN1/GluN3B. Naproti tomu při aplikaci lektinů v kontinuální přítomnosti 500 μM glycinu jsme nepozorovali žádný nebo jen nepatrný účinek (obr. 8C); zdá se tedy, že schopnost lektinů modulovat receptory

GluN1/GluN3B je závislá na konformaci, podobně jako v případě receptorů GluN1/GluN3A.

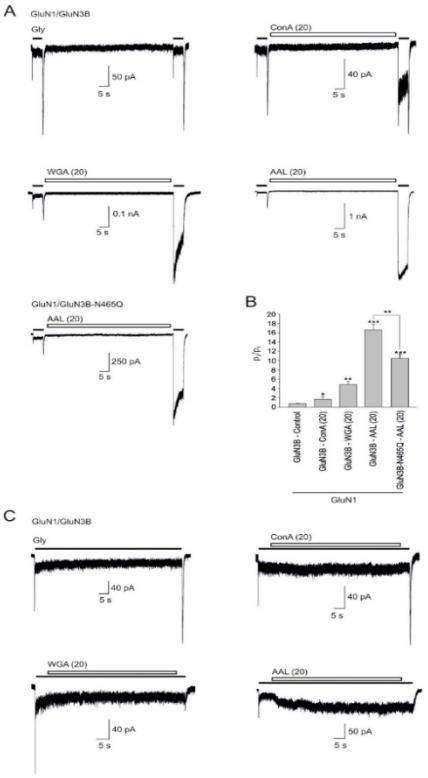

Obrázek 8. Zkoumání mechanismu působení vybraných lektinů na receptory GluN1/GluN3B. (A) Reprezentativní záznamy měření v HEK293 buňkách exprimujících receptory GluN1/GluN3B byly vyvolány 5 sekundovým pulzem 500 μM glycinu (vyznačeno černým pruhem) před a po 1 minutové aplikaci 20 μg/ml ConA, WGA nebo AAL. (B) Souhrn p_2/p_1 snímání z HEK293 buněk exprimujících buď GluN1/GluN3B WT, nebo GluN1/GluN3B-N465Q receptory; kde je uvedeno, bylo mezi dvěma pulzy glycinu aplikováno 20 μg/ml ConA, WGA nebo AAL ($n \geq 5$ buněk/skupinu). (C) Reprezentativní proudy z celé buňky přes receptory GluN1/GluN3B vyvolané aplikací 500 μM glycinu (označeno černým pruhem); kde je uvedeno, bylo aplikováno 20 μg/ml ConA, WGA nebo AAL po dobu 1 minuty v kontinuální přítomnosti glycinu. Pouze AAL měl mírný zesilující účinek, s průměrným zvýšením amplitudy ustáleného proudu o 310 ± 60 % ($n = 5$) na konci 1 minutové aplikace AAL. *$p < 0,05$, **$p < 0,01$, ***$p < 0,001$ oproti buňkám ošetřeným kontrolní skupinou nebo mezi jednotlivými skupinami (ANOVA).

6. Diskuse

6.1. Tři patogenní mutace v doméně M3 podjednotky GluN1 regulují povrchovou expresi a farmakologickou citlivost NMDAR

Zaměřili jsme se na tři patogenní mutace v doméně M3 podjednotky GluN1 – M641I, A645S a Y647S – spojované s mentálním postižením, pohybovými poruchami a epileptickými záchvaty (Lemke et al., 2016). Ukázali jsme, že tyto mutace ovlivňují povrchovou expresi NMDAR v buňkách HEK293 v závislosti na podjednotce - konkrétně mutace

GluN1-M641I významně snižuje povrchovou expresi receptorů GluN1/GluN2A, ale nikoli receptorů GluN1/GluN2B nebo GluN1/GluN3A, mutace GluN1-Y647S snižuje povrchovou expresi receptorů GluN1/GluN2A a GluN1/GluN2B, ale nikoli receptorů GluN1/GluN3A, a mutace GluN1-A645S neovlivnila úroveň povrchové exprese, ať už byla exprimována společně s podjednotkou GluN2A, GluN2B nebo GluN3A. Naše mikroskopická data získaná z hipokampálních neuronů (DIV14) navíc prokázala stejné změny v povrchové expresi, jaké byly pozorovány v HEK293 buňkách v případě společné exprese mutované podjednotky GluN1 s podjednotkou GluN2A. Tyto výsledky jsou v souladu s tím, že hipokampální neurony mají nízkou expresi endogenní podjednotky GluN3 a vysokou expresi podjednotky GluN2A (Hansen et al., 2021; Henson et al., 2010; Paoletti et al., 2013; Vieira et al., 2020). Dále bylo prokázáno, že *de novo* mutace GluN1-G620R – spojovaná s opožděním vývoje a poruchami chování – snižuje povrchovou expresi receptorů GluN1/GluN2B, ale nikoli receptorů GluN1/GluN2A (Chen et al., 2017).

Dále naše skupina již dříve prokázala, že specifické aminokyselinové zbytky v doméně M3 podjednotek GluN1 a GluN2 (GluN1-W636, GluN2A-W634, GluN2B-W635) přispívají k regulaci přenosu NMDAR na povrch buněk (Kaniakova et al., 2012). Patogenní mutace GluN2B-W607C a GluN2B-S628F v TMD – spojované s mentálním postižením a opožděným vývojem – navíc snižují povrchovou expresi

NMDAR a také citlivost NMDAR na inhibici Mg^{2+} (Vyklický et al., 2018). V dalším experimentu jsme také pozorovali změny funkčních vlastností receptoru, konkrétně jsme zjistili, že hodnota EC_{50} pro glycin je u receptorů GluN1-M641I/GluN3A zvýšená ve srovnání s WT GluN1/GluN3A, a dále že receptory GluN1-A645S/GluN3A mají pomalejší τ_w desenzitizace. Změny v desenzitizaci jsou v souladu s důkazy, že mutace v TMD, včetně motivu SYTANLAAF, mění proudovou kinetiku receptoru GluN1/GluN2A (Hu a Zheng, 2005). Ačkoli jsme zjistili, že mutace GluN1-Y647S nemění expresi receptorů GluN1/GluN3A, naše elektrofyziologické experimenty neodhalily žádný proud indukovaný glycinem, pokud nebyla provedena aplikace CGP-78608 (Grand et al., 2018). Proto předpokládáme, že mutace GluN1-Y647S pravděpodobně mění specifické funkční vlastnosti receptorů GluN1/GluN3A, jako je míra otevření iontového kanálu. Tuto domněnku však nemůžeme testovat, protože na rozdíl od možnosti blokace receptorů GluN1/GluN2 blokátorem otevřeného kanálu MK-801 v současné době neexistuje žádný specifický blokátor pro receptory GluN1/GluN3A (Chatterton et al., 2002).

Snížení citlivosti na agonisty a/nebo antagonisty bylo zaznamenáno také u dalších patogenních mutací, jako je GluN2B-N615I, nacházející se na začátku linkeru M2-M3, a GluN2B-V618G, která se nacházíse v linkeru M2-M3 a která je spojována s Westovým syndromem. Obě uvedené mutacesnižují citlivost NMDAR na Mg^{2+} a memantin (Fedele

et al., 2018). Výše zmíněná mutace GluN1-G620R rovněž snižuje citlivost na agonisty a inhibici Mg^{2+} (Chen et al., 2017). V naší studii jsme však nepozorovali změny v citlivosti GluN1/GluN2 receptorů na Mg^{2+} u žádné ze zkoumaných mutací. Nicméně jsme pozorovali, že mutace GluN1-A645S snižuje citlivost receptorů GluN1/GluN2 na memantin v nepřítomnosti extracelulárního Mg^{2+}, což je v souladu s předchozími výsledky získanými pomocí oocytů Xenopus exprimujících receptory GluN1/GluN2B (Kashiwagi et al., 2002). Zjistili jsme, že v přítomnosti fyziologické koncentrace Mg^{2+} se hodnota IC_{50} pro memantin snížila pro receptory GluN1-M641I/GluN2A, ale zvýšila se pro receptory GluN1-A645S/GluN2A ve srovnání s receptory WT GluN1/GluN2A. Podobné výsledky jsme získali při měření receptorů skládajících se z těchto mutovaných GluN1 podjednotek exprimovaných v hipokampálních neuronech, navíc naše analýza NMDA indukované excitotoxicity v hipokampálních neuronech toto zjištění rovněž potvrdila. Konkrétně memantin značně snižoval excitotoxicitu neuronů exprimujících podjednotku GluN1-M641I, ale byl významně méně neuroprotektivní u neuronů exprimujících podjednotku GluN1-A645S ve srovnání s neurony exprimujícími podjednotku WT GluN1.

Dále jsme zjistili, že mutace M641I-GluN1 a A645S-GluN1 odlišně ovlivňují kinetiku nástupu (τon) a posunu (τoff) inhibice memantinem a také schopnost memantinu vyvolat SSI u NMDAR. Konkrétně jsme zjistili, že τoff inhibice

memantinem je pomalejší u receptorů GluN1-M641I/GluN2A a rychlejší u receptorů GluN1-A645S/GluN2A v nepřítomnosti a přítomnosti Mg^{2+} ve srovnání s receptory WT GluN1/GluN2A. Předchozí studie zjistily, že pomalá složka τoff (τslow) představuje odvázání memantinu z jeho druhého nízkoafinitního vazebného místa na receptoru GluN1/GluN2 (Glasgow et al., 2018). Když jsme se tedy zaměřili na τslow, získali jsme zvýšené hodnoty pro receptory GluN1-M641I/GluN2A a snížené hodnoty pro receptory GluN1-A645S/GluN2A ve srovnání s receptory WT GluN1/GluN2A za všech testovaných experimentálních podmínek. Tato data naznačují, že tyto dvě patogenní mutace v doméně M3 podjednotky GluN1 rozdílně ovlivňují kinetiku vazby i rozvázání memantinu a mohou případně ovlivnit SSI memantinu nebo, na základě nedávných studií, ovlivnit přenos memantinu z membrány na kanál (Wilcox et al., 2022). Souhrnně naše data naznačují, že specifické patogenní mutace v doméně M3 podjednotky GluN1 rozdílně ovlivňují farmakologickou citlivost a povrchovou expresiNMDAR.

6.2. Přítomnost předpokládaných *N*-glykosylačních míst a jejich interakce se specifickými lektiny reguluje funkční vlastnosti receptorů GluN1/GluN3

Zaměřili jsme se na studium role specifických N-glykanů podjednotek GluN1, GluN3A a GluN3B v regulaci funkčních vlastností NMDAR a také na roli různých lektinů v modulaci receptorů GluN1/GluN3A. Již dříve bylo zjištěno, že

inhibice glykosylace NMDAR tunikamycinem snižuje EC_{50} pro glutamát GluN1/GluN2B receptorů (Everts et al., 1997), stejně jako EC_{50} pro NMDA nativních NMDAR (Lichnerova et al., 2015). Bylo také prokázáno, že N-glykosylační místa v podjednotce GluN1 jsou nutná pro uvolnění NMDAR z ER (Skrenkova et al., 2018). Zde jsme ukázali, že narušení předpokládaných N-glykosylačních míst v podjednotkách GluN1 nebo GluN3A nemá vliv na desenzitizaci receptorů GluN1/GluN3A nezávisle na koncentraci glycinu. Toto pozorování je v souladu s naším předchozím zjištěním, že mutovaná N-glykosylační místa nemění váženou časovou konstantu (τw) desenzitizace pro receptory GluN1/GluN3A v reakci na 500 μM glycin (Skrenkova et al., 2018). Naproti tomu jsme zjistili, že mutované aminokyselinové zbytky N440 a N674 v podjednotce GluN1 a N786 v podjednotce GluN3B mění funkční vlastnosti receptorů GluN1/GluN3B. V našich předchozích studiích jsme ukázali, že 11 z 12 N-glykosylačních míst v podjednotce GluN1 je modifikováno glykany, ale aminokyselinový zbytek N674 glykosylovaný není (Kaniakova et al., 2016). Předpokládáme tedy, že glykosylace N440 reguluje desenzitizační vlastnosti receptorů GluN1/GluN3B, zatímco pozorované změny u mutovaného zbytku N674 jsou způsobeny strukturní změnou v LBD podjednotky GluN1. Pokud jde o aminokyselinový zbytek N786 v podjednotce GluN3B, v současné době není známo, zda je toto místo v rekombinantní podjednotce GluN3B glykosylováno. Vzhledem k tomu, že jsme pozorovali změny

v amplitudě proudu "ocasu" receptorů GluN1/GluN3B s mutovaným zbytkem N786, předpokládáme, že glykosylace na tomto zbytku mění aktivaci receptorů GluN1/GluN3B spíše změnou LBD v podjednotce GluN3B, než ovlivněním kinetiky desenzitizace prostřednictvím LBD podjednotky GluN1.

Již dříve jsme prokázali silnou asociaci NMDAR obsahujících GluN3A s četnými lektiny, jako jsou ConA, WGA a AAL, které jsou selektivní především pro manózové zbytky, N-acetylglukosaminové zbytky a fukózové zbytky. Navíc naše předchozí biochemická data naznačují, že v NMDAR obsahujících GluN3A se vyskytuje široká škála glykanových struktur (Kaniakova et al., 2016). Zde jsme tato zjištění doplnili tím, že jsme ukázali, že lektiny modulují funkční vlastnosti receptorů GluN1/GluN3. Vzhledem k tomu, že 14 z 19 testovaných lektinů významně zpomalilo τ_w desenzitizace a změnilo amplitudu píku, předpokládali jsme, že tento modulační účinek je zprostředkován snížením kinetiky desenzitizace. Skutečně, po zavedení mutací do podjednotky GluN1, které ji činí necitlivou na glycin až do 30 mM (Kvist Trine, Greenwood Jeremy, 2013), jsme po aplikaci lektinů nepozorovali žádné změny. Tyto výsledky potvrdily naši hypotézu, že lektiny modulují desenzitizaci receptorů, a jsou v souladu s předchozími zjištěními, že lektin ConA snižuje desenzitizaci u AMPAR a KAR, ačkoli nemá výrazný vliv na receptory GluN1/GluN2 (Everts et al., 1997; M. L. Mayer a Vyklicky, 1989).

Je zajímavé, že nejsilnější modulační účinek na receptory GluN1/GluN3A a GluN1/GluN3B jsme pozorovali u AAL, avšak receptory obsahující záměnu v místě N565 podjednotky GluN3A a místě N465 podjednotky GluN3B vykazovaly podobnou citlivost na AAL jako WT GluN1/GluN3 na ConA a WGA. Toto pozorování naznačuje, že zbytek N565 v podjednotce GluN3A a jeho homologní zbytek N465 v podjednotce GluN3B se podílejí na zesílení modulačního účinku AAL, což lze vysvětlit vyšší specifitou nebo afinitou AAL k různým glykanům ve srovnání s WGA nebo ConA (Dam a Fred Brewer, 2009; Moremen a kol., 2014). Dále jsme pozorovali, že aplikace ConA, WGA nebo AAL v trvalé přítomnosti glycinu neměla prakticky žádný vliv na desenzitizaci receptorů GluN1/GluN3A nebo GluN1/GluN3B; toto zjištění je v souladu s výsledkem dřívější studie, že snížení desenzitizace KAR vyvolané ConA je proces závislý na konformaci (Everts a kol., 1999). Celkově naše data odhalují nové informace o úloze N-glykanů při regulaci funkčních vlastností receptorů GluN1/GluN3 v savčích buňkách a poskytují nové poznatky o lektinech jako nástroji pro modulaci nekonvenčních NMDAR.

7. Závěr

Správná regulace fungování a povrchové exprese NMDAR je klíčová pro fyziologický synaptický přenos, učení a paměť a tato regulace probíhá na více úrovních. V této disertační práci jsme se zaměřili především na studium role

integrity ATD a TMD v regulaci funkčních vlastností různých NMDAR. Pomocí elektrofyziologických technik jsme prokázali předpokládanou roli N-glykosylačních míst a různých lektinů v regulaci funkčních vlastností receptorů GluN1/GluN3. Ukázali jsme, že lektiny ovlivňují funkční vlastnosti receptorů GluN1/GluN3, a to pravděpodobně snížením desenzitizace. Ukázali jsme také, že integrita LBD podjednotek GluN1 a GluN3A je klíčová pro správnou funkci a transport NMDAR na povrch buněk. V neposlední řadě jsme poskytli nové informace o třech dříve identifikovaných patogenních mutacích v doméně M3 podjednotky GluN1 z hlediska jejich vlivu na funkční a farmakologické vlastnosti různých podtypů NMDAR. Tyto informace mohou být využity pro další pochopení úlohy různých NMDAR jak za fyziologických podmínek, tak při rozvoji různých neurodegenerativních onemocnění.

8. Použitá literatura

Amin, J. B., Gochman, A., He, M., Certain, N., & Wollmuth, L. P. (2021). NMDA Receptors Require Multiple Pre-opening Gating Steps for Efficient Synaptic Activity. Neuron, 109(3): 488-501.

Ataman, Z. A., Gakhar, L., Sorensen, B. R., Hell, J. W., & Shea, M. A. (2007). The NMDA Receptor NR1 C1 Region Bound to Calmodulin: Structural Insights into Functional Differences between Homologous Domains. Structure, 15(12): 1603–1617.

Chatterton, J. E., Awobuluyi, M., Premkumar, L. S., Takahashi, H., Talantova, M., Shin, Y., Cul, J., Tu, S., Sevarino, K. A., Nakanishi, N., Tong, G., Lipton, S. A., & Zhang, D. (2002). Excitatory glycine receptors containing the NR3 family of NMDA receptor subunits. Nature, 415(6873): 793–798.

Chen, W., Shieh, C., Swanger, S. A., Tankovic, A., Au, M., McGuire, M., Tagliati, M., Graham, J. M., Madan-Khetarpal, S., Traynelis, S. F., Yuan, H., & Pierson, T. M. (2017). GRIN1 mutation associated with intellectual disability alters NMDA receptor trafficking and function. Journal of Human Genetics, 62(6): 589–597.

Dam, T. K., & Fred Brewer, C. (2009). Lectins as pattern recognition molecules: The effects of epitope density in innate immunity. Glycobiology, 20(3): 270–279.

Everts, I., Petroski, R., Kizelsztein, P., Teichberg, V. I., Heinemann, S. F., & Hollmann, M. (1999). Lectin-induced inhibition of desensitization of the kainate receptor GluR6 depends on the activation state and can be mediated by a single native or ectopic N-linked carbohydrate side chain. Journal of Neuroscience, 19(3): 916–927.

Everts, I., Villmann, C., Hollmann, M. (1997). N-

glycosylation is not a prerequisite for glutamate receptor function but is essential for lectin modulation. Molecular Pharmacology, 52(5): 861–873.

Fedele, L., Newcombe, J., Topf, M., Gibb, A., Harvey, R. J., & Smart, T. G. (2018). Disease-associated missense mutations in GluN2B subunit alter NMDA receptor ligand binding and ion channel properties. Nature Communications, 9(1). Furukawa, H., & Gouaux, E. (2003). Mechanisms of activation, inhibition and specificity: Crystal structures of the NMDA receptor NR1 ligand-binding core. EMBO Journal, 22(12): 2873–2885.

Furukawa, K. (2014). Crystal structure of a heterotetrameric NMDA receptor ion channel. Scienc, 344(6187): 992–997.

Glasgow, G. N., Madeleine, R. W., Johnsona, J.W., (2019). Effects of Mg^{2+} on recovery of NMDA receptors from inhibition by memantine and ketamine reveal properties of a second site. Physiology & Behavior, 176(3): 139–148.

Grand, T., Abi Gerges, S., David, M., Diana, M. A., Paoletti, P. (2018). Unmasking GluN1/GluN3A excitatory glycine NMDA receptors. Nature Communications, 9(1).

Hatton, C. J., & Paoletti, P. (2005). Modulation of triheteromeric NMDA receptors by N-terminal domain ligands. Neuron, 46(2): 261–274.

Henson, M. A., Roberts, A. C., Pérez-Otaño, I., & Philpot, B. D. (2010). Influence of the NR3A subunit on NMDA receptor functions. Progress in Neurobiology, 91(1): 23–37.

Hu, B., & Zheng, F. (2005). Differential effects on current kinetics by point mutations in the lurcher motif of NR1/NR2A receptors. Journal of Pharmacology and Experimental Therapeutics, 312(3), 899–904.

Huettner, J. E. (2015). Glutamate receptor pores. Journal of Physiology, 593(1): 49–59.

Johansen Amin, Aaron Gochman, Miaomiao He, Certain, N., & Wollmuth, L. P. (2021). NMDA receptors require multiple pre-opening gating steps for efficient synaptic activity. Physiology & Behavior, 109(3): 488–501.

Johnson, J. W. (2019). Effects of Mg^{2+} on recovery of NMDA receptors from inhibition by memantine and ketamine reveal properties of a second site. *Physiology and Behavior* 176, 139–148.

Kaniakova, M., Krausova, B., Vyklicky, V., Korinek, M., Lichnerova, K., Vyklicky, L., & Horak, M. (2012). Key amino acid residues within the third membrane domains of NR1 and NR2 subunits contribute to the regulation of the surface delivery of N-methyl-D-aspartate receptors. Journal of Biological Chemistry, 287(31): 26423–26434.

Kaniakova, M., Lichnerova, K., Skrenkova, K., Vyklicky, L., & Horak, M. (2016). Biochemical and electrophysiological characterization of N-glycans on NMDA receptor subunits. Journal of Neurochemistry, 546–556.

Kashiwagi, K., Masuko, T., Nguyen, C. D., Kuno, T., Tanaka, I., Igarashi, K., & Williams, K. (2002). Channel blockers acting at N-methyl-D-aspartate receptors: Differential effects of mutations in the vestibule and ion channel pore. Molecular Pharmacology, 61(3): 533–545.

Kotermanski, Sh. E., Johnson, J. W. (2009). Mg^{2+} imparts NMDA receptor subtype selectivity to the Alzheimer's drug memantine. Journal of Neuroscience, 29(9):2774-2779

Kvist Trine, Greenwood Jeremy, H. K. (2013). Structure-based discovery of antagonists for GluN3-containing N-methyl-D-aspartate receptors. Neuropharmacology,

23(1): 1–7.
Lee, C. H., Lü, W., Michel, J. C., Goehring, A., Du, J., Song, X., & Gouaux, E. (2014). NMDA receptor structures reveal subunit arrangement and pore architecture. Nature, 511(7508): 191–197.
Lemke, J. R., Geider, K., Helbig, K. L., Heyne, H. O., Schütz, H., Hentschel, J., Courage, C., Depienne, C., Nava, C., Heron, D., Møller, R. S., Hjalgrim, H., Lal, D., Neubauer, B. A., Nürnberg, P., Thiele, H., Kurlemann, G., Arnold, G. L., Bhambhani, V., Syrbe, S. (2016). Delineating the GRIN1 phenotypic spectrum: A distinct genetic NMDA receptor encephalopathy. Neurology, 86(23): 2171–2178.
Li, Z., Liang, D., & Chen, L. (2008). Receptor Ion Channels. Assay And Drug Development Technologies, 6(2): 298–487.
Lichnerova, K., Kaniakova, M., Park, S. P., Skrenkova, K., Wang, Y. X., Petralia, R. S., Suh, Y. H., & Horak, M. (2015). Two N-glycosylation sites in the GluN1 subunit are essential for releasing N-methyl-D-aspartate (NMDA) receptors from the endoplasmic reticulum. Journal of Biological Chemistry, 290(30), 18379–18390.
Mayer, M. L., & Vyklicky, L. (1989). Concanavalin A selectively reduces desensitization of mammalian neuronal quisqualate receptors. Proceedings of the National Academy of Sciences of the United States of America, 86(4): 1411–1415.
Meddows, E., Le Bourdellès, B., Grimwood, S., Wafford, K., Sandhu, S., Whiting, P., & McIlhinney, R. A. J. (2001). Identification of Molecular Determinants That Are Important in the Assembly of N-Methyl-D-aspartate Receptors. Journal of Biological Chemistry, 276(22): 18795–18803.
Moremen, K. W., Tiemeyer, M., Nairn, A. V.

(2012)Vertebrate protein glycosylation: diversity, synthesis and function. Nature Reviews Molecular Cell Biology, 13(7): 448-62.

Paoletti, P., Bellone, C., & Zhou, Q. (2013). NMDA receptor subunit diversity: Impact on receptor properties, synaptic plasticity and disease. Nature Reviews Neuroscience, 14(6): 383-400

Sanz-Clemente, A., Nicoll, R. A., & Roche, K. W. (2013). Diversity in NMDA receptor composition: Many regulators, many consequences. Neuroscientist, 19(1): 62-75.

Skrenkova, K., Lee, S., Lichnerova, K., Kaniakova, M., Hansikova, H., Zapotocky, M., Suh, Y. H., & Horak, M. (2018). N-glycosylation regulates the trafficking and surface mobility of GluN3A-containing NMDA receptors. Frontiers in Molecular Neuroscience,11: 188.

Smothers, C. T., Woodward, J. J., (2009). Expression of glycine-activated diheteromeric NR1/NR3 receptors in human embryonic kidney 293 cells Is NR1 splice variant-dependent. Journal of Pharmacology and Experimental Therapeutics, (3): 975-84.

Traynelis, S. F., Wollmuth, L. P., McBain, C. J., Menniti, F. S., Vance, K. M., Ogden, K. K., Hansen, K. B., Yuan, H., Myers, S. J., & Dingledine, R. (2010). Glutamate receptor ion channels: Structure, regulation, and function. Pharmacological Reviews, 62(3): 405–496

Vieira, M., Yong, X. L. H., Roche, K. W., Anggono, V. (2020). Regulation of NMDA glutamate receptor functions by the GluN2 subunits. Journal of Neurochemistry, 154(2): 121-143.

Vyklicky, V., Krausova, B., Cerny, J., Ladislav, M., Smejkalova, T., Kysilov, B., Korinek, M., Danacikova, S., Horak, M., Chodounska, H., Kudova, E., & Vyklicky, L. (2018). Surface expression, function, and

pharmacology of disease-associated mutations in the membrane domain of the human GluN2B subunit. Frontiers in Molecular Neuroscience, 11: 110.

Warnet, X. L., Bakke KroWarnet, X. L., Bakke Krog, H., Sevillano-Quispe, O. G., Poulsen, H., & Kjaergaard, M. (2020). The C-terminal domains of the NMDA receptor: How intrinsically disordered tails affect signalling, plasticity and disease. European Journal of Neuroscience, 54(8):6713-6739

Wilcox, M. R., Nigam, A., Glasgow, N. G., Narangoda, C., Phillips, M. B., Patel, D. S., Mesbahi-vasey, S., Turcu, A. L., Vázquez, S., Kurnikova, M. G., Johnson, J. W. (2022). Inhibition of NMDA receptors through a membrane-to-channel path. Nature Communications, 13(1): 4114

Wollmuth, L. P., & Sobolevsky, A. I. (2004). Structure and gating of the glutamate receptor ion channel. Trends in Neurosciences. 27: 321– 328

9. Seznam publikací

9.1. Publikace *in extenso*, související s touto dizertační prací

1. Marharyta Kolcheva, Stepan Kortus, Barbora Hrcka Krausova, Petra Barackova, Anna Misiachna, Sarka Danacikova, Martina Kaniakova, Katarina Hemelikova, Matej Hotovec, Kristyna Rehakova, Martin Horak (2021) Specific pathogenic mutations in the M3 domain of the GluN1 subunit regulate the surface delivery and pharmacological sensitivity of NMDA receptors. *Neuropharmacology*, 189:108528. IF= 5.25 (2021/2022).

2. Katarina Hemelikova*****, **Marharyta Kolcheva***, Kristyna Skrenkova, Martina Kanikova, Martin Horak (2019) Lectins modulate the functional properties of GluN1/GluN3A – containg receptors. *Neuropharmacology*, 157:107671. IF= 5.25 (2021/2022).

3. Kristyna Skrenkova, Katarina Hemelikova, Marharyta Kolcheva, Stepan Kortus, Martina Kaniakova, Barbora Krausova, Martin Horak (2019) Structural features in the glycine-binding sites of the GluN1 and GluN3A subunits regulate the surface delivery of NMDA receptors. *Scientific Reports*, 9(1):12303. IF=4.996 (2021/2022).

4. Kristyna Skrenkova, Jae-man Song, Stepan Kortus, **Marharyta Kolcheva**, Jakub Netolicky, Katarina Hemelikova, Martina Kaniakova, Barbora Hrcka Krausova, Tomas Kucera, Jan Korabecny, Young Ho Suh, Martin Horak (2020) The pathogenic S688Y mutation in the ligand-binding

domain of the GluN1 subunit regulates the properties of NMDA receptors. *Scientific Reports*, 10:18576. IF=4.996 (2021/2022).

** co-first authorship*

9.2. Publikace nesouvisející s touto dizertační prací

1. Jan Konecny, Anna Misiachna, Martina Hrabinova, Lenka Pulkrabkova, Marketa Benkova, Lukas Prchal, Tomas Kucera, Tereza Kobrlova, Vladimir Finger, **Marharyta Kolcheva**, Stepan Kortus, Daniel Jun, Marian Valko, Martin Horak, Ondrej Soukup, Jan Korabecny (2020) Pursuing the Complexity of Alzheimer's Disease: Discovery of Fluoren-9-Amines as Selective Butyrylcholinesterase Inhibitors and N-Methyl-d-Aspartate Receptor Antagonists. *Biomolecules*, 11(1):3. IF=4.569 (2021/2022).

2. Lukas Gorecki, Anna Misiachna, Jiri Damborsky, Rafael Dolezal, Jan Korabecny, Lada Cejkova, Kristina Hakenova, Marketa Chvojkova, Jana Zdarova Karasova, Lukas Prchal, Martin Novak, **Marharyta Kolcheva**, Stepan Kortus, Karel Vales, Martin Horak, Ondrej Soukup (2021) Structure-activity relationships of dually-acting acetylcholinesterase inhibitors derived from tacrine on N-methyl-d-Aspartate receptors. *European Journal of Medicinal Chemistry*, 219:113434. IF=6.514 (2021/2022)

10. Životopis

Mgr. Marharyta Kolcheva

OSOBNÍ ÚDAJE

Datum narození: 30.12.1992
Občanství: UKR
E-mail: marharyta.kolcheva@iem.cas.cz

VZDĚLÁVÁNÍ

2017 – nyní: Doktorský studijní program Fyziologie živočichů Univerzita Karlova v Praze, Přírodovědecká fakulta

2013 – 2015: Magisterský studijní program Biofyzika, vědecké centrum " Ústav biologie", Národní univerzity Tarase Ševčenka v Kyjevě

2009 – 2013: Bakalářský studijní program Biologie, vědecké centrum " Ústav biologie", Národní univerzity Tarase Ševčenka v Kyjevě

PRACOVNÍ ZKUŠENOSTI

2017 – nyní: Fyziologický ústav AV ČR

Laboratoř buněčné neurofyziologie

2017 – nyní: Ústav experimentální medicíny AV ČR

oddělení Neurochemie

LABORATORNÍ DOVEDNOSTI

− příprava a kultivace lidských embryonálních ledvinných buněk 293 (HEK293) a embryonálních hipokampálních neuronů
− transfekce kultivovaných buněk HEK293
− elektrofyziologická měření pomocí techniky patch-clamp

− mutageneze řízená místem, mutageneze řízená více místy
− NMDA indukovaná excitotoxicita
− imunofluorescenční mikroskopie - povrchové a celkové barvení, pořízení obrazu a zpracování analýzy

KONFERENCE

Regionální schůze FENS 2019 Bělehrad, Srbsko
Fórum FENS 2022 Paříž, Francie

Charles University
Faculty of Science
Department of Animal Physiology

Mgr. Kolcheva Marharyta

Ph.D. thesis summary:

Functional and pharmacological properties of GluN1/GluN2 and GluN1/GluN3 subtypes of NMDA receptors

Supervisor

Mgr. Martin Horak, Ph.D

Prague 2022

Doctoral Study programs in Biomedicine
Charles University
and The Czech Academy of Sciences

Study programme: Animal physiology

Chairman of the Sector Board: doc. RNDr. Jiří Novotný, DSc

Institute and Department:

Institute of Physiology, CAS
Department of Cellular
Neurophysiology

Institute of Experimental
Medicine, CAS
Department of Neurochemistry

Author: Mgr. Marharyta Kolcheva
Supervisor: Mgr. Martin Horak, Ph.D.

The Ph.D. Thesis is available in the library of the Faculty of Science, Charles University.

Contents

1. Abstract 60

2. Introduction 61

3. Hypotheses and objectives 64

4. Materials and methods 65

5. Results 71

5.1. Three pathogenic mutations in the M3 domain of the GluN1 subunit regulate the surface delivery and pharmacological sensitivity of NMDARs 71
5.2. The presence of putative N-glycosylation sites and their interaction with specific lectins regulates the functional properties of GluN1/GluN3 receptors 88
6. Discussion 94

6.1. Three pathogenic mutations in the M3 domain of the GluN1 subunit regulate the surface delivery and pharmacological sensitivity of NMDARs 94
6.2. The presence of putative N-glycosylation sites and their interaction with specific lectins regulates the functional properties of GluN1/GluN3 receptors 98
7. Conclusion 101

8. References 103

9. List of publications 109

9.1. Publications *in extenso*, related to this thesis 109
9.2. Publications *in extenso*, unrelated to this thesis 110
10. Curriculum Vitae 111

1. Abstract

N-methyl-D-aspartate receptors (NMDARs) are ionotropic glutamate receptors and they play a critical role in excitatory synaptic transmission in the mammalian central nervous system (CNS). Hyperactivity or hypoactivity of NMDARs can lead to a wide spectrum of pathological conditions and psychiatric disorders, such as Alzheimer's disease, Parkinson's disease, Huntington's disease, epilepsy, schizophrenia. NMDARs form a heterotetrameric complex made up of GluN1, GluN2(A-D) and/or GluN3(A, B) subunits. Different subtypes of NMDARs could have various effects on disease pathogenesis and therefore it is crucial to investigate the specific role of each subunit in the regulation of normal NMDAR functioning. The regulation of NMDARs occurs at different levels, from early processing, including synthesis, assembly, quality control in the endoplasmic reticulum (ER), trafficking to the cell surface, to internalization, recycling, and degradation. In this dissertation, we mainly focused on determining the roles of extracellular and transmembrane regions of different subtypes of NMDARs in the regulation of their function. In particular, using electrophysiology and microscopy methods on HEK293 cells and cultured hippocampal neurons, we investigated: (i) the impact of *N*-glycosylation and different lectins on the regulation of the functional properties of GluN1/GluN3 receptors; (ii) the effects of pathogenic mutations in the transmembrane domain (TMD) of the GluN1 subunit on surface delivery, and the functional and pharmacological properties of conventional and non-conventional di-heteromeric NMDARs; (iii) the role of

glycine-binding site integrity of the GluN1 and GluN3A subunits in the trafficking and functional properties of NMDARs.

2. Introduction

N-methyl-D-aspartate receptors (NMDARs) are ionotropic glutamate receptors that play a key role in the mammalian central nervous system (CNS). Normal functioning of NMDARs is important for excitatory synaptic transmission and memory formation. However, hyperactivity or hypoactivity of NMDARs can lead to a wide range of pathological conditions and psychiatric disorders, such as Alzheimer's disease, Parkinson's disease, Huntington's disease, epilepsy, and schizophrenia (Paoletti et al., 2013; Zhou and Duan, 2018).

NMDARs are heterotetrameric complex made up of two obligatory GluN1 subunits (which has eight splicing variants), GluN2 (GluN2A to GluN2D) subunits and/or GluN3 (GluN3A and GluN3B) subunits. All GluN subunits share the same topology, including the extracellular *N*-terminal domain (NTD) formed by amino-terminal domain (ATD) and ligand-binding domain (LBD), transmembrain domane (TMD) and the intracellular C-terminal domain (CTD).

ATD is defined by the first ~ 400 amino acid residues, has a “clamshell-like” structure formed by segments R1 and R2, and contains binding sites for allosteric modulators such as ifenprodil, protons, Zn^{2+}, polyamines (H. Furukawa and Gouaux, 2003; K. Furukawa, 2014). Also, evidence suggests that ATD mediates the assembly of the initial GluN

subunit dimers in the ER (Meddows et al., 2001). ATD is linked to LBD via ATD-LBD linkers. Similar to ATD, LBD is composed of two segments – S1 and S2, which create a binding pocket for ligands (Amin et al., 2021; H. Furukawa and Gouaux, 2003; C. H. Lee et al., 2014; Paoletti et al., 2013). LBD of GluN1 and GluN3 subunits contain a glycine-binding sites while LBD of GluN2 subunits contains glutamate-binding site (Traynelis et al., 2010).

The transmembrane domain (TMD) make up of tree transmembrane α-helices (M1, M3, and M4) and the M2 loop, where the M2 loop and the M3 segment are the major pore-lining domains (Wollmuth and Sobolevsky, 2004). The M2 loop forms the narrowest part of the ion channel and is a selective filter for ions as well as a binding site for Mg^{2+} and open-channel blockers (Hatton and Paoletti, 2005; Huettner, 2015). The M3 helices form a very tight arrangement around the receptor's pore, whereas the remaining M1 and M4 helices are located more at the periphery, around the ion channel (Karakas and Furukawa, 2014; Lee et al., 2014). The M3 helix is also in contact with the short pre-M1 helix that is oriented parallel to the membrane (Lee et al., 2014; Sanz-Clemente et al., 2013; Traynelis et al., 2010). The M3 helix include a conserved amino acid SYTANLAAF motif that can be found in all types of glutamate receptors. The LBD and TMD are connected through the three short linkers, that are labeled according to their position and orientation: S1-M1, M3-S2, and S2-M4, where S indicates the LBD segment and M the transmembrane helix. M3-S2 linkers are central polypeptide chains, directly connecting S2 segments from LBD with M3

helices, forming an ion channel. S1-M1 and S2-M4 linkers are located more in the periphery and participate in gating regulation, however, their exact contribution remains unknown (K. Furukawa, 2014; Johansen Amin et al., 2021).

CTD is the most variable part of the NMDARs, the length differs considerably between subunits, from ~50 residues in the GluN1 subunit and up to 660 residues in the the GluN2B subunit. CTD plays an important role in the stabilisation and anchoring of NMDARs to the cell cytoskeleton, as it contains binding sites for many regulatory molecules (Ataman et al., 2007; Warnet et al., 2020). Interestingly, the structure of the CTD remains undefined, only some short recognition motifs have been identified in the complexes with binding partners (e.g., short Ca2+/calmodulin-binding part) (Ataman et al., 2007). The lack of structures is probably due to the fact that CTDs belong to a class of intrinsically disordered regions (IDRs) that do not contain enough hydrophobic amino acids for folding into a defined 3D structure (Wright and Dyson, 2015). However, this region can be robustly predicted based on sequence alone (Nielsen and Mulder, 2019).

Different subtypes of NMDARs could have various effects on disease pathogenesis and therefore it is crucial to investigate the specific role of each subunit in the regulation of normal functioning of NMDARs. The regulation of NMDARs occurs at different levels, from early processing, including synthesis, assembly, quality control in the endoplasmic reticulum (ER), trafficking to the cell surface, to internalization, recycling, and degradation. In this dissertation

thesis, we mainly focused on determining the roles of extracellular and transmembrane regions of different subtypes of NMDARs in the regulation of their function. In particular, using electrophysiological and microscopical methods on both HEK293 cells and cultured hippocampal neurons, we investigated: (i) the impact of *N*-glycosylation and different lectins on the regulation of the functional properties of GluN1/GluN3 receptors; (ii) the effects of pathogenic mutations in the transmembrane domain (TMD) of GluN1 subunit on surface delivery, functional and pharmacological properties of conventional and non-conventional di-heteromeric NMDARs; (iii) the role of glycine-binding site integrity of the GluN1 and GluN3A subunits in the trafficking and functional properties of NMDARs.

3. Hypotheses and objectives

1) Previous studies found that GluN1/GluN2 receptors and GluN3A-containing NMDARs are extensively *N*-glycosylated. Several types of plant lectins have been shown to bind to NMDARs and affect the functional properties of the receptors. Also, earlier studies have shown that the functional properties of di-heteromeric GluN1/GluN2 receptors and native NMDARs are less sensitive to modulation by lectins compared to AMPARs and KARs (Everts et al., 1997; M. L. Mayer and Vyklicky, 1989), however, the specific effect of lectins on the functional properties of GluN1/GluN3 receptors has not yet been fully elucidated.

Objective: to examine whether the presence of specific *N*-glycans regulates the functional properties of

GluN1/GluN3 receptors, as well as test a panel of lectins for their potential to modulate the functional properties of GluN1/GluN3 receptors.

2) Previous studies found that the range of pathogenic mutations identified in GluN subunits – including mutations surrounding the binding site for open-channel blockers – alter the surface delivery, glutamate and glycine potency, sensitivity to Mg^{2+} and memantine (Chen et al., 2017; Fedele et al., 2018; Vyklicky et al., 2018). Memantine is FDA-approved compound commonly used for the treatment of Alzheimer's disease with a complex mechanism of action, including second site inhibition (SSI) (Glasgow et al., 2018), also referred to as membrane-to-channel inhibition (MCI) (Wilcox et al., 2022). Moreover, physiological concentrations of Mg^{2+} (on the order of 1 mM) alter inhibitory effects of memantine on GluN1/GluN2 receptors and thus, are an important factor when considering the therapeutic use of memantine (Johnson, 2019).

Objective: to examined whether three previously reported pathogenic mutations in the lower region of the M3 domain in GluN1 subunit – M641I, A645S and Y647S – affect the surface delivery, functional properties, and/or pharmacological properties of NMDARs expressed in HEK293 cells and cultured rat hippocampal neurons.

4. Materials and methods

Preparation of primary hippocampal neurons

All animal procedures were performed in accordance with ARRIVE guidelines and the European Commission Council Directive 2010/63/EU for experiments on animals.

Primary cultures hippocampal neurons were prepared from 18-day-old Wistar rat embryos (Lichnerova et al., 2015). In brief: the hippocampi were dissected in a cold dissection solution consisting of Hanks' balanced salt solution supplemented with 10 mM HEPES (pH 7.4) and penicillin-streptomycin (Life Technologies), then incubated for 20 minutes at 37 °C in dissection medium. The cells were then washed, dissociated using a glass pipette, resuspended and plated at a density of $2x10^4$ cells per cm^2 on poly-*L*-lysine–coated glass coverslips in plating medium consisting of minimum essential medium (MEM) supplemented with 10% heat-inactivated horse serum, N2 supplement (1X), 1 mM sodium pyruvate, 20 mM *D*-Glucose, 25 mM HEPES and 1 % penicillin-streptomycin; after 2 h, the plating medium was replaced with Neurobasal medium supplemented with B-27 and *L*-glutamine (Thermo Fisher Scientific).

Preparation of transfected HEK293 cells

HEK293 cells were cultured in Opti-MEM (Thermo Fisher Scientific) containing 5% fetal bovine serum (Thermo Fisher Scientific) (Kaniakova et al., 2012; Lichnerova et al., 2015). For electrophysiology, HEK293 cells were grown in 24-well plates and transfected with a total of 0.9 μg of cDNA constructs encoding the GluN1/GluN2 or GluN1/GluN3 subunits and GFP (to identify successfully transfected cells) mixed with 0.9 μl MATra-A Reagent (IBA) in 50 μl Opti-MEM I; the cells were then trypsinized and grown at lower density on poly-L-lysine–coated glass coverslips. For microscopy, HEK293 cells grown in 12-well plates were

transfected with a total of 0.45 µg of cDNA constructs encoding the GluN subunits (at a 1:2 ratio of tagged:untagged subunits) mixed with 1 µl Lipofectamine 2000 reagent (Thermo Fisher Scientific) in 50 µl Opti- MEM I.

Immunofluorescence microscopy

Surface NMDARs were labelled as described previously (Kaniakova et al., 2012; Lichnerova et al., 2015). In brief: cells were washed in phosphate-buffered saline (PBS), then incubated in blocking solution – PBS with 10% normal goat serum (NGS). Then, surface NMDARs were labeled using a rabbit anti-GFP primary antibody (15 min; 1:1000; Merck) followed by an anti-rabbit secondary antibody conjugated to Alexa Fluor 647 (15 min; 1:1000; Thermo Fisher Scientific). Then, the cells were fixed in 4% paraformaldehyde (PFA) in PBS, permeabilized with 0.25% Triton X-100 in PBS, and labeled with a mouse anti-GFP primary antibody (30 min; 1:1000; Merck) followed by a goat anti-mouse secondary antibody conjugated to Alexa Fluor 488 (30 min; 1:1000; Thermo Fisher Scientific). The cells were then mounted on glass slides using ProLong Antifade reagent (Thermo Fisher Scientific).

Images were obtained at room temperature using a fluorescence microscope (Olympus Scan) with an objective 60x/1.35 oil immersion or a confocal scanning microscope (Leica TCS SP8) equipped with solid-state lasers and apochromatic objective for an oil immersion of 63x/1.30. The images obtained were analyzed using the software ImageJ (NIH). In hippocampal neurons, the surface and total

fluorescence signal intensity was analyzed in 10 µm long segments of secondary and tertiary dendrites (Lichnerova et al., 2015).

Electrophysiology

Whole-cell patch-clamp recordings were made on transfected HEK293 cells using the Axopatch 200B amplifier (Molecular Devices). Borosilicate glass patch pipettes (3–6 MΩ tip resistance) were prepared using a P-97 puller (Sutter Instruments) and filled with intracellular recording solution containing (in mM): 125 gluconic acid, 15 CsCl, 5 BAPTA, 10 HEPES, 3 MgCl2, 0.5 CaCl2 and 2 ATP-Mg salts (pH 7.2 with CsOH). The standard extracellular solution (ECS) contained (in mM): 160 NaCl, 2.5 KCl, 10 HEPES, 10 D-glucose, 0.2 EDTA, and 0.7 CaCl2 (pH 7.3 with NaOH). For measuring the IC_{50} values for Mg^{2+} and measuring currents in the presence of 1 $MgCl_2$, EDTA was omitted from the ECS. For application extracellular solutions, a multi-barrel rapid perfusion system with a time constant of solution exchange around the cell of approximately 20 ms. Unless stated otherwise, all ECSs contained 50 µM glycine. For the recording from hippocampal neurons, the ECS contained 1 µM tetrodotoxin (TTX) and 10 µM bicuculine. All electrophysiological recordings were performed at room temperature, and the reported holding potential values were corrected for the calculated liquid junction potential of approximately 14 mV (Vyklicky et al., 2018). The NMDAR activation curves for glutamate and glycine were obtained using the following equation:
Equation (1):

$$I = I_{max}/(1 + (EC_{50}/[agonist])^h),$$

where I_{max} is the maximal response, EC_{50} is the concentration eliciting the half-maximal response, [agonist] is the glutamate or glycine concentration, and h is the Hill coefficient. The NMDARs inhibition curves were obtained using the following equation:

Equation (2):

$$I = 1/(1 + ([antagonist]/IC_{50})^h),$$

where IC_{50} is the concentration of Mg^{2+} or memantine that produced 50% inhibition of the agonist-evoked current, [antagonist] is the Mg^{2+} or memantine concentration, and h is the Hill coefficient. Time course of MK-801 or memantine inhibition was analyzed using single or double exponential function, a weighted time constants (τ_w) were obtained using the following equation:

Equation (3):

$$\tau_w = (\tau_{fast}*A_{fast} + \tau_{slow}*A_{slow})/(A_{fast} + A_{slow}),$$

where τ_{fast} and A_{fast} are the time constant and area, respectively, of the fast component, and τ_{slow} and A_{slow} are the time constant and area, respectively, of the slower component; normalized A_{fast} values were obtained by dividing each value by (A_{fast} + A_{slow}).

SSI was measured as described previously (Glasgow et al., 2018). In brief, the minimum fractional response after SSI (minimum $I_{SSI}/I_{control}$) was calculated as the average $I_{SSI}/I_{control}$ value measured over a 200-ms window centered on the minimum ratio value; $I_{control}$ was calculated as the average of Icontrol1 and $I_{control2}$; responses in which the $I_{control2}/I_{control1}$ value was <0.8 were excluded from the analysis.

NMDA-induced excitotoxicity

To induce excitotoxicity, neurons at DIV14 were placed overnight in a minimal defined medium containing 10% MEM (Invitrogen) and 90% Salt-Glucose (SG) medium containing (in mM): 114 NaCl, 0.219% NaHCO3, 5.292 KCl, 1 MgCl2, 2 CaCl2, 10 HEPES, 30 glucose, 0.5 sodium pyruvate, and 0.1% phenol red (McQueen et al., 2017; Skrenkova et al., 2020). The following day, the neurons were placed in 100% SG medium containing glycine, NMDA, and memantine (Hello Bio) at the indicated concentrations. After 1 h, the medium was changed to 10% MEM and 90% SG medium, and after an additional 22–23 h, the neurons were labelled with 5 μM Hoechst 33342 (Molecular Probes) for 30 min and then fixed in 4% PFA in PBS. After the neurons were permeabilized using Triton X-100, the YFP-GluN1 subunits were labelled with mouse anti-GFP and goat anti-mouse Alexa Fluor 488 antibodies as described above.

Images (1024 × 1024 pixels with a pixel size of 1.243 μm × 1.243 μm, thus covering a field of view 1272 μm × 1272 μm in size) were acquired using an Olympus FV10i confocal microscope equipped with a 10x/0.4 NA super apochromat objective. For each field of view, three images were obtained: the YFP signal (to indicate infected cells), Hoechst (for nuclear staining), and a DIC image. Nuclear area was measured using software ImageJ (NIH), and a custom-made macro script was used to automatically measure nuclear area exclusively in infected cells identified by YFP expression. The number of cells per condition was 519–1407, 17446-24758 cells were collected in each experiment (all conditions summed). The

MATLAB (2019b) was used to classify cells as pyknotic or non-pyknotic based on the nuclear area measured for each cell.

5. Results

5.1. Three pathogenic mutations in the M3 domain of the GluN1 subunit regulate the surface delivery and pharmacological sensitivity of NMDARs

First, we asked whether three pathogenic mutations in the M3 domain of the GluN1 subunit (Lemke et al., 2016) alter the surface delivery of GluN1/GluN2A, GluN1/GluN2B, and GluN1/GluN3A receptors expressed in HEK293 cells; these mutations are shown schematically in Fig. 1A. For this purpose, we generated YFP-tagged GluN1-1a subunits containing the pathogenic mutations M641I, A645S, Y647S; we then co-expressed these subunits together with the GluN2A, GluN2B, and GluN3A subunits and measured their surface and total expression levels using immunostaining with an anti-GFP antibody; example images of transfected cells are shown in Fig. 1B. We found that cells expressing GluN1-1a-M641I/GluN2A, GluN1-Y647S/GluN2A, and GluN1-1a-Y647S/GluN2B receptors had significantly reduced surface delivery; all other NMDARs combinations studied were delivered to the cell surface at the same level as their corresponding wild-type receptors (Fig. 1C). These results indicate that specific pathogenic mutations in the M3 domain of the GluN1-1a subunit differentially alter the trafficking of NMDARs subtypes. Similar to our results obtained with the GluN1-1a splice variant, we found that the GluN1-4a-M641I/GluN2A, GluN1-4a-Y647S/GluN2A, and GluN1-4a-

Y647S/GluN2B receptors – but not any other NMDAR combinations tested – had significantly reduced surface delivery compared to wild-type receptors (Fig. 1D). Taken together, these data confirm that specific pathogenic mutations in the M3 domain of the GluN1 subunit affect the surface delivery of NMDARs, and this effect is apparently independent of the GluN1 splice variant.

Next, we examined whether these pathogenic mutations in the M3 domain of GluN1 subunit affect the surface delivery of NMDARs in neurons. Ten days after viral infection, we performed immunostaining using an anti-GFP antibody and measured surface and total levels of the GluN1-1a subunits using confocal microscopy (Fig. 1E). Our analysis revealed that the GluN1-1a-A645S subunit was expressed at the surface at the same level as the wild-type subunit, whereas the GluN1-1a-M641I and GluN1-1a-Y647S subunits were significantly reduced at the cell surface (Fig. 1F). These findings are consistent with our data obtained with HEK293 cells and confirm that specific pathogenic mutations in the M3 domain of the GluN1 subunit affect the surface delivery of NMDARs.

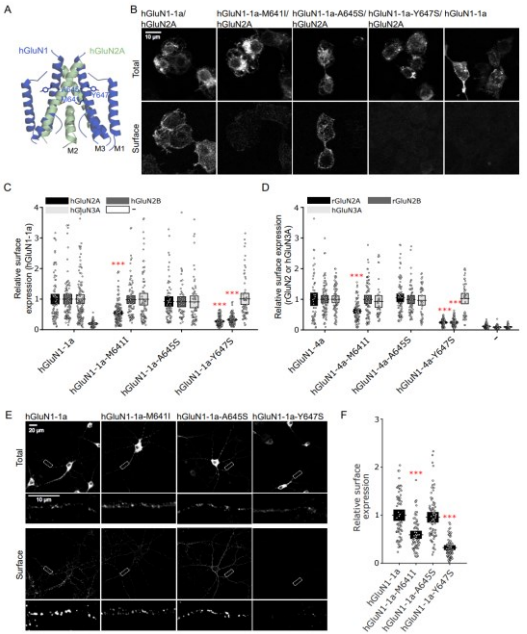

Fig. 1. Pathogenic mutations in GluN1 subunit differentially alter the surface delivery of NMDARs in a subunit-dependent manner. (A) Structural model of the M1, M2, and M3 domains in the GluN1/GluN2A heterotetramer (PDB code: 6IRA); the three amino acid residues studied here are indicated. (B) Representative images of HEK293 cells transfected with the GluN2A subunit and the indicated wild-type or mutant YFP-

GluN1-1a (GluN1-1a) subunits; total and surface GluN1-1a subunits were labeled 24 h after transfection using an anti-GFP antibody. (C–D) Summary of the relative surface expression of wild-type and mutant GluN1-1a (C) or GluN1-4a (D) subunits co-transfected with the indicated untagged GluN2 or GluN3A subunits (C) or GFP-GluN2 (GluN2) and GFP-GluN3A (GluN3A) subunits (D), measured using fluorescence microscopy ($n \geq 70/49$ cells per group); ***$p < 0.001$ vs. the corresponding wild-type NMDARs, (one-way ANOVA). (E) Representative images of cultured rat hippocampal neurons infected with lentiviruses encoding the indicated YFP-GluN1-1a (GluN1-1a) subunits; total and surface GluN1-1a subunits were labeled using an anti-GFP antibody. (F) Summary of the relative surface expression of the indicated GluN1-1a subunits measured in 10-μm segments of secondary or tertiary dendrites ($n \geq 30$ segments in ≥6 different cells per group); ***$p < 0.001$ vs. GluN1- 1a, (one-way ANOVA).

Next, we measured the dose-response curves for Mg^{2+} block of wild-type and mutant GluN1-4a/GluN2A and GluN1-4a/GluN2B receptors in the presence of saturating concentration (1 mM) of glutamate (Fig. 2A, C). We found that neither the M641I mutation nor the A645S mutation in the GluN1-4a subunit affected the IC_{50} value for Mg^{2+}, regardless of the GluN2 subunit co-expressed in the HEK293 cells (Fig. 2B, D). Thus, neither of these pathogenic mutations affects the sensitivity of GluN1-4a/GluN2 receptors to Mg^{2+}.

We then measured NMDARs sensitivity to memantine using the same approach as above; for these experiments, the ECS contained 0 mM Mg^{2+} (Fig. 2E–H). Our analysis revealed that memantine inhibited both GluN1-4a/GluN2A and GluN1-4a/GluN2B receptors with an IC_{50}

value of approximately 1 μM (Fig. 2F, H), which is consistent with previously published data (Kotermanski and Johnson, 2009). In contrast to our experiments involving Mg^{2+}, we found that the IC_{50} value for memantine was significantly increased for receptors containing the GluN1-4a-A645S subunit (2 E-H), but was unaffected in receptors containing the GluN1-4a-M641I subunit (Fig. 2F, H). Thus, the two pathogenic mutations in the GluN1 subunit do not affect the sensitivity of NMDARs to Mg^{2+}, but differentially affect the sensitivity of NMDARs to memantine.

A previous study found that physiological levels of extracellular Mg^{2+} (approximately 1 mM) affect the selectivity of NMDARs to memantine (Kotermanski and Johnson, 2009). We therefore examined whether the pathogenic mutations in the M3 domain of GluN1 subunit affect the sensitivity of NMDARs to memantine in the presence of 1 mM Mg^{2+} by measuring whole-cell currents induced by 1 mM glutamate at membrane potential of −60 mV, and increasing concentrations of memantine (Fig. 2I). For these experiments, we focused on GluN2A-containing NMDARs, as they generally yield larger currents in HEK293 cells compared to GluN2B-containing NMDARs, thus allowing us to more readily examine the effect of memantine on glutamate-induced currents in the presence of 1 mM Mg^{2+}. In the presence of 1 mM Mg^{2+}, we observed that the IC_{50} value for memantine was approximately 14 μM at wild-type GluN1-4a/GluN2A receptors (Fig. 2J and K), consistent with previously published data (Kotermanski and Johnson, 2009). Interestingly, we found that GluN1-4a-M641I/GluN2A receptors had a significantly decreased IC_{50}

value (~2 μM), whereas GluN1-4a-A645S/GluN2A receptors had a significantly increased IC_{50} value (~32 μM) for memantine in the presence of 1 mM Mg^{2+} compared to wild-type GluN1-4a/GluN2A receptors; the IC_{50} values for memantine in the absence and presence of 1 mM Mg^{2+} for various GluN1-4a/GluN2A receptors are summarized in Fig. 2K. In addition, we examined the sensitivity of NMDARs to memantine in HEK293 cells voltage-clamped at membrane potentials of −20 mV and +40 mV and found that IC_{50} values for memantine were significantly decreased at GluN1-4a-M641I/GluN2A receptors and significantly increased at GluN1-4a-A645S/GluN2A receptors compared to wild-type GluN1-4a/GluN2A receptors at both membrane potentials (Fig. 2L–N). Taken together, these data indicate that the M641I and A645S mutations in the M3 domain of the GluN1 subunit increase and decrease, respectively, sensitivity of the GluN1/GluN2 receptor to memantine in physiologically relevant levels of extracellular Mg^{2+} and membrane potentials.

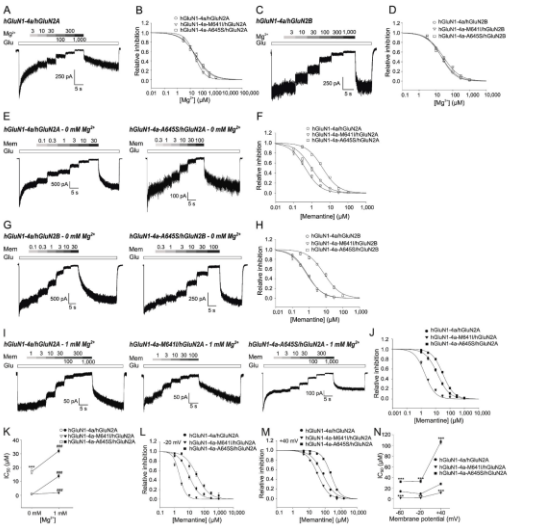

Fig. 2. Specific pathogenic mutations in the M3 domain of GluN1 subunit differentially affect the sensitivity of GluN1/GluN2 receptors to memantine but not to Mg^{2+}. (A, C) Representative whole-cell recordings of HEK293 cells transfected with GluN1-4a/GluN2A (A) or GluN1-4a/GluN2B (C) receptors voltage-clamped at a membrane potential of −60 mV. The indicated concentrations of Mg^{2+} (in μM) were applied in the continuous presence of 1 mM glutamate (Glu). (B, D) Normalized dose-response curves for Mg^{2+} block obtained by fitting the data with Equation (2) (see Methods). Each data point represents the mean normalized current obtained from ≥5 cells ± SEM. (E, G) Representative whole-cell recordings of HEK293 cells transfected with the indicated

GluN1-4a/GluN2A (E) or GluN1-4a/GluN2B (G) receptors voltage-clamped at a membrane potential of −60 mV. The indicated concentrations of memantine (Mem, in μM) were applied in the continuous presence of 1 mM Glu. (F, H) Normalized dose-response curves for memantine inhibition (measured in 0 mM Mg^{2+}) were obtained by fitting the data with Equation (2). Each data point represents the mean normalized current obtained from ≥5 cells ± SEM. (I) Representative whole-cell recordings of HEK293 cells transfected with the indicated GluN1-4a/GluN2A receptors voltage-clamped at a membrane potential of −60 mV measured in the presence of 1 mM Mg^{2+}. The indicated concentrations of Mem (in μM) were applied in the continuous presence of Glu and 1 mM Mg^{2+}. (J) Normalized dose-response curves for memantine inhibition measured in 1 mM Mg^{2+} were obtained by fitting the experimental data with Equation (2). Each data point represents the mean normalized current obtained from ≥4 cells ± SEM. (K) The IC_{50} values for memantine plotted against extracellular Mg^{2+} concentration for the indicated GluN1-4a/GluN2A receptors. ***$p < 0.001$ vs. GluN1-4a/GluN2A receptors (one-way ANOVA with Tukey's post hoc test); ###$p < 0.001$ vs. 0 mM Mg^{2+} (Student's t-test). (L, M) Normalized dose-response curves for memantine inhibition measured in HEK293 cells at a holding membrane potential of −20 mV (L) or +40 mV (M). (N) The IC_{50} values for memantine measured in 1 mM Mg^{2+} plotted against membrane potentials for the indicated GluN1-4a/GluN2A receptors. **$p < 0.010$ and ***$p < 0.001$ vs. wild-type GluN1-4a/GluN2A receptors (one-way ANOVA with Tukey's post hoc test).

Importantly, memantine can also act upon GluN1/GluN2 receptors via a second site that is accessible in the absence of agonists, a phenomenon known as second-site inhibition (SSI)

(Glasgow et al., 2018), also referred to as membrane-to-channel inhibition (MCI) (Wilcox et al., 2022). To induce SSI, HEK293 cells were treated with 100 μM memantine; after removal of memantine, 1 mM glutamate is added, and the glutamate-induced current was compared to currents elicited without and prior treatment with memantine (Fig. 3A). To quantify these data, we calculated the minimum ratio between SSI currents and control currents ("minimum $I_{SSI}/I_{control}$"); these results are summarized in Fig. 3B. Consistent with previous reports (Blanpied et al., 1997; Glasgow et al., 2018; Kotermanski and Johnson, 2009), we observed that the minimum $I_{SSI}/I_{control}$ for GluN1-4a/GluN2A receptors was approximately 0.5 in control conditions and in HEK293 cells treated with both memantine and either D-APV (a competitive antagonist for the glutamate-binding site in the GluN2 subunit) or 1 mM Mg^{2+}; moreover, the minimum $I_{SSI}/I_{control}$ increased to approximately 0.9 when 1 mM Mg^{2+} was present throughout the entire experiment (Fig. 3B). In addition, we found that the time constant of the recovery from SSI ($\tau_{recovery}$) was approximately 6 s for wild-type GluN1-4a/GluN2A receptors under control conditions (Fig. 3C). We then examined NMDARs containing pathogenic mutations in the GluN1 subunit and found that the minimum $I_{SSI}/I_{control}$ for GluN1-4a-M641I/GluN2A receptors was similar to wild-type GluN1-4a/GluN2A receptors under all conditions, with the exception of a significant decrease of the minimum $I_{SSI}/I_{control}$ in the continuous presence of 1 mM Mg^{2+} (Fig. 3B); $\tau_{recovery}$ for the GluN1-4a-M641I/GluN2A receptors was also similar to wild-type GluN1-4a/GluN2A receptors (Fig. 3C). In contrast, we

found that the minimum $I_{SSI}/I_{control}$ for GluN1-4a-A645S/GluN2A receptors was significantly increased in comparison to wild-type Glu-N1-4a/GluN2A receptors (~0.8) under all conditions and was not different from wild-type GluN1-4a/GluN2A receptors when measured in the continuous presence of 1 mM Mg^{2+} (Fig. 3B); we could not calculate $\tau_{recovery}$ for GluN1-4a-A645S/GluN2A receptors because of the relatively weak memantine-induced SSI measured at these receptors. Glasgow et al. reported that SSI requires memantine to transit from the second site to the deep site (Glasgow et al., 2018). Consistent with previous data (Glasgow et al., 2018), we found that holding the membrane potential at +40 mV (instead of −60 mV) eliminated memantine-induced SSI (i.e., $I_{SSI}/I_{control}$ was approximately 1) for both wild-type and mutant GluN1-4a/GluN2A receptors (Fig. 3D, F). In contrast, we found that stepping (i.e., "jumping") the membrane potential from −60 mV to +40 mV only when applying memantine had no effect on memantine-induced SSI compared to holding the membrane potential at −60 mV throughout the entire recording (Fig. 3E and F). Taken together, these data indicate that the M641I and A645S mutations in the GluN1 subunit differentially affect ability of memantine to induce SSI at NMDARs.

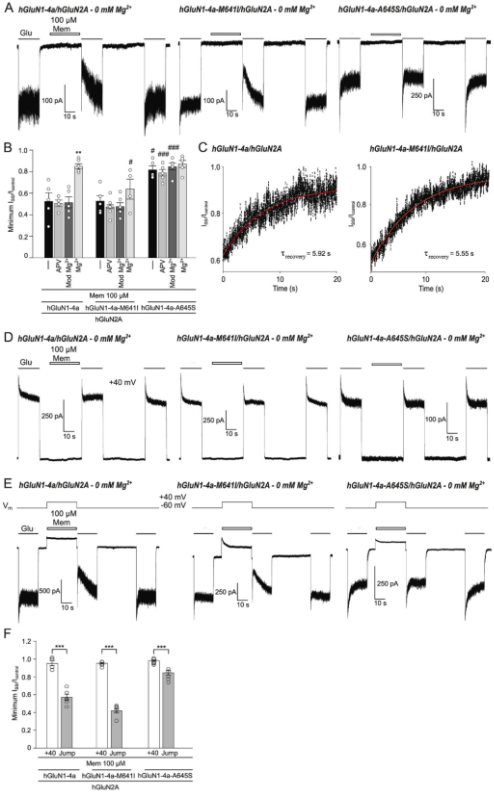

Fig. 3. Specific pathogenic mutations in the M3 domain of the GluN1 subunit differentially affect memantine-mediated SSI

of GluN1/GluN2A receptors. (A) Representative whole-cell recordings of HEK293 cells expressing the indicated GluN1-4a/GluN2A receptors voltage-clamped at a membrane potential of −60 mV. Where indicated, 1 mM glutamate (Glu) and 100 μM memantine (Mem) were applied. (B) Summary of minimum $I_{SSI}/I_{control}$ calculated for the indicated GluN1-4a/GluN2A receptors (see Methods). "–", control condition; "APV", 50 μM D-APV was co-applied with Mem; "Mod Mg^{2+}", 1 mM Mg^{2+} was co-applied with Mem; "Mg^{2+}", 1 mM Mg^{2+} was present throughout the entire recording (see text for more details); $n \geq 5$ cells per each condition. **$p < 0.001$ vs. control condition (one-way ANOVA); #$p < 0.050$ and ###$p < 0.001$ vs. the wild-type GluN1-4a/GluN2A receptors (one-way ANOVA). (C) $I_{SSI}/I_{control}$ is plotted from the example traces shown in panel A, with the corresponding time constant of recovery from SSI ($\tau_{recovery}$) shown. The average $\tau_{recovery}$ values were 6.25 ± 0.72 s and 6.83 ± 0.66s for cells expressing GluN1-4a/GluN2A and GluN1-4a-M641I/GluN2A receptors, respectively ($n \geq 5$ cells per each group; $p > 0.05$; Student's t-test). (D, E) Representative whole-cell recordings of HEK293 cells expressing the indicated GluN1-4a/GluN2A receptors voltage-clamped at a fixed membrane potential of +40 mV (D) or at −60 mV with a step ("jump") to +40 mV during Mem application (E). (F) Summary of minimum $I_{SSI}/I_{control}$ calculated for the indicated GluN1-4a/GluN2A receptors recorded as shown in panels D (+40; gray bars) and E (Jump, black bars); $n \geq 5$ cells per each group. ***$p < 0.001$ vs. +40 mV (Student's t-test).

Next, we performed electrophysiological measurements from cultured hippocampal neurons expressing either wild-type or mutant GluN1-1a subunits to analyze the memantine sensitivity in the presence of 1 mM Mg^{2+} at a membrane potential of −60 mV; for these experiments, we used 300 μM

NMDA instead of glutamate to activate the NMDARs, and both TTX and bicuculine were present throughout the recordings. Similar to our findings obtained with HEK293 cells, we found that the IC_{50} value for memantine was significantly decreased for YFP-GluN1-1a-M641I-expressing neurons, whereas significantly increased for YFP-GluN1-1a-A645S-expressing neurons, when compared to wild-type YFP-GluN1-1a-expressing neurons (Fig. 4 A–B). Furthermore, when we recorded at membrane potentials from −80 mV to +80 mV (in 20 mV incremental steps), we observed that 30 μM memantine more effectively inhibited NMDARs from neurons expressing YFP-GluN1-1a-M641I, but less effectively NMDARs from neurons expressing YFP-GluN1-1a-A645S, both compared to neurons expressing YFP-GluN1-1a (except for neurons expressing YFP-GluN1- 1a-A645S measured at membrane potentials of −20 mV and 0 mV; Fig. 4C–D). Thus, as in HEK293 cells, two different mutations in the M3 domain of the GluN1 subunit differentially affect the sensitivity of NMDARs to memantine when expressed in hippocampal neurons.

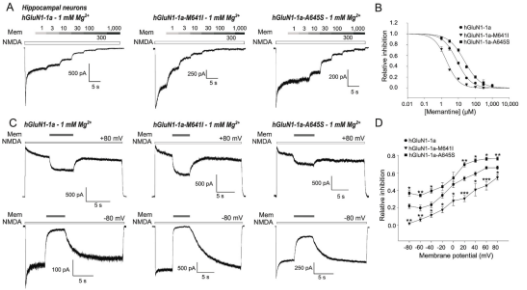

Fig. 4. Specific pathogenic mutations in the M3 domain of the GluN1 subunit differentially affect the sensitivity of neuronal NMDARs to memantine. (A) Representative whole-cell recordings of cultured hippocampal neurons infected with lentiviruses expressing the indicated YFP-tagged GluN1-1a (GluN1-1a) subunits; the membrane potential was voltage-clamped at −60 mV. Endogenous GluN1 subunits were knocked down by expressing a shRNA-GluN1. The indicated concentrations of memantine (Mem; in μM) were applied in the continuous presence of 300 μM NMDA, 50 μM glycine, 1 μM TTX, 10 μM bicuculine, and 1 mM Mg^{2+}. (B) Normalized dose-response curves for memantine inhibition in the continuous presence of 1 mM Mg^{2+} were obtained by fitting the data with Equation (2). Each data point represents the mean normalized current obtained from ≥4 cells ± SEM. (C) Representative whole-cell patch-clamp recordings measured from cultured infected hippocampal neurons held at a

membrane voltage of −80 mV or +80 mV. NMDARs were activated exactly as described in A, 30 μM memantine was used for all conditions. (D) Graph summarizing the relative inhibition induced by 30 μM memantine, measured from hippocampal neurons expressing the GluN1-1a, GluN1-1a-M641I and GluN1-1a-A645S at the indicated membrane potentials. n ≥ 5 cells per each condition; one-way ANOVA with Tukey's post hoc test); *p < 0.050, **p < 0.010, and ***p < 0.001 vs. GluN1-1a.

Lastly, we examined whether the mutations in the GluN1 subunit affect NMDA-induced excitotoxicity in cultured hippocampal neurons. We therefore expressed either wild-type or mutant YFP-GluN1-1a subunits in neurons; we then cultured the neurons in medium containing 1 mM Mg^{2+} together with 10 μM glycine and 0, 30, or 100 μM NMDA as well as in various concentrations of memantine for 1 h, followed by an additional culturing for 22–23 h. The percentage of dead cells was then determined by staining the nuclei with Hoechst 33342 and measuring nuclear area (Fig. 5A). Using this protocol, we found that neurons expressing the wild-type YFP-GluN1-1a subunit underwent significant excitotoxicity (~80%) upon treatment with either 30 μM or 100 μM NMDA, and memantine significantly reduced excitotoxicity in a dose- dependent manner (Fig. 5B–E). Neurons expressing either the YFP- GluN1-1a-M641I or YFP-GluN1-1a-A645S subunits were also susceptible to NMDA-induced excitotoxicity, with a percentage of death cells similar to wild-type YFP-GluN1-1a-expressing neurons.

Interestingly, and consistent with our electrophysiology data, we found that memantine differentially affected NMDA-induced excitotoxicity in neurons expressing the mutant GluN1 subunits. Specifically, memantine significantly reduced excitotoxicity in neurons expressing the YFP-GluN1-1a-M641I subunit but was significantly less neuro- protective in neurons expressing the YFP-GluN1-1a-A645S subunit in comparison to neurons expressing wild-type YFP-GluN1-1a subunit (Fig. 5D and E). These data indicate that specific pathogenic mutations in the M3 domain of the GluN1 subunit differentially affect the pharmacological sensitivity of NMDARs in hippocampal neurons.

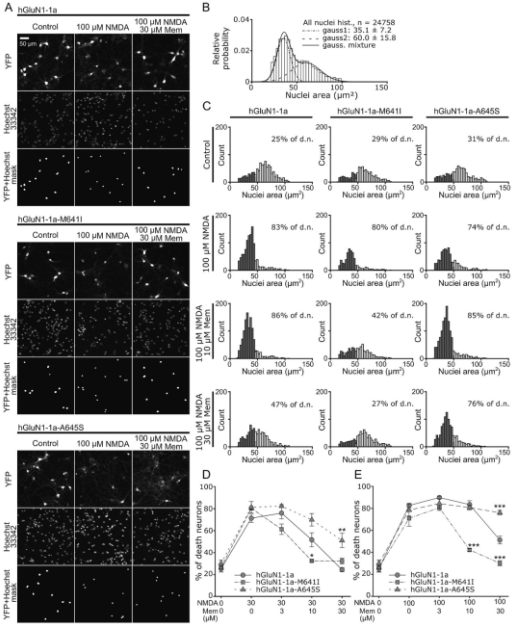

Fig. 5. Memantine differentially affects NMDA-induced excitotoxicity in hippocampal neurons expressing mutated GluN1 subunits. (A) Representative fluorescence images of YFP and Hoechst 33342 staining in hippocampal neurons expressing YFP-GluN1-1a (GluN1-1a), YFP-GluN1-1a-M641I (GluN1-1a-M641I), or YFP-GluN1-1a-A645S (GluN1-1a- A645S) subunits. Where indicated, the neurons were untreated (Control; left column) or treated with either 10 µM glycine and 100 µM NMDA (middle column) or 10 µM

glycine, 100 μM NMDA, and 30 μM memantine (Mem) (right column). Upper rows: the YFP channel; middle rows: the Hoechst 33342 channel; and bottom rows: a mask was applied to select only the nuclei of cells expressing YFP. (B) Histogram showing the distribution of the nuclear size measured for all neurons, revealing two clearly distinguishable groups representing pyknotic (i.e., dead) and non-pyknotic neurons. The data were fitted with a mixture of two Gaussian distribution models (the solid line), and the Gaussian parameters (mean and sigma values) were estimated for each distribution and are shown. The estimated individual Gaussian distributions are shown as a dotted line (pyknotic cells) and as a dashed line (non-pyknotic cells). (C) Histograms showing the distributions of nuclear area for the neurons in the indicated conditions. For each condition, the neurons were classified based on the probability of being pyknotic (dark gray bars) or non-pyknotic (white bars), with the corresponding percentage of dead (i.e., pyknotic) neurons indicated (D–E) Summary of the percentage of dead (i.e., pyknotic). neurons expressing the indicated GluN1-1a subunits and treated with the indicated concentrations of memantine (Mem) in the presence of 30 μM (D) or 100 μM (E) NMDA; the classified nuclei were counted for each condition, and the number of pyknotic cells is expressed as the percentage of the total number of cells analyzed. The error bars indicate the SEM; $n \geq 5214$ cells per each condition collected from 5 independent experiments. *$p < 0.050$, **$p < 0.010$, and ***$p < 0.001$ vs. wild-type GluN1-1a subunit (one-way ANOVA; all data passed the Shapiro–Wilk normality test, $p < 0.05$).

5.2. The presence of putative N-glycosylation sites and their interaction with specific lectins regulates the functional properties of GluN1/GluN3 receptors

As shown in Fig. 6A and B, the GluN1 and GluN3A subunits each contain 12 putative *N*-glycosylation consensus

sites (N-X-S/T) (Skrenkova et al., 2018); in contrast, the GluN3B subunit contains 6 putative *N*-glycosylation consensus sites (Fig. 6B). Here, we combined electrophysiology with a rapid solution exchange system in which we applied a wide range of glycine concentrations (from 10 μM to 10 mM) to HEK293 cells transfected with wild-type or mutant (N→Q) forms of GluN1/GluN3 receptors. We found no difference between wild-type and mutated GluN1/GluN3A receptors with respect to the normalized peak current amplitude or τ_w of desensitization measured in response to various concentrations of glycine, however, we found differences in functional properties between wild-type and mutated GluN1/GluN3B receptors. Since, GluN1/GluN3B receptors produce a large tail current at the end of the glycine application (Smothers and Woodward, 2009), where appropriate, we measured the ratio of the steady-state current amplitude to the peak current amplitude (ss/p), as well as the ratio of the peak tail current amplitude to the steady-state current (t/ss) of wild-type GluN1/GluN3B and GluN1/GluN3B that lack triplet sets as well as single putative N-glycosylation sites. Our analysis revealed that the t/ss ratio was increased for the GluN1-N440Q/GluN3B, GluN1-4/4N→Q/GluN3B and GluN1-N674Q/GluN3B receptors, but was unchanged in the remaining GluN1/GluN3B receptors tested (Fig. 6C).

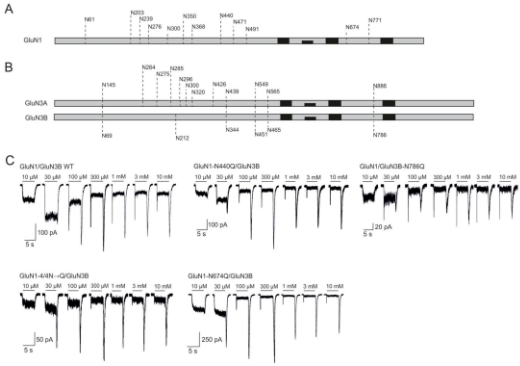

Fig. 6. Overview of putative *N*-glycosylation sites in GluN1, GluN3A, and GluN3B subunits. (A–B) Schematic diagram showing the approximate location of the 12 putative N-glycosylation consensus sites (N-X-S/T) in the GluN1 (A) and GluN3A (B) subunits, and the 6 putative N-glycosylation consensus sites in the GluN3B subunit (B); the four solid black boxes in each subunit indicate the membrane-spanning domains. (C) Representative whole-cell voltage-clamp recordings of human embryonic kidney 293 (HEK293) cells transfected with the indicated GluN1/GluN3B receptors. Currents were elicited by application of the indicated concentrations of glycine (indicated by the horizontal black bars).

Next, we examined the effect of lectins on the functional properties of GluN1/GluN3B receptors. We pre-treated HEK293 cells expressing GluN1/GluN3B receptors for 8 min in each lectin at 200 μg/ml, and then measured the properties

of glycine-induced currents (Fig. 7A). Our analysis revealed that 14 of the 19 lectins tested significantly reduced the t/ss ratio measured in GluN1/GluN3B receptors (Fig. 7B and Table 1). We then focused our analysis on ConA, WGA, and AAL and found that all three lectins significantly increased both the ss/p ratio (Fig. 7C) and the 10–90% rise time for the onset of glycine-induced currents (Fig. 7D) of the GluN1/GluN3B receptors. We also found that 20 μg/ml ConA, WGA, and AAL was sufficient to reduce the t/ss ratio to the same extent as 200 μg/ml (Fig. 7E; compare with Fig. 7B).

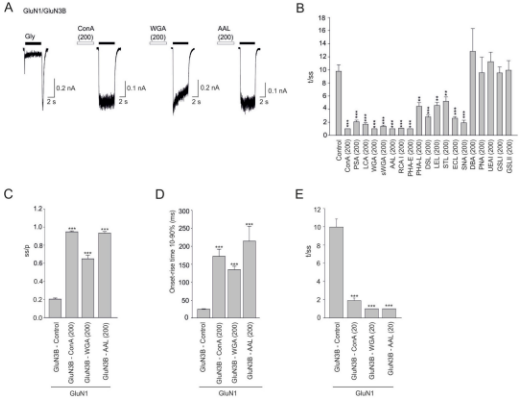

Fig. 7. GluN1/GluN3B receptors are modulated by specific lectins. (A) Whole-cell currents were elicited with a 5-s pulse of 500 μM glycine (indicated by the black bar) in HEK293 cells expressing GluN1/GluN3B receptors. Where indicated, the cells were pre-

incubated with 200 μg/ml ConA, WGA, or AAL for 8 min (indicated by the white bars, not to scale). (B) Summary of t/ss ratio measured for GluN1/GluN3B receptors; where indicated, the cells were pre-incubated with 200 μg/ml of the indicated lectins (n≥5 cells/group). (C–E) The ss/p ratio, 10–90% onset rise time, and t/ss ratio were measured during a 5-s application of 500 μM glycine in cells expressing GluN1/GluN3B receptors; where indicated, the cells were pre-incubated with 200 μg/ml (C and D) or 20 μg/ml (E) ConA, WGA, or AAL (n ≥ 5 cells/group). **p < 0.01, ***p < 0.001 versus control-treated cells (one-way ANOVA).

Next, we examined whether the effect of lectins on GluN1/GluN3B receptors is conformation-dependent. We therefore measured glycine-induced currents before and after a 1-min application of 20 μg/ml ConA, WGA, or AAL and analyzed the p_2/p_1 ratio of GluN1/GluN3B receptors (Fig. 8A–B). Our analysis revealed that all three lectins significantly increased the p_2/p_1 ratio of GluN1/GluN3B receptors (Fig. 8B). Interestingly, we observed that compared to wild-type receptors the effect of AAL was significantly lower in receptors containing GluN3B–N465Q subunit (Fig. 8A, B), supporting the notion that N465 in the GluN3B subunit plays a role in the ability of AAL to modulate the functional properties of GluN1/GluN3B receptors. In contrast, when we applied the lectins in the continuous presence of 500 μM glycine, we found no or minor effect (Fig. 8C); thus, similar to our findings with respect to GluN1/GluN3A receptors, the

ability of lectins to modulate GluN1/GluN3B receptors appears to be dependent on the conformation.

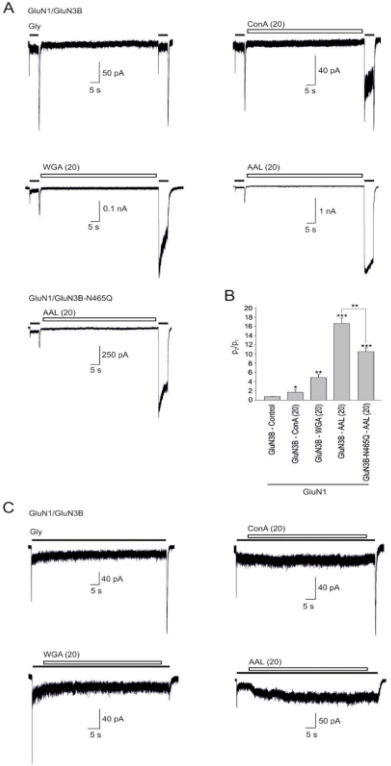

Fig. 8. Investigating the mechanism of action of selected lectins on GluN1/GluN3B receptors. (A) Whole-cell currents through GluN1/GluN3B receptors were elicited with a 5-sec pulse of 500 μM glycine (indicated by the black bar) before and after a 1-min application of 20 μg/ml ConA, WGA, or AAL. (B) Summary of p2/p1 measured in cells expressing either wild-type GluN1/GluN3B or GluN1/GluN3B–N465Q receptors; where indicated, 20 μg/ ml ConA, WGA, or AAL was applied between the two glycine pulses ($n \geq 5$ cells/group). (C) Representative whole-cell currents through GluN1/ GluN3B receptors elicited with an application of 500 μM glycine (indicated by the black bar); where indicated, 20 μg/ml ConA, WGA, or AAL was applied for 1 min in the continued presence of glycine. Only AAL had a slight potentiating effect, with a mean increase of the steady-state current amplitude of 310 ± 60% ($n = 5$) by the end of the 1-min application of AAL. *$p < 0.05$, **$p < 0.01$, ***$p < 0.001$ versus control-treated cells or between the in- dicated groups (ANOVA).

6. Discussion

6.1. Three pathogenic mutations in the M3 domain of the GluN1 subunit regulate the surface delivery and pharmacological sensitivity of NMDARs

We focused on three pathogenic mutations in the M3 domain of the GluN1 subunit - M641I, A645S, and Y647S - associated with intellectual disability, movement disorders, and seizures (Lemke et al., 2016). We showed that this mutations affect the surface delivery of NMDARs in HEK293 cells in subunit-dependent manner – specifically, GluN1-M641I mutation significantly reduces surface expression of GluN1/GluN2A receptors, but not GluN1/GluN2B or GluN1/GluN3A receptors, GluN1-Y647S mutation reduces

surface expression of GluN1/GluN2A and GluN1/GluN2B receptors, but not GluN1/GluN3A receptors and GluN1-A645S mutation did not affect the level of surface expression whether was co-expressed with GluN2A, GluN2B or GluN3A subunits. Moreover, our microscopy data obtained on using hippocampal neurons (DIV14) demonstrated the same changes in surface expression as observed in HEK293 cells when mutated GluN1 subunits were co-expressed with the GluN2A subunit. These results are consistent with the finding that hippocampal neurons have low expression of endogenous GluN3 subunit and high expression of GluN2A subunit (Hansen et al., 2021; Henson et al., 2010; Paoletti et al., 2013; Vieira et al., 2020). Similarly to this finding, it has been shown that *de novo* mutation GluN1-G620R – associated with developmental delay and behavioural abnormalities – reduces surface delivery of GluN1/GluN2B receptors, but not GluN1/GluN2A receptors (Chen et al., 2017).

Moreover, our group previously showed that specific amino acid residues in the M3 domain of GluN1 and GluN2 subunits (GluN1-W636, GluN2A-W634, GluN2B-W635) contribute to the regulation of trafficking of NMDARs to the cell surface (Kaniakova et al., 2012). Furthermore, pathogenic mutations GluN2B-W607C and GluN2B-S628F in the TMD - associated with intellectual disability and developmental delay - reduce surface delivery of NMDARs, as well as sensitivity of NMDARs to glutamate, glycine and Mg^{2+} block (Vyklicky et al., 2018). In our further experiment we also observed changes in the receptor's functional properties, specifically – we found that the EC_{50} value for glycine was increased for GluN1-

M641I/GluN3A receptors compared to WT GluN1/GluN3A, and we found that GluN1-A645S/GluN3A receptors had a slower τ_w of desensitization. The changes in desensitisation are consistent with evidences that mutations in the TMD, including SYTANLAAF motif, alter current kinetics of GluN1/GluN2A receptor (Hu and Zheng, 2005). Although we found that the GluN1-Y647S mutation does not alter expression of GluN1/GluN3A receptors, our electrophysiological experiments revealed no glycine-induced current unless CGP-78608 application was applied (Grand et al., 2018). Therefore, we hypothesise that GluN1-Y647S mutation presumably changes specific functional properties of GluN1/GluN3A receptors, such as P_o. However, we cannot test this assumption because, unlike the open-channel blocker of GluN1/GluN2 receptor MK-801, no specific open-channel blocker of GluN1/GluN3A receptor exists at present (Chatterton et al., 2002).

Reduction in agonist and/or antagonist sensitivity was also reported for other pathogenic mutations, such as N615I-GluN2B located at the beginning of the M2–M3 linker, and V618G-GluN2B, located in the M2–M3 linker – associated with West syndrome – reduce the sensitivity of NMDARs to Mg^{2+} and memantine (Fedele et al., 2018). The GluN1-G620R mutation, mentioned above, also reduces agonist sensitivity and Mg^{2+} block (Chen et al., 2017). However, in our study, we did not observe changes in the Mg^{2+} sensitivity of GluN1/GluN2 receptors with any of the examined mutation. Nevertheless, we observed that GluN1-A645S mutation reduces sensitivity of GluN1/GluN2 receptors to memantine

in the absence of extracellular Mg^{2+}, which is consistent with previous results obtained using *Xenopus* oocytes expressing GluN1/GluN2B receptors (Kashiwagi et al., 2002). Interestingly, we found that in the presence of physiological concentration of Mg^{2+}, IC_{50} value for memantine was decreased for GluN1-M641I/GluN2A receptors but increased for GluN1-A645S/GluN2A receptors, when compared to WT GluN1/GluN2A receptors. Similar results were obtained when we measured these GluN1 subunits expressed in hippocampal neurons, moreover, our analysis of NMDA-induced excitotoxicity in hippocampal neurons also supported this finding. Specifically, memantine significantly reduced excitotoxicity in neurons expressing GluN1-M641I subunit but was significantly less neuroprotective in neurons expressing GluN1-A645S subunit in comparison to neurons expressing WT GluN1 subunit.

In addition, we found that M641I-GluN1 and A645S-GluN1 mutations differentially affect the onset (τ_{on}) and offset (τ_{off}) kinetics of inhibition by memantine, as well as affect memantine's ability to induce SSI at NMDARs. Specifically, we found that τ_{off} of memantine inhibition was slower for GluN1-M641I/GluN2A receptors and faster for GluN1-A645S/GluN2A receptors in absent and present of Mg^{2+}, when compared to WT GluN1/GluN2A receptors. Previous studies found that the slow component of τ_{off} (τ_{slow}) represents memantine unbinding from its second low-affinity binding site, at the GluN1/GluN2 receptor (Glasgow et al., 2018). Thus, when we focused on τ_{slow}, we found increased values for GluN1-M641I/GluN2A receptors and decreased values for

GluN1-A645S/GluN2A receptors, when compared to WT GluN1/GluN2A receptors under all experimental condition tested. These findings indicate that these two pathogenic mutations in the M3 domain of GluN1 subunit differentially affect both the binding and unbinding kinetic of memantine, and may possibly affect the SSI of memantine or, based on the recent studies, affect the membrane-to-channel transfer of memantine (Wilcox et al., 2022). Taking together, our data indicate that specific pathogenic mutations in the M3 domain of the GluN1 subunit differentially affect the pharmacological sensitivity and surface delivery of NMDARs.

6.2. The presence of putative N-glycosylation sites and their interaction with specific lectins regulates the functional properties of GluN1/GluN3 receptors

We focused on studying the role of specific *N*-glycans of the GluN1, GluN3A and GluN3B subunits in the regulation of functional properties of NMDARs as well as the role of different lectins in the modulation of GluN1/GluN3A receptors. It has been previously reported that inhibition of glycosylation of NMDARs with tunicamycin decreases EC_{50} for glutamate of GluN1/GluN2B receptors (Everts et al., 1997), as well as EC_{50} for NMDA of native NMDARs (Lichnerova et al., 2015). It was also shown that *N*-glycosylation sites in the GluN1 subunit are required for the release of NMDARs from the ER (Skrenkova et al., 2018). Here we showed that disruption of putative *N*-glycosylation sites in GluN1 or GluN3A subunits do not affects the desensitisation of GluN1/GluN3A receptors independent of the glycine concentration. This observation is in agreement

with our previous finding that mutated *N*-glycosylation sites do not change weighted time constant (τ_w) of desensitization for GluN1/GluN3A receptors in response to 500 μM glycine (Skrenkova et al., 2018). In contrast, we found that mutated residues N440 and N674 in the GluN1 subunit and N786 in the GluN3B subunit altered functional properties of GluN1/GluN3B receptors. In our previous studies, we showed that 11 out of 12 *N*-glycosylation sites in the GluN1 subunit are modified by glycans but N674 residue is not glycosylated (Kaniakova et al., 2016). Thus, we suggest that glycosylation of N440 residue regulates desensitization properties of GluN1/GluN3B receptors, whereas the observed changes with the mutated N674 residue are caused by a structural change in the LBD of the GluN1 subunit. As for the N786 residue in the GluN3B subunit, it is currently unknown whether this site is glycosylated in the recombinant GluN3B subunit, however, since we observed changes in the "tail" current amplitude of GluN1/GluN3B receptors with the N786 mutated residue, we suggest that glycosylation at this residue alters the activation of GluN1/GluN3B receptors by altering the LBD in the GluN3B subunit, rather than affecting the desensitization kinetics via the LBD of the GluN1 subunit.

We have previously shown a strong association of GluN3A-containing NMDARs with numerous lectins such as ConA, WGA and AAL mainly selective for mannose residues, *N*-acetylglucosamine residues, and fucose residues respectively. Moreover, our previous biochemical data indicating that GluN3A-containing NMDARs comprise a wide variety of glycan structures (Kaniakova et al., 2016). Here, we

complemented these findings by showing that lectins modulate the functional properties of GluN1/GluN3 receptors. Considering that 14 out of 19 tested lectins significantly slowed τ_w of desensitization and altered peak amplitude, we hypothesized that this modulating effect is mediated by a decrease in desensitisation kinetics. Indeed, after introducing mutations into GluN1 subunit that makes it insensitive to glycine up to 30 mM (Kvist Trine, Greenwood Jeremy, 2013), we observed no changes after lectin application. These results confirmed our hypothesis that lectins modulate eceptor desensitisation, and are consistent with previous findings that the ConA lectin reduces desensitisation at AMPARs and KARs, though has no pronounced effect on GluN1/GluN2 receptors (Everts et al., 1997; M. L. Mayer and Vyklicky, 1989).

Interestingly, we observed the strongest modulating effect on GluN1/GluN3A and GluN1/GluN3B receptors with AAL, however, receptors, containing replacement in N565 site of GluN3A subunit and N465 site of GluN3B subunit showed s9milar sensitivity to AAL as WT GluN1/GluN3 to ConA and WGA. This observation suggests that the N565 residue in GluN3A subunit and its homologue residue N465 in GluN3B subunit re involved in potentiating the modulatory effect of AAL, which could be explained by the higher specificity or affinity of AAL for different glycans compared to WGA or ConA (Dam and Fred Brewer, 2009; Moremen et al., 2014). Furthermore, we observed that application of ConA, WGA or AAL in the persistent presence of glycine had virtually no effect on GluN1/GluN3A or GluN1/GluN3B receptors

desensitization; this finding is consistent with a previous report that ConA-induced reduction of KARs desensitization is conformation-dependent process (Everts et al., 1999). Taking together, our findings reveal new information on the role of *N*-glycans in regulating the functional properties of GluN1/GluN3 receptors in mammalian cells and provide new clues about lectins as a tool for modulating non-conventional NMDARs.

7. Conclusion

Proper regulation functioning and trafficking of NMDARs is crucial for normal synaptic transmission, learning, and memory and this regulation occurs at multiple levels. In this dissertation, we mainly focused on studying the role of NTD and TMD integrity in the regulation of the functional properties of different NMDARs. Using electrophysiological technique, we demonstrated the putative role of *N*-glycosylation sites and various lectins in the regulation of the functional properties of GluN1/GluN3 receptors. We showed that lectins affect functional properties of GluN1/GluN3 receptors, more likely by reducing desensitization. We also showed that integrity of LBD of GluN1 and GluN3A subunits is crucial for proper functioning and delivery of NMDARs to the cell surface. Finally, we provided new information about three previously identified pathogenic mutations in the M3 domain of the GluN1 subunit in terms of their impact on the functional and pharmacological properties of different subtypes of NMDARs. This information can be used for further understanding of the role of different

NMDARs both in normal conditions and in the development of various neurodegenerative diseases

8. References

Amin, J. B., Gochman, A., He, M., Certain, N., & Wollmuth, L. P. (2021). NMDA Receptors Require Multiple Pre-opening Gating Steps for Efficient Synaptic Activity. Neuron, 109(3): 488-501.

Ataman, Z. A., Gakhar, L., Sorensen, B. R., Hell, J. W., & Shea, M. A. (2007). The NMDA Receptor NR1 C1 Region Bound to Calmodulin: Structural Insights into Functional Differences between Homologous Domains. Structure, 15(12): 1603–1617.

Chatterton, J. E., Awobuluyi, M., Premkumar, L. S., Takahashi, H., Talantova, M., Shin, Y., Cul, J., Tu, S., Sevarino, K. A., Nakanishi, N., Tong, G., Lipton, S. A., & Zhang, D. (2002). Excitatory glycine receptors containing the NR3 family of NMDA receptor subunits. Nature, 415(6873): 793–798.

Chen, W., Shieh, C., Swanger, S. A., Tankovic, A., Au, M., McGuire, M., Tagliati, M., Graham, J. M., Madan-Khetarpal, S., Traynelis, S. F., Yuan, H., & Pierson, T. M. (2017). GRIN1 mutation associated with intellectual disability alters NMDA receptor trafficking and function. Journal of Human Genetics, 62(6): 589–597.

Dam, T. K., & Fred Brewer, C. (2009). Lectins as pattern recognition molecules: The effects of epitope density in innate immunity. Glycobiology, 20(3): 270–279.

Everts, I., Petroski, R., Kizelsztein, P., Teichberg, V. I., Heinemann, S. F., & Hollmann, M. (1999). Lectin-induced inhibition of desensitization of the kainate receptor GluR6 depends on the activation state and can be mediated by a single native or ectopic N-linked carbohydrate side chain. Journal of Neuroscience, 19(3): 916–927.

Everts, I., Villmann, C., Hollmann, M. (1997). N-glycosylation is not a prerequisite for glutamate

receptor function but is essential for lectin modulation. Molecular Pharmacology, 52(5): 861–873.

Fedele, L., Newcombe, J., Topf, M., Gibb, A., Harvey, R. J., & Smart, T. G. (2018). Disease-associated missense mutations in GluN2B subunit alter NMDA receptor ligand binding and ion channel properties. Nature Communications, 9(1). Furukawa, H., & Gouaux, E. (2003). Mechanisms of activation, inhibition and specificity: Crystal structures of the NMDA receptor NR1 ligand-binding core. EMBO Journal, 22(12): 2873–2885.

Furukawa, K. (2014). Crystal structure of a heterotetrameric NMDA receptor ion channel. Scienc, 344(6187): 992–997.

Glasgow, G. N., Madeleine, R. W., Johnsona, J.W., (2019). Effects of Mg^{2+} on recovery of NMDA receptors from inhibition by memantine and ketamine reveal properties of a second site. Physiology & Behavior, 176(3): 139–148.

Grand, T., Abi Gerges, S., David, M., Diana, M. A., Paoletti, P. (2018). Unmasking GluN1/GluN3A excitatory glycine NMDA receptors. Nature Communications, 9(1).

Hatton, C. J., & Paoletti, P. (2005). Modulation of triheteromeric NMDA receptors by N-terminal domain ligands. Neuron, 46(2): 261–274.

Henson, M. A., Roberts, A. C., Pérez-Otaño, I., & Philpot, B. D. (2010). Influence of the NR3A subunit on NMDA receptor functions. Progress in Neurobiology, 91(1): 23–37.

Hu, B., & Zheng, F. (2005). Differential effects on current kinetics by point mutations in the lurcher motif of NR1/NR2A receptors. Journal of Pharmacology and Experimental Therapeutics, 312(3), 899–904.

Huettner, J. E. (2015). Glutamate receptor pores. Journal of

Physiology, 593(1): 49–59.
Johansen Amin, Aaron Gochman, Miaomiao He, Certain, N., & Wollmuth, L. P. (2021). NMDA receptors require multiple pre-opening gating steps for efficient synaptic activity. Physiology & Behavior, 109(3): 488–501.
Johnson, J. W. (2019). Effects of Mg^{2+} on recovery of NMDA receptors from inhibition by memantine and ketamine reveal properties of a second site. *Physiology and Behavior* 176, 139–148.
Kaniakova, M., Krausova, B., Vyklicky, V., Korinek, M., Lichnerova, K., Vyklicky, L., & Horak, M. (2012). Key amino acid residues within the third membrane domains of NR1 and NR2 subunits contribute to the regulation of the surface delivery of N-methyl-D-aspartate receptors. Journal of Biological Chemistry, 287(31): 26423–26434.
Kaniakova, M., Lichnerova, K., Skrenkova, K., Vyklicky, L., & Horak, M. (2016). Biochemical and electrophysiological characterization of N-glycans on NMDA receptor subunits. Journal of Neurochemistry, 546–556.
Kashiwagi, K., Masuko, T., Nguyen, C. D., Kuno, T., Tanaka, I., Igarashi, K., & Williams, K. (2002). Channel blockers acting at N-methyl-D-aspartate receptors: Differential effects of mutations in the vestibule and ion channel pore. Molecular Pharmacology, 61(3): 533–545.
Kotermanski, Sh. E., Johnson, J. W. (2009). Mg^{2+} imparts NMDA receptor subtype selectivity to the Alzheimer's drug memantine. Journal of Neuroscience, 29(9):2774-9
Kvist Trine, Greenwood Jeremy, H. K. (2013). Structure-based discovery of antagonists for GluN3-containing N-methyl-D-aspartate receptors. Neuropharmacology, 23(1): 1–7.

Lee, C. H., Lü, W., Michel, J. C., Goehring, A., Du, J., Song, X., & Gouaux, E. (2014). NMDA receptor structures reveal subunit arrangement and pore architecture. Nature, 511(7508): 191–197.

Lemke, J. R., Geider, K., Helbig, K. L., Heyne, H. O., Schütz, H., Hentschel, J., Courage, C., Depienne, C., Nava, C., Heron, D., Møller, R. S., Hjalgrim, H., Lal, D., Neubauer, B. A., Nürnberg, P., Thiele, H., Kurlemann, G., Arnold, G. L., Bhambhani, V., Syrbe, S. (2016). Delineating the GRIN1 phenotypic spectrum: A distinct genetic NMDA receptor encephalopathy. Neurology, 86(23): 2171–2178.

Li, Z., Liang, D., & Chen, L. (2008). Receptor Ion Channels. Assay And Drug Development Technologies, 6(2): 298–487.

Lichnerova, K., Kaniakova, M., Park, S. P., Skrenkova, K., Wang, Y. X., Petralia, R. S., Suh, Y. H., & Horak, M. (2015). Two N-glycosylation sites in the GluN1 subunit are essential for releasing N-methyl-D-aspartate (NMDA) receptors from the endoplasmic reticulum. Journal of Biological Chemistry, 290(30), 18379–18390.

Mayer, M. L., & Vyklicky, L. (1989). Concanavalin A selectively reduces desensitization of mammalian neuronal quisqualate receptors. Proceedings of the National Academy of Sciences of the United States of America, 86(4): 1411–1415.

Meddows, E., Le Bourdellès, B., Grimwood, S., Wafford, K., Sandhu, S., Whiting, P., & McIlhinney, R. A. J. (2001). Identification of Molecular Determinants That Are Important in the Assembly of N-Methyl-D-aspartate Receptors. Journal of Biological Chemistry, 276(22): 18795–18803.

Moremen, K. W., Tiemeyer, M., Nairn, A. V. (2012)Vertebrate protein glycosylation: diversity,

synthesis and function. Nature Reviews Molecular Cell Biology, 13(7): 448-62.
Paoletti, P., Bellone, C., & Zhou, Q. (2013). NMDA receptor subunit diversity: Impact on receptor properties, synaptic plasticity and disease. Nature Reviews Neuroscience, 14(6): 383-400
Sanz-Clemente, A., Nicoll, R. A., & Roche, K. W. (2013). Diversity in NMDA receptor composition: Many regulators, many consequences. Neuroscientist, 19(1): 62-75.
Skrenkova, K., Lee, S., Lichnerova, K., Kaniakova, M., Hansikova, H., Zapotocky, M., Suh, Y. H., & Horak, M. (2018). N-glycosylation regulates the trafficking and surface mobility of GluN3A-containing NMDA receptors. Frontiers in Molecular Neuroscience,11: 188.
Smothers, C. T., Woodward, J. J., (2009). Expression of glycine-activated diheteromeric NR1/NR3 receptors in human embryonic kidney 293 cells Is NR1 splice variant-dependent. Journal of Pharmacology and Experimental Therapeutics, (3): 975-84.
Traynelis, S. F., Wollmuth, L. P., McBain, C. J., Menniti, F. S., Vance, K. M., Ogden, K. K., Hansen, K. B., Yuan, H., Myers, S. J., & Dingledine, R. (2010). Glutamate receptor ion channels: Structure, regulation, and function. Pharmacological Reviews, 62(3): 405–496
Vieira, M., Yong, X. L. H., Roche, K. W., Anggono, V. (2020). Regulation of NMDA glutamate receptor functions by the GluN2 subunits. Journal of Neurochemistry, 154(2): 121-143.
Vyklicky, V., Krausova, B., Cerny, J., Ladislav, M., Smejkalova, T., Kysilov, B., Korinek, M., Danacikova, S., Horak, M., Chodounska, H., Kudova, E., & Vyklicky, L. (2018). Surface expression, function, and pharmacology of disease-associated mutations in the

membrane domain of the human GluN2B subunit. Frontiers in Molecular Neuroscience, 11: 110.

Warnet, X. L., Bakke KroWarnet, X. L., Bakke Krog, H., Sevillano-Quispe, O. G., Poulsen, H., & Kjaergaard, M. (2020). The C-terminal domains of the NMDA receptor: How intrinsically disordered tails affect signalling, plasticity and disease. European Journal of Neuroscience, 54(8):6713-6739

Wilcox, M. R., Nigam, A., Glasgow, N. G., Narangoda, C., Phillips, M. B., Patel, D. S., Mesbahi-vasey, S., Turcu, A. L., Vázquez, S., Kurnikova, M. G., Johnson, J. W. (2022). Inhibition of NMDA receptors through a membrane-to-channel path. Nature Communications, 13(1): 4114

Wollmuth, L. P., & Sobolevsky, A. I. (2004). Structure and gating of the glutamate receptor ion channel. Trends in Neurosciences. 27: 321– 328

9. List of publications

9.1. Publications *in extenso*, related to this thesis

1. Marharyta Kolcheva, Stepan Kortus, Barbora Hrcka Krausova, Petra Barackova, Anna Misiachna, Sarka Danacikova, Martina Kaniakova, Katarina Hemelikova, Matej Hotovec, Kristyna Rehakova, Martin Horak (2021) Specific pathogenic mutations in the M3 domain of the GluN1 subunit regulate the surface delivery and pharmacological sensitivity of NMDA receptors. *Neuropharmacology*, 189:108528. IF= 5.25 (2021/2022).

2. Katarina Hemelikova*****, **Marharyta Kolcheva***, Kristyna Skrenkova, Martina Kanikova, Martin Horak (2019) Lectins modulate the functional properties of GluN1/GluN3A – containg receptors. *Neuropharmacology*, 157:107671. IF= 5.25 (2021/2022).

3. Kristyna Skrenkova, Katarina Hemelikova, Marharyta Kolcheva, Stepan Kortus, Martina Kaniakova, Barbora Krausova, Martin Horak (2019) Structural features in the glycine-binding sites of the GluN1 and GluN3A subunits regulate the surface delivery of NMDA receptors. *Scientific Reports*, 9(1):12303. IF=4.996 (2021/2022).

4. Kristyna Skrenkova, Jae-man Song, Stepan Kortus, **Marharyta Kolcheva**, Jakub Netolicky, Katarina Hemelikova, Martina Kaniakova, Barbora Hrcka Krausova, Tomas Kucera, Jan Korabecny, Young Ho Suh, Martin Horak (2020) The pathogenic S688Y mutation in the ligand-binding domain of the GluN1 subunit regulates the properties of NMDA receptors. *Scientific Reports*, 10:18576. IF=4.996 (2021/2022).

** co-first authorship*

9.2. Publications *in extenso*, unrelated to this thesis

1. Jan Konecny, Anna Misiachna, Martina Hrabinova, Lenka Pulkrabkova, Marketa Benkova, Lukas Prchal, Tomas Kucera, Tereza Kobrlova, Vladimir Finger, **Marharyta Kolcheva**, Stepan Kortus, Daniel Jun, Marian Valko, Martin Horak, Ondrej Soukup, Jan Korabecny (2020) Pursuing the Complexity of Alzheimer's Disease: Discovery of Fluoren-9-Amines as Selective Butyrylcholinesterase Inhibitors and N-Methyl-d-Aspartate Receptor Antagonists. *Biomolecules*, 11(1):3. IF=4.569 (2021/2022).

2. Lukas Gorecki, Anna Misiachna, Jiri Damborsky, Rafael Dolezal, Jan Korabecny, Lada Cejkova, Kristina Hakenova, Marketa Chvojkova, Jana Zdarova Karasova, Lukas Prchal, Martin Novak, **Marharyta Kolcheva**, Stepan Kortus, Karel Vales, Martin Horak, Ondrej Soukup (2021) Structure-activity relationships of dually-acting acetylcholinesterase inhibitors derived from tacrine on N-methyl-d-Aspartate receptors. *European Journal of Medicinal Chemistry*, 219:113434. IF=6.514 (2021/2022).

10. Curriculum Vitae

Mgr. Marharyta Kolcheva

PERSONAL DATA

Date of birth: 30.12.1992
Citizenship: UKR
E-mail: marharyta.kolcheva@iem.cas.cz

EDUCATION

2017 – now: Ph.D. student of the Faculty of Science of the Charles Universit in Prague, department of *Animal Physiology.*

2013 – 2015: Master's degree in Biophysics Educational and Scientific Center „Institute of Biology“of the Taras Shevchenko National University of Kyiv

2009 – 2013: Bachelor's degree in Biology Educational and Scientific Center „Institute of Biology“ of the Taras Shevchenko National University of Kyiv

RESEARCH

2017 – now: Institute of Physiology CAS, Laboratory of Cellular Neurophysiology
2017 – now: Institute of the Experimental Medicine CAS, Department of Neurochemistry

LABORATORY SKILLS

- preparation and culture of human embryonic kidney 293 cells (HEK293) and embryonic hippocampal neurons
- transfection of cultivated HEK293 cells
- electrophysiological measurements using the patch-clamp technique in the whole-cell configuration
- site-directed, multi-site-directed mutagenesis
- NMDA-induced excitotoxicity
- immunofluorescence microscopy - surface and total staining, image acquisition, and analysis processing

CONFERENCES

FENS regional meeting 2019 Belgrade, Serbia
FENS Forum 2022 Paris, France

Charles University
Faculty of Science
Department of Animal Physiology

Mgr. Kolcheva Marharyta

Ph.D. thesis summary:

Functional and pharmacological properties of GluN1/GluN2 and GluN1/GluN3 subtypes of NMDA receptors

Supervisor

Mgr. Martin Horak, Ph.D

Prague 2022

Doctoral Study programs in Biomedicine
Charles University
and The Czech Academy of Sciences

Study programme: Animal physiology

Chairman of the Sector Board: doc. RNDr. Jiří Novotný, DSc

Institute and Department:

Institute of Physiology, CAS
Department of Cellular
Neurophysiology

Institute of Experimental
Medicine, CAS
Department of Neurochemistry

Author: Mgr. Marharyta Kolcheva
Supervisor: Mgr. Martin Horak, Ph.D.

The Ph.D. Thesis is available in the library of the Faculty of Science, Charles University.

Contents

1. Abstract 4

2. Introduction 5

3. Hypotheses and objectives 8

4. Materials and methods 9

5. Results 15

5.1. Three pathogenic mutations in the M3 domain of the GluN1 subunit regulate the surface delivery and pharmacological sensitivity of NMDARs 15

5.2. The presence of putative N-glycosylation sites and their interaction with specific lectins regulates the functional properties of GluN1/GluN3 receptors 32

6. Discussion 38

6.1. Three pathogenic mutations in the M3 domain of the GluN1 subunit regulate the surface delivery and pharmacological sensitivity of NMDARs 38

6.2. The presence of putative N-glycosylation sites and their interaction with specific lectins regulates the functional properties of GluN1/GluN3 receptors 42

7. Conclusion 45

8. References 47

9. List of publications 53

9.1. Publications *in extenso*, related to this thesis 53

9.2. Publications *in extenso*, unrelated to this thesis 54

10. Curriculum Vitae 55

1. Abstract

N-methyl-D-aspartate receptors (NMDARs) are ionotropic glutamate receptors and they play a critical role in excitatory synaptic transmission in the mammalian central nervous system (CNS). Hyperactivity or hypoactivity of NMDARs can lead to a wide spectrum of pathological conditions and psychiatric disorders, such as Alzheimer's disease, Parkinson's disease, Huntington's disease, epilepsy, schizophrenia. NMDARs form a heterotetrameric complex made up of GluN1, GluN2(A-D) and/or GluN3(A, B) subunits. Different subtypes of NMDARs could have various effects on disease pathogenesis and therefore it is crucial to investigate the specific role of each subunit in the regulation of normal NMDAR functioning. The regulation of NMDARs occurs at different levels, from early processing, including synthesis, assembly, quality control in the endoplasmic reticulum (ER), trafficking to the cell surface, to internalization, recycling, and degradation. In this dissertation, we mainly focused on determining the roles of extracellular and transmembrane regions of different subtypes of NMDARs in the regulation of their function. In particular, using electrophysiology and microscopy methods on HEK293 cells and cultured hippocampal neurons, we investigated: (i) the impact of *N*-glycosylation and different lectins on the regulation of the functional properties of GluN1/GluN3 receptors; (ii) the effects of pathogenic mutations in the transmembrane domain (TMD) of the GluN1 subunit on surface delivery, and the functional and pharmacological properties of conventional and non-conventional di-heteromeric NMDARs; (iii) the role of

glycine-binding site integrity of the GluN1 and GluN3A subunits in the trafficking and functional properties of NMDARs.

2. Introduction

N-methyl-D-aspartate receptors (NMDARs) are ionotropic glutamate receptors that play a key role in the mammalian central nervous system (CNS). Normal functioning of NMDARs is important for excitatory synaptic transmission and memory formation. However, hyperactivity or hypoactivity of NMDARs can lead to a wide range of pathological conditions and psychiatric disorders, such as Alzheimer's disease, Parkinson's disease, Huntington's disease, epilepsy, and schizophrenia (Paoletti et al., 2013; Zhou and Duan, 2018).

NMDARs are heterotetrameric complex made up of two obligatory GluN1 subunits (which has eight splicing variants), GluN2 (GluN2A to GluN2D) subunits and/or GluN3 (GluN3A and GluN3B) subunits. All GluN subunits share the same topology, including the extracellular *N*-terminal domain (NTD) formed by amino-terminal domain (ATD) and ligand-binding domain (LBD), transmembrain domane (TMD) and the intracellular C-terminal domain (CTD).

ATD is defined by the first ~ 400 amino acid residues, has a “clamshell-like” structure formed by segments R1 and R2, and contains binding sites for allosteric modulators such as ifenprodil, protons, Zn^{2+}, polyamines (H. Furukawa and Gouaux, 2003; K. Furukawa, 2014). Also, evidence suggests that ATD mediates the assembly of the initial GluN

subunit dimers in the ER (Meddows et al., 2001). ATD is linked to LBD via ATD-LBD linkers. Similar to ATD, LBD is composed of two segments – S1 and S2, which create a binding pocket for ligands (Amin et al., 2021; H. Furukawa and Gouaux, 2003; C. H. Lee et al., 2014; Paoletti et al., 2013). LBD of GluN1 and GluN3 subunits contain a glycine-binding sites while LBD of GluN2 subunits contains glutamate-binding site (Traynelis et al., 2010).

The transmembrane domain (TMD) make up of tree transmembrane α-helices (M1, M3, and M4) and the M2 loop, where the M2 loop and the M3 segment are the major pore-lining domains (Wollmuth and Sobolevsky, 2004). The M2 loop forms the narrowest part of the ion channel and is a selective filter for ions as well as a binding site for Mg^{2+} and open-channel blockers (Hatton and Paoletti, 2005; Huettner, 2015). The M3 helices form a very tight arrangement around the receptor's pore, whereas the remaining M1 and M4 helices are located more at the periphery, around the ion channel (Karakas and Furukawa, 2014; Lee et al., 2014). The M3 helix is also in contact with the short pre-M1 helix that is oriented parallel to the membrane (Lee et al., 2014; Sanz-Clemente et al., 2013; Traynelis et al., 2010). The M3 helix include a conserved amino acid SYTANLAAF motif that can be found in all types of glutamate receptors. The LBD and TMD are connected through the three short linkers, that are labeled according to their position and orientation: S1-M1, M3-S2, and S2-M4, where S indicates the LBD segment and M the transmembrane helix. M3-S2 linkers are central polypeptide chains, directly connecting S2 segments from LBD with M3

helices, forming an ion channel. S1-M1 and S2-M4 linkers are located more in the periphery and participate in gating regulation, however, their exact contribution remains unknown (K. Furukawa, 2014; Johansen Amin et al., 2021).

CTD is the most variable part of the NMDARs, the length differs considerably between subunits, from ~50 residues in the GluN1 subunit and up to 660 residues in the the GluN2B subunit. CTD plays an important role in the stabilisation and anchoring of NMDARs to the cell cytoskeleton, as it contains binding sites for many regulatory molecules (Ataman et al., 2007; Warnet et al., 2020). Interestingly, the structure of the CTD remains undefined, only some short recognition motifs have been identified in the complexes with binding partners (e.g., short Ca2+/calmodulin-binding part) (Ataman et al., 2007). The lack of structures is probably due to the fact that CTDs belong to a class of intrinsically disordered regions (IDRs) that do not contain enough hydrophobic amino acids for folding into a defined 3D structure (Wright and Dyson, 2015). However, this region can be robustly predicted based on sequence alone (Nielsen and Mulder, 2019).

Different subtypes of NMDARs could have various effects on disease pathogenesis and therefore it is crucial to investigate the specific role of each subunit in the regulation of normal functioning of NMDARs. The regulation of NMDARs occurs at different levels, from early processing, including synthesis, assembly, quality control in the endoplasmic reticulum (ER), trafficking to the cell surface, to internalization, recycling, and degradation. In this dissertation

thesis, we mainly focused on determining the roles of extracellular and transmembrane regions of different subtypes of NMDARs in the regulation of their function. In particular, using electrophysiological and microscopical methods on both HEK293 cells and cultured hippocampal neurons, we investigated: (i) the impact of *N*-glycosylation and different lectins on the regulation of the functional properties of GluN1/GluN3 receptors; (ii) the effects of pathogenic mutations in the transmembrane domain (TMD) of GluN1 subunit on surface delivery, functional and pharmacological properties of conventional and non-conventional di-heteromeric NMDARs; (iii) the role of glycine-binding site integrity of the GluN1 and GluN3A subunits in the trafficking and functional properties of NMDARs.

3. Hypotheses and objectives

1) Previous studies found that GluN1/GluN2 receptors and GluN3A-containing NMDARs are extensively *N*-glycosylated. Several types of plant lectins have been shown to bind to NMDARs and affect the functional properties of the receptors. Also, earlier studies have shown that the functional properties of di-heteromeric GluN1/GluN2 receptors and native NMDARs are less sensitive to modulation by lectins compared to AMPARs and KARs (Everts et al., 1997; M. L. Mayer and Vyklicky, 1989), however, the specific effect of lectins on the functional properties of GluN1/GluN3 receptors has not yet been fully elucidated.

Objective: to examine whether the presence of specific *N*-glycans regulates the functional properties of

GluN1/GluN3 receptors, as well as test a panel of lectins for their potential to modulate the functional properties of GluN1/GluN3 receptors.

2) Previous studies found that the range of pathogenic mutations identified in GluN subunits – including mutations surrounding the binding site for open-channel blockers – alter the surface delivery, glutamate and glycine potency, sensitivity to Mg^{2+} and memantine (Chen et al., 2017; Fedele et al., 2018; Vyklicky et al., 2018). Memantine is FDA-approved compound commonly used for the treatment of Alzheimer's disease with a complex mechanism of action, including second site inhibition (SSI) (Glasgow et al., 2018), also referred to as membrane-to-channel inhibition (MCI) (Wilcox et al., 2022). Moreover, physiological concentrations of Mg^{2+} (on the order of 1 mM) alter inhibitory effects of memantine on GluN1/GluN2 receptors and thus, are an important factor when considering the therapeutic use of memantine (Johnson, 2019).

Objective: to examined whether three previously reported pathogenic mutations in the lower region of the M3 domain in GluN1 subunit – M641I, A645S and Y647S – affect the surface delivery, functional properties, and/or pharmacological properties of NMDARs expressed in HEK293 cells and cultured rat hippocampal neurons.

4. Materials and methods

Preparation of primary hippocampal neurons

All animal procedures were performed in accordance with ARRIVE guidelines and the European Commission Council Directive 2010/63/EU for experiments on animals.

Primary cultures hippocampal neurons were prepared from 18-day-old Wistar rat embryos (Lichnerova et al., 2015). In brief: the hippocampi were dissected in a cold dissection solution consisting of Hanks' balanced salt solution supplemented with 10 mM HEPES (pH 7.4) and penicillin-streptomycin (Life Technologies), then incubated for 20 minutes at 37 °C in dissection medium. The cells were then washed, dissociated using a glass pipette, resuspended and plated at a density of $2x10^4$ cells per cm^2 on poly-*L*-lysine–coated glass coverslips in plating medium consisting of minimum essential medium (MEM) supplemented with 10% heat-inactivated horse serum, N2 supplement (1X), 1 mM sodium pyruvate, 20 mM *D*-Glucose, 25 mM HEPES and 1 % penicillin-streptomycin; after 2 h, the plating medium was replaced with Neurobasal medium supplemented with B-27 and *L*-glutamine (Thermo Fisher Scientific).

Preparation of transfected HEK293 cells

HEK293 cells were cultured in Opti-MEM (Thermo Fisher Scientific) containing 5% fetal bovine serum (Thermo Fisher Scientific) (Kaniakova et al., 2012; Lichnerova et al., 2015). For electrophysiology, HEK293 cells were grown in 24-well plates and transfected with a total of 0.9 µg of cDNA constructs encoding the GluN1/GluN2 or GluN1/GluN3 subunits and GFP (to identify successfully transfected cells) mixed with 0.9 µl MATra-A Reagent (IBA) in 50 µl Opti-MEM I; the cells were then trypsinized and grown at lower density on poly-L-lysine–coated glass coverslips. For microscopy, HEK293 cells grown in 12-well plates were

transfected with a total of 0.45 µg of cDNA constructs encoding the GluN subunits (at a 1:2 ratio of tagged:untagged subunits) mixed with 1 µl Lipofectamine 2000 reagent (Thermo Fisher Scientific) in 50 µl Opti- MEM I.

Immunofluorescence microscopy

Surface NMDARs were labelled as described previously (Kaniakova et al., 2012; Lichnerova et al., 2015). In brief: cells were washed in phosphate-buffered saline (PBS), then incubated in blocking solution – PBS with 10% normal goat serum (NGS). Then, surface NMDARs were labeled using a rabbit anti-GFP primary antibody (15 min; 1:1000; Merck) followed by an anti-rabbit secondary antibody conjugated to Alexa Fluor 647 (15 min; 1:1000; Thermo Fisher Scientific). Then, the cells were fixed in 4% paraformaldehyde (PFA) in PBS, permeabilized with 0.25% Triton X-100 in PBS, and labeled with a mouse anti-GFP primary antibody (30 min; 1:1000; Merck) followed by a goat anti-mouse secondary antibody conjugated to Alexa Fluor 488 (30 min; 1:1000; Thermo Fisher Scientific). The cells were then mounted on glass slides using ProLong Antifade reagent (Thermo Fisher Scientific).

Images were obtained at room temperature using a fluorescence microscope (Olympus Scan) with an objective 60x/1.35 oil immersion or a confocal scanning microscope (Leica TCS SP8) equipped with solid-state lasers and apochromatic objective for an oil immersion of 63x/1.30. The images obtained were analyzed using the software ImageJ (NIH). In hippocampal neurons, the surface and total

fluorescence signal intensity was analyzed in 10 μm long segments of secondary and tertiary dendrites (Lichnerova et al., 2015).

Electrophysiology

Whole-cell patch-clamp recordings were made on transfected HEK293 cells using the Axopatch 200B amplifier (Molecular Devices). Borosilicate glass patch pipettes (3–6 MΩ tip resistance) were prepared using a P-97 puller (Sutter Instruments) and filled with intracellular recording solution containing (in mM): 125 gluconic acid, 15 CsCl, 5 BAPTA, 10 HEPES, 3 MgCl2, 0.5 CaCl2 and 2 ATP-Mg salts (pH 7.2 with CsOH). The standard extracellular solution (ECS) contained (in mM): 160 NaCl, 2.5 KCl, 10 HEPES, 10 D-glucose, 0.2 EDTA, and 0.7 CaCl2 (pH 7.3 with NaOH). For measuring the IC_{50} values for Mg^{2+} and measuring currents in the presence of 1 $MgCl_2$, EDTA was omitted from the ECS. For application extracellular solutions, a multi-barrel rapid perfusion system with a time constant of solution exchange around the cell of approximately 20 ms. Unless stated otherwise, all ECSs contained 50 μM glycine. For the recording from hippocampal neurons, the ECS contained 1 μM tetrodotoxin (TTX) and 10 μM bicuculine. All electrophysiological recordings were performed at room temperature, and the reported holding potential values were corrected for the calculated liquid junction potential of approximately 14 mV (Vyklicky et al., 2018). The NMDAR activation curves for glutamate and glycine were obtained using the following equation:
Equation (1):

$$I = I_{max}/(1 + (EC_{50}/[agonist])^h),$$

where I_{max} is the maximal response, EC_{50} is the concentration eliciting the half-maximal response, [agonist] is the glutamate or glycine concentration, and h is the Hill coefficient. The NMDARs inhibition curves were obtained using the following equation:

Equation (2):

$$I = 1/(1 + ([antagonist]/IC_{50})^h),$$

where IC_{50} is the concentration of Mg^{2+} or memantine that produced 50% inhibition of the agonist-evoked current, [antagonist] is the Mg^{2+} or memantine concentration, and h is the Hill coefficient. Time course of MK-801 or memantine inhibition was analyzed using single or double exponential function, a weighted time constants (τ_w) were obtained using the following equation:

Equation (3):

$$\tau_w = (\tau_{fast} * A_{fast} + \tau_{slow} * A_{slow})/(A_{fast} + A_{slow}),$$

where τ_{fast} and A_{fast} are the time constant and area, respectively, of the fast component, and τ_{slow} and A_{slow} are the time constant and area, respectively, of the slower component; normalized A_{fast} values were obtained by dividing each value by (A_{fast} + A_{slow}).

SSI was measured as described previously (Glasgow et al., 2018). In brief, the minimum fractional response after SSI (minimum $I_{SSI}/I_{control}$) was calculated as the average $I_{SSI}/I_{control}$ value measured over a 200-ms window centered on the minimum ratio value; $I_{control}$ was calculated as the average of Icontrol1 and $I_{control2}$; responses in which the $I_{control2}/I_{control1}$ value was <0.8 were excluded from the analysis.

NMDA-induced excitotoxicity

To induce excitotoxicity, neurons at DIV14 were placed overnight in a minimal defined medium containing 10% MEM (Invitrogen) and 90% Salt-Glucose (SG) medium containing (in mM): 114 NaCl, 0.219% $NaHCO_3$, 5.292 KCl, 1 $MgCl_2$, 2 $CaCl_2$, 10 HEPES, 30 glucose, 0.5 sodium pyruvate, and 0.1% phenol red (McQueen et al., 2017; Skrenkova et al., 2020). The following day, the neurons were placed in 100% SG medium containing glycine, NMDA, and memantine (Hello Bio) at the indicated concentrations. After 1 h, the medium was changed to 10% MEM and 90% SG medium, and after an additional 22–23 h, the neurons were labelled with 5 μM Hoechst 33342 (Molecular Probes) for 30 min and then fixed in 4% PFA in PBS. After the neurons were permeabilized using Triton X-100, the YFP-GluN1 subunits were labelled with mouse anti-GFP and goat anti-mouse Alexa Fluor 488 antibodies as described above.

Images (1024 × 1024 pixels with a pixel size of 1.243 μm × 1.243 μm, thus covering a field of view 1272 μm × 1272 μm in size) were acquired using an Olympus FV10i confocal microscope equipped with a 10x/0.4 NA super apochromat objective. For each field of view, three images were obtained: the YFP signal (to indicate infected cells), Hoechst (for nuclear staining), and a DIC image. Nuclear area was measured using software ImageJ (NIH), and a custom-made macro script was used to automatically measure nuclear area exclusively in infected cells identified by YFP expression. The number of cells per condition was 519–1407, 17446-24758 cells were collected in each experiment (all conditions summed). The

MATLAB (2019b) was used to classify cells as pyknotic or non-pyknotic based on the nuclear area measured for each cell.

5. Results

5.1. Three pathogenic mutations in the M3 domain of the GluN1 subunit regulate the surface delivery and pharmacological sensitivity of NMDARs

First, we asked whether three pathogenic mutations in the M3 domain of the GluN1 subunit (Lemke et al., 2016) alter the surface delivery of GluN1/GluN2A, GluN1/GluN2B, and GluN1/GluN3A receptors expressed in HEK293 cells; these mutations are shown schematically in Fig. 1A. For this purpose, we generated YFP-tagged GluN1-1a subunits containing the pathogenic mutations M641I, A645S, Y647S; we then co-expressed these subunits together with the GluN2A, GluN2B, and GluN3A subunits and measured their surface and total expression levels using immunostaining with an anti-GFP antibody; example images of transfected cells are shown in Fig. 1B. We found that cells expressing GluN1-1a-M641I/GluN2A, GluN1-Y647S/GluN2A, and GluN1-1a-Y647S/GluN2B receptors had significantly reduced surface delivery; all other NMDARs combinations studied were delivered to the cell surface at the same level as their corresponding wild-type receptors (Fig. 1C). These results indicate that specific pathogenic mutations in the M3 domain of the GluN1-1a subunit differentially alter the trafficking of NMDARs subtypes. Similar to our results obtained with the GluN1-1a splice variant, we found that the GluN1-4a-M641I/GluN2A, GluN1-4a-Y647S/GluN2A, and GluN1-4a-

Y647S/GluN2B receptors – but not any other NMDAR combinations tested – had significantly reduced surface delivery compared to wild-type receptors (Fig. 1D). Taken together, these data confirm that specific pathogenic mutations in the M3 domain of the GluN1 subunit affect the surface delivery of NMDARs, and this effect is apparently independent of the GluN1 splice variant.

Next, we examined whether these pathogenic mutations in the M3 domain of GluN1 subunit affect the surface delivery of NMDARs in neurons. Ten days after viral infection, we performed immunostaining using an anti-GFP antibody and measured surface and total levels of the GluN1-1a subunits using confocal microscopy (Fig. 1E). Our analysis revealed that the GluN1-1a-A645S subunit was expressed at the surface at the same level as the wild-type subunit, whereas the GluN1-1a-M641I and GluN1-1a-Y647S subunits were significantly reduced at the cell surface (Fig. 1F). These findings are consistent with our data obtained with HEK293 cells and confirm that specific pathogenic mutations in the M3 domain of the GluN1 subunit affect the surface delivery of NMDARs.

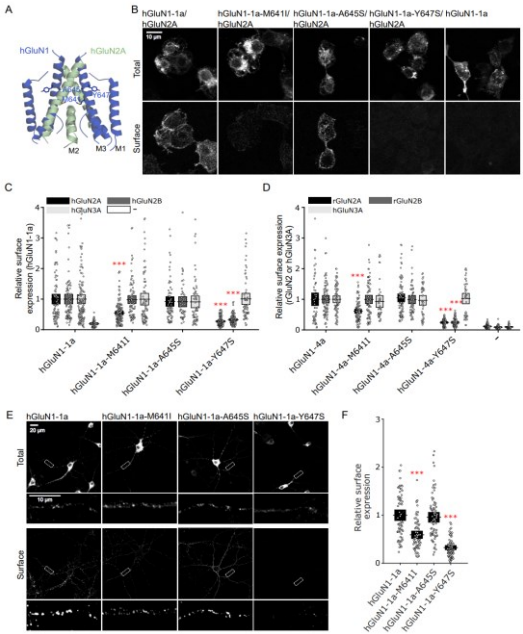

Fig. 1. Pathogenic mutations in GluN1 subunit differentially alter the surface delivery of NMDARs in a subunit-dependent manner. (A) Structural model of the M1, M2, and M3 domains in the GluN1/GluN2A heterotetramer (PDB code: 6IRA); the three amino acid residues studied here are indicated. (B) Representative images of HEK293 cells transfected with the GluN2A subunit and the indicated wild-type or mutant YFP-GluN1-1a (GluN1-1a) subunits; total and surface GluN1-1a

subunits were labeled 24 h after transfection using an anti-GFP antibody. (C–D) Summary of the relative surface expression of wild-type and mutant GluN1-1a (C) or GluN1-4a (D) subunits co-transfected with the indicated untagged GluN2 or GluN3A subunits (C) or GFP-GluN2 (GluN2) and GFP-GluN3A (GluN3A) subunits (D), measured using fluorescence microscopy ($n \geq 70/49$ cells per group); ***$p < 0.001$ vs. the corresponding wild-type NMDARs, (one-way ANOVA). (E) Representative images of cultured rat hippocampal neurons infected with lentiviruses encoding the indicated YFP-GluN1-1a (GluN1-1a) subunits; total and surface GluN1-1a subunits were labeled using an anti-GFP antibody. (F) Summary of the relative surface expression of the indicated GluN1-1a subunits measured in 10-μm segments of secondary or tertiary dendrites ($n \geq 30$ segments in ≥6 different cells per group); ***$p < 0.001$ vs. GluN1- 1a, (one-way ANOVA).

Next, we measured the dose-response curves for Mg^{2+} block of wild-type and mutant GluN1-4a/GluN2A and GluN1-4a/GluN2B receptors in the presence of saturating concentration (1 mM) of glutamate (Fig. 2A, C). We found that neither the M641I mutation nor the A645S mutation in the GluN1-4a subunit affected the IC_{50} value for Mg^{2+}, regardless of the GluN2 subunit co-expressed in the HEK293 cells (Fig. 2B, D). Thus, neither of these pathogenic mutations affects the sensitivity of GluN1-4a/GluN2 receptors to Mg^{2+}.

We then measured NMDARs sensitivity to memantine using the same approach as above; for these experiments, the ECS contained 0 mM Mg^{2+} (Fig. 2E–H). Our analysis revealed that memantine inhibited both GluN1-4a/GluN2A and GluN1-4a/GluN2B receptors with an IC_{50} value of approximately 1 μM (Fig. 2F, H), which is consistent

with previously published data (Kotermanski and Johnson, 2009). In contrast to our experiments involving Mg^{2+}, we found that the IC_{50} value for memantine was significantly increased for receptors containing the GluN1-4a-A645S subunit (2 E-H), but was unaffected in receptors containing the GluN1-4a-M641I subunit (Fig. 2F, H). Thus, the two pathogenic mutations in the GluN1 subunit do not affect the sensitivity of NMDARs to Mg^{2+}, but differentially affect the sensitivity of NMDARs to memantine.

A previous study found that physiological levels of extracellular Mg^{2+} (approximately 1 mM) affect the selectivity of NMDARs to memantine (Kotermanski and Johnson, 2009). We therefore examined whether the pathogenic mutations in the M3 domain of GluN1 subunit affect the sensitivity of NMDARs to memantine in the presence of 1 mM Mg^{2+} by measuring whole-cell currents induced by 1 mM glutamate at membrane potential of −60 mV, and increasing concentrations of memantine (Fig. 2I). For these experiments, we focused on GluN2A-containing NMDARs, as they generally yield larger currents in HEK293 cells compared to GluN2B-containing NMDARs, thus allowing us to more readily examine the effect of memantine on glutamate-induced currents in the presence of 1 mM Mg^{2+}. In the presence of 1 mM Mg^{2+}, we observed that the IC_{50} value for memantine was approximately 14 μM at wild-type GluN1-4a/GluN2A receptors (Fig. 2J and K), consistent with previously published data (Kotermanski and Johnson, 2009). Interestingly, we found that GluN1-4a-M641I/GluN2A receptors had a significantly decreased IC_{50} value (~2 μM), whereas GluN1-4a-A645S/GluN2A receptors

had a significantly increased IC_{50} value (~32 μM) for memantine in the presence of 1 mM Mg^{2+} compared to wild-type GluN1-4a/GluN2A receptors; the IC_{50} values for memantine in the absence and presence of 1 mM Mg^{2+} for various GluN1-4a/GluN2A receptors are summarized in Fig. 2K. In addition, we examined the sensitivity of NMDARs to memantine in HEK293 cells voltage-clamped at membrane potentials of −20 mV and +40 mV and found that IC_{50} values for memantine were significantly decreased at GluN1-4a-M641I/GluN2A receptors and significantly increased at GluN1-4a-A645S/GluN2A receptors compared to wild-type GluN1-4a/GluN2A receptors at both membrane potentials (Fig. 2L–N). Taken together, these data indicate that the M641I and A645S mutations in the M3 domain of the GluN1 subunit increase and decrease, respectively, sensitivity of the GluN1/GluN2 receptor to memantine in physiologically relevant levels of extracellular Mg^{2+} and membrane potentials.

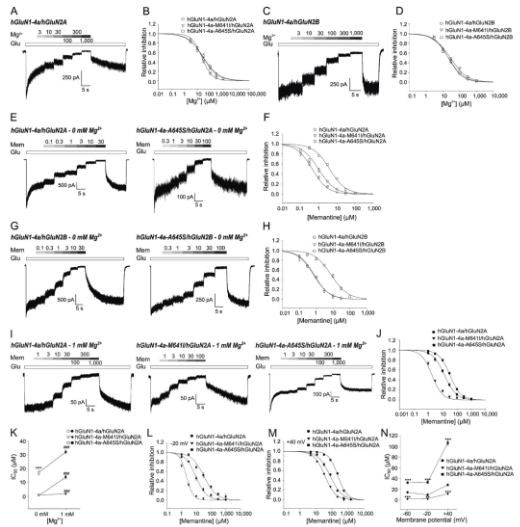

Fig. 2. Specific pathogenic mutations in the M3 domain of GluN1 subunit differentially affect the sensitivity of GluN1/GluN2 receptors to memantine but not to Mg^{2+}. (A, C) Representative whole-cell recordings of HEK293 cells transfected with GluN1-4a/GluN2A (A) or GluN1-4a/GluN2B (C) receptors voltage-clamped at a membrane potential of −60 mV. The indicated concentrations of Mg^{2+} (in μM) were applied in the continuous presence of 1 mM glutamate (Glu). (B, D) Normalized dose-response curves for Mg^{2+} block obtained by fitting the data with Equation (2) (see Methods). Each data point represents the mean normalized current obtained from ≥5 cells ± SEM. (E, G) Representative whole-cell recordings of HEK293 cells transfected with the indicated

GluN1-4a/GluN2A (E) or GluN1-4a/GluN2B (G) receptors voltage-clamped at a membrane potential of −60 mV. The indicated concentrations of memantine (Mem, in μM) were applied in the continuous presence of 1 mM Glu. (F, H) Normalized dose-response curves for memantine inhibition (measured in 0 mM Mg^{2+}) were obtained by fitting the data with Equation (2). Each data point represents the mean normalized current obtained from ≥5 cells ± SEM. (I) Representative whole-cell recordings of HEK293 cells transfected with the indicated GluN1-4a/GluN2A receptors voltage-clamped at a membrane potential of −60 mV measured in the presence of 1 mM Mg^{2+}. The indicated concentrations of Mem (in μM) were applied in the continuous presence of Glu and 1 mM Mg^{2+}. (J) Normalized dose-response curves for memantine inhibition measured in 1 mM Mg^{2+} were obtained by fitting the experimental data with Equation (2). Each data point represents the mean normalized current obtained from ≥4 cells ± SEM. (K) The IC_{50} values for memantine plotted against extracellular Mg^{2+} concentration for the indicated GluN1-4a/GluN2A receptors. ***$p < 0.001$ vs. GluN1-4a/GluN2A receptors (one-way ANOVA with Tukey's post hoc test); ###$p < 0.001$ vs. 0 mM Mg^{2+} (Student's t-test). (L, M) Normalized dose-response curves for memantine inhibition measured in HEK293 cells at a holding membrane potential of −20 mV (L) or +40 mV (M). (N) The IC_{50} values for memantine measured in 1 mM Mg^{2+} plotted against membrane potentials for the indicated GluN1-4a/GluN2A receptors. **$p < 0.010$ and ***$p < 0.001$ vs. wild-type GluN1-4a/GluN2A receptors (one-way ANOVA with Tukey's post hoc test).

Importantly, memantine can also act upon GluN1/GluN2 receptors via a second site that is accessible in the absence of agonists, a phenomenon known as second-site inhibition (SSI)

(Glasgow et al., 2018), also referred to as membrane-to-channel inhibition (MCI) (Wilcox et al., 2022). To induce SSI, HEK293 cells were treated with 100 μM memantine; after removal of memantine, 1 mM glutamate is added, and the glutamate-induced current was compared to currents elicited without and prior treatment with memantine (Fig. 3A). To quantify these data, we calculated the minimum ratio between SSI currents and control currents ("minimum $I_{SSI}/I_{control}$"); these results are summarized in Fig. 3B. Consistent with previous reports (Blanpied et al., 1997; Glasgow et al., 2018; Kotermanski and Johnson, 2009), we observed that the minimum $I_{SSI}/I_{control}$ for GluN1-4a/GluN2A receptors was approximately 0.5 in control conditions and in HEK293 cells treated with both memantine and either D-APV (a competitive antagonist for the glutamate-binding site in the GluN2 subunit) or 1 mM Mg^{2+}; moreover, the minimum $I_{SSI}/I_{control}$ increased to approximately 0.9 when 1 mM Mg^{2+} was present throughout the entire experiment (Fig. 3B). In addition, we found that the time constant of the recovery from SSI ($\tau_{recovery}$) was approximately 6 s for wild-type GluN1-4a/GluN2A receptors under control conditions (Fig. 3C). We then examined NMDARs containing pathogenic mutations in the GluN1 subunit and found that the minimum $I_{SSI}/I_{control}$ for GluN1-4a-M641I/GluN2A receptors was similar to wild-type GluN1-4a/GluN2A receptors under all conditions, with the exception of a significant decrease of the minimum $I_{SSI}/I_{control}$ in the continuous presence of 1 mM Mg^{2+} (Fig. 3B); $\tau_{recovery}$ for the GluN1-4a-M641I/GluN2A receptors was also similar to wild-type GluN1-4a/GluN2A receptors (Fig. 3C). In contrast, we

found that the minimum $I_{SSI}/I_{control}$ for GluN1-4a-A645S/GluN2A receptors was significantly increased in comparison to wild-type Glu-N1-4a/GluN2A receptors (~0.8) under all conditions and was not different from wild-type GluN1-4a/GluN2A receptors when measured in the continuous presence of 1 mM Mg^{2+} (Fig. 3B); we could not calculate $\tau_{recovery}$ for GluN1-4a-A645S/GluN2A receptors because of the relatively weak memantine-induced SSI measured at these receptors. Glasgow et al. reported that SSI requires memantine to transit from the second site to the deep site (Glasgow et al., 2018). Consistent with previous data (Glasgow et al., 2018), we found that holding the membrane potential at +40 mV (instead of −60 mV) eliminated memantine-induced SSI (i.e., $I_{SSI}/I_{control}$ was approximately 1) for both wild-type and mutant GluN1-4a/GluN2A receptors (Fig. 3D, F). In contrast, we found that stepping (i.e., "jumping") the membrane potential from −60 mV to +40 mV only when applying memantine had no effect on memantine-induced SSI compared to holding the membrane potential at −60 mV throughout the entire recording (Fig. 3E and F). Taken together, these data indicate that the M641I and A645S mutations in the GluN1 subunit differentially affect ability of memantine to induce SSI at NMDARs.

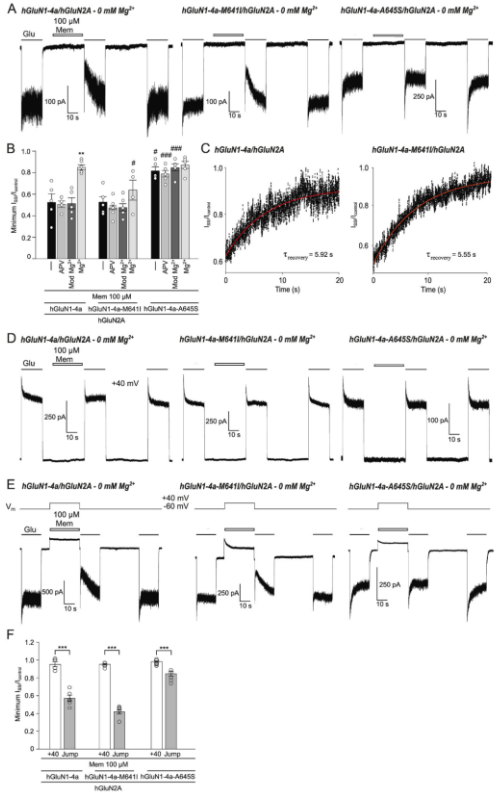

Fig. 3. Specific pathogenic mutations in the M3 domain of the GluN1 subunit differentially affect memantine-mediated SSI

of GluN1/GluN2A receptors. (A) Representative whole-cell recordings of HEK293 cells expressing the indicated GluN1-4a/GluN2A receptors voltage-clamped at a membrane potential of −60 mV. Where indicated, 1 mM glutamate (Glu) and 100 μM memantine (Mem) were applied. (B) Summary of minimum $I_{SSI}/I_{control}$ calculated for the indicated GluN1-4a/GluN2A receptors (see Methods). "–", control condition; "APV", 50 μM D-APV was co-applied with Mem; "Mod Mg^{2+}", 1 mM Mg^{2+} was co-applied with Mem; "Mg^{2+}", 1 mM Mg^{2+} was present throughout the entire recording (see text for more details); $n \geq 5$ cells per each condition. **$p < 0.001$ vs. control condition (one-way ANOVA); #$p < 0.050$ and ###$p < 0.001$ vs. the wild-type GluN1-4a/GluN2A receptors (one-way ANOVA). (C) $I_{SSI}/I_{control}$ is plotted from the example traces shown in panel A, with the corresponding time constant of recovery from SSI ($\tau_{recovery}$) shown. The average $\tau_{recovery}$ values were 6.25 ± 0.72 s and 6.83 ± 0.66s for cells expressing GluN1-4a/GluN2A and GluN1-4a-M641I/GluN2A receptors, respectively ($n \geq 5$ cells per each group; $p > 0.05$; Student's t-test). (D, E) Representative whole-cell recordings of HEK293 cells expressing the indicated GluN1-4a/GluN2A receptors voltage-clamped at a fixed membrane potential of +40 mV (D) or at −60 mV with a step ("jump") to +40 mV during Mem application (E). (F) Summary of minimum $I_{SSI}/I_{control}$ calculated for the indicated GluN1-4a/GluN2A receptors recorded as shown in panels D (+40; gray bars) and E (Jump, black bars); $n \geq 5$ cells per each group. ***$p < 0.001$ vs. +40 mV (Student's t-test).

Next, we performed electrophysiological measurements from cultured hippocampal neurons expressing either wild-type or mutant GluN1-1a subunits to analyze the memantine sensitivity in the presence of 1 mM Mg^{2+} at a membrane potential of −60 mV; for these experiments, we used 300 μM

NMDA instead of glutamate to activate the NMDARs, and both TTX and bicuculine were present throughout the recordings. Similar to our findings obtained with HEK293 cells, we found that the IC_{50} value for memantine was significantly decreased for YFP-GluN1-1a-M641I-expressing neurons, whereas significantly increased for YFP-GluN1-1a-A645S-expressing neurons, when compared to wild-type YFP-GluN1-1a-expressing neurons (Fig. 4 A–B). Furthermore, when we recorded at membrane potentials from −80 mV to +80 mV (in 20 mV incremental steps), we observed that 30 μM memantine more effectively inhibited NMDARs from neurons expressing YFP-GluN1-1a-M641I, but less effectively NMDARs from neurons expressing YFP-GluN1-1a-A645S, both compared to neurons expressing YFP-GluN1-1a (except for neurons expressing YFP-GluN1- 1a-A645S measured at membrane potentials of −20 mV and 0 mV; Fig. 4C–D). Thus, as in HEK293 cells, two different mutations in the M3 domain of the GluN1 subunit differentially affect the sensitivity of NMDARs to memantine when expressed in hippocampal neurons.

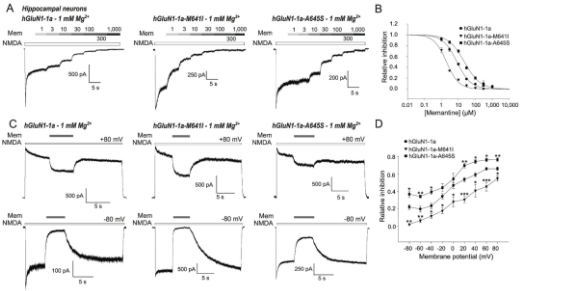

Fig. 4. Specific pathogenic mutations in the M3 domain of the GluN1 subunit differentially affect the sensitivity of neuronal NMDARs to memantine. (A) Representative whole-cell recordings of cultured hippocampal neurons infected with lentiviruses expressing the indicated YFP-tagged GluN1-1a (GluN1-1a) subunits; the membrane potential was voltage-clamped at −60 mV. Endogenous GluN1 subunits were knocked down by expressing a shRNA-GluN1. The indicated concentrations of memantine (Mem; in μM) were applied in the continuous presence of 300 μM NMDA, 50 μM glycine, 1 μM TTX, 10 μM bicuculine, and 1 mM Mg^{2+}. (B) Normalized dose-response curves for memantine inhibition in the continuous presence of 1 mM Mg^{2+} were obtained by fitting the data with Equation (2). Each data point represents the mean normalized current obtained from ≥4 cells ± SEM. (C) Representative whole-cell patch-clamp recordings measured from cultured infected hippocampal neurons held at a membrane voltage of −80 mV or +80 mV.

NMDARs were activated exactly as described in A, 30 μM memantine was used for all conditions. (D) Graph summarizing the relative inhibition induced by 30 μM memantine, measured from hippocampal neurons expressing the GluN1-1a, GluN1-1a-M641I and GluN1-1a-A645S at the indicated membrane potentials. $n \geq 5$ cells per each condition; one-way ANOVA with Tukey's post hoc test); *$p < 0.050$, **$p < 0.010$, and ***$p < 0.001$ vs. GluN1-1a.

Lastly, we examined whether the mutations in the GluN1 subunit affect NMDA-induced excitotoxicity in cultured hippocampal neurons. We therefore expressed either wild-type or mutant YFP-GluN1-1a subunits in neurons; we then cultured the neurons in medium containing 1 mM Mg^{2+} together with 10 μM glycine and 0, 30, or 100 μM NMDA as well as in various concentrations of memantine for 1 h, followed by an additional culturing for 22–23 h. The percentage of dead cells was then determined by staining the nuclei with Hoechst 33342 and measuring nuclear area (Fig. 5A). Using this protocol, we found that neurons expressing the wild-type YFP-GluN1-1a subunit underwent significant excitotoxicity (~80%) upon treatment with either 30 μM or 100 μM NMDA, and memantine significantly reduced excitotoxicity in a dose- dependent manner (Fig. 5B–E). Neurons expressing either the YFP- GluN1-1a-M641I or YFP-GluN1-1a-A645S subunits were also susceptible to NMDA-induced excitotoxicity, with a percentage of death cells similar to wild-type YFP-GluN1-1a-expressing neurons. Interestingly, and consistent with our electrophysiology data,

we found that memantine differentially affected NMDA-induced excitotoxicity in neurons expressing the mutant GluN1 subunits. Specifically, memantine significantly reduced excitotoxicity in neurons expressing the YFP-GluN1-1a-M641I subunit but was significantly less neuro- protective in neurons expressing the YFP-GluN1-1a-A645S subunit in comparison to neurons expressing wild-type YFP-GluN1-1a subunit (Fig. 5D and E). These data indicate that specific pathogenic mutations in the M3 domain of the GluN1 subunit differentially affect the pharmacological sensitivity of NMDARs in hippocampal neurons.

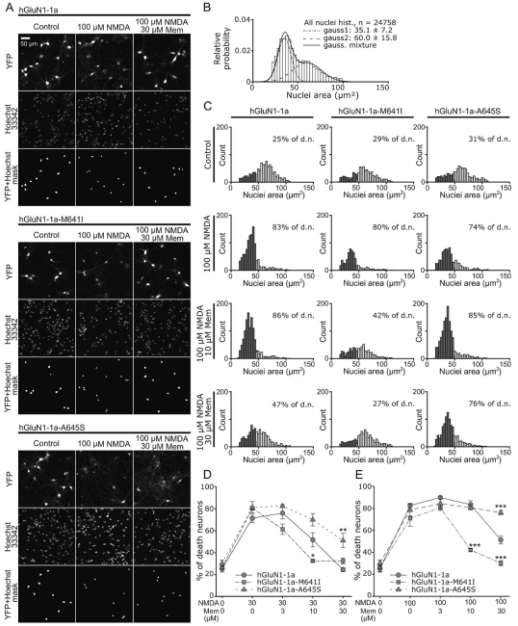

Fig. 5. Memantine differentially affects NMDA-induced excitotoxicity in hippocampal neurons expressing mutated GluN1 subunits. (A) Representative fluorescence images of YFP and Hoechst 33342 staining in hippocampal neurons expressing YFP-GluN1-1a (GluN1-1a), YFP-GluN1-1a-M641I (GluN1-1a-M641I), or YFP-GluN1-1a-A645S (GluN1-1a- A645S) subunits. Where indicated, the neurons were untreated (Control; left column) or treated with either 10 µM glycine and 100 µM NMDA (middle column) or 10 µM

glycine, 100 μM NMDA, and 30 μM memantine (Mem) (right column). Upper rows: the YFP channel; middle rows: the Hoechst 33342 channel; and bottom rows: a mask was applied to select only the nuclei of cells expressing YFP. (B) Histogram showing the distribution of the nuclear size measured for all neurons, revealing two clearly distinguishable groups representing pyknotic (i.e., dead) and non-pyknotic neurons. The data were fitted with a mixture of two Gaussian distribution models (the solid line), and the Gaussian parameters (mean and sigma values) were estimated for each distribution and are shown. The estimated individual Gaussian distributions are shown as a dotted line (pyknotic cells) and as a dashed line (non-pyknotic cells). (C) Histograms showing the distributions of nuclear area for the neurons in the indicated conditions. For each condition, the neurons were classified based on the probability of being pyknotic (dark gray bars) or non-pyknotic (white bars), with the corresponding percentage of dead (i.e., pyknotic) neurons indicated (D–E) Summary of the percentage of dead (i.e., pyknotic). neurons expressing the indicated GluN1-1a subunits and treated with the indicated concentrations of memantine (Mem) in the presence of 30 μM (D) or 100 μM (E) NMDA; the classified nuclei were counted for each condition, and the number of pyknotic cells is expressed as the percentage of the total number of cells analyzed. The error bars indicate the SEM; $n \geq 5214$ cells per each condition collected from 5 independent experiments. *$p < 0.050$, **$p < 0.010$, and ***$p < 0.001$ vs. wild-type GluN1-1a subunit (one-way ANOVA; all data passed the Shapiro–Wilk normality test, $p < 0.05$).

5.2. The presence of putative N-glycosylation sites and their interaction with specific lectins regulates the functional properties of GluN1/GluN3 receptors

As shown in Fig. 6A and B, the GluN1 and GluN3A subunits each contain 12 putative *N*-glycosylation consensus

sites (N-X-S/T) (Skrenkova et al., 2018); in contrast, the GluN3B subunit contains 6 putative *N*-glycosylation consensus sites (Fig. 6B). Here, we combined electrophysiology with a rapid solution exchange system in which we applied a wide range of glycine concentrations (from 10 μM to 10 mM) to HEK293 cells transfected with wild-type or mutant (N→Q) forms of GluN1/GluN3 receptors. We found no difference between wild-type and mutated GluN1/GluN3A receptors with respect to the normalized peak current amplitude or τ_w of desensitization measured in response to various concentrations of glycine, however, we found differences in functional properties between wild-type and mutated GluN1/GluN3B receptors. Since, GluN1/GluN3B receptors produce a large tail current at the end of the glycine application (Smothers and Woodward, 2009), where appropriate, we measured the ratio of the steady-state current amplitude to the peak current amplitude (ss/p), as well as the ratio of the peak tail current amplitude to the steady-state current (t/ss) of wild-type GluN1/GluN3B and GluN1/GluN3B that lack triplet sets as well as single putative N-glycosylation sites. Our analysis revealed that the t/ss ratio was increased for the GluN1-N440Q/GluN3B, GluN1-4/4N→Q/GluN3B and GluN1-N674Q/GluN3B receptors, but was unchanged in the remaining GluN1/GluN3B receptors tested (Fig. 6C).

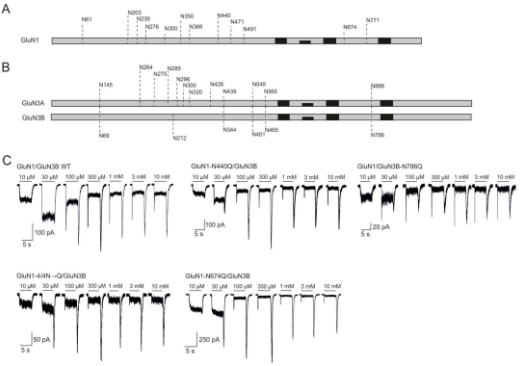

Fig. 6. Overview of putative *N*-glycosylation sites in GluN1, GluN3A, and GluN3B subunits. (A–B) Schematic diagram showing the approximate location of the 12 putative N-glycosylation consensus sites (N-X-S/T) in the GluN1 (A) and GluN3A (B) subunits, and the 6 putative N-glycosylation consensus sites in the GluN3B subunit (B); the four solid black boxes in each subunit indicate the membrane-spanning domains. (C) Representative whole-cell voltage-clamp recordings of human embryonic kidney 293 (HEK293) cells transfected with the indicated GluN1/GluN3B receptors. Currents were elicited by application of the indicated concentrations of glycine (indicated by the horizontal black bars).

Next, we examined the effect of lectins on the functional properties of GluN1/GluN3B receptors. We pre-treated HEK293 cells expressing GluN1/GluN3B receptors for 8 min in each lectin at 200 μg/ml, and then measured the properties

of glycine-induced currents (Fig. 7A). Our analysis revealed that 14 of the 19 lectins tested significantly reduced the t/ss ratio measured in GluN1/GluN3B receptors (Fig. 7B and Table 1). We then focused our analysis on ConA, WGA, and AAL and found that all three lectins significantly increased both the ss/p ratio (Fig. 7C) and the 10–90% rise time for the onset of glycine-induced currents (Fig. 7D) of the GluN1/GluN3B receptors. We also found that 20 μg/ml ConA, WGA, and AAL was sufficient to reduce the t/ss ratio to the same extent as 200 μg/ml (Fig. 7E; compare with Fig. 7B).

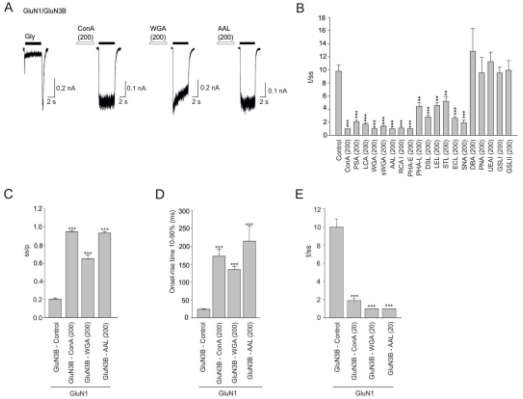

Fig. 7. GluN1/GluN3B receptors are modulated by specific lectins. (A) Whole-cell currents were elicited with a 5-s pulse of 500 μM glycine (indicated by the black bar) in HEK293 cells expressing GluN1/GluN3B receptors. Where indicated, the cells were pre-incubated with 200 μg/ml ConA, WGA, or

AAL for 8 min (indicated by the white bars, not to scale). (B) Summary of t/ss ratio measured for GluN1/GluN3B receptors; where indicated, the cells were pre-incubated with 200 μg/ml of the indicated lectins (n≥5 cells/group). (C–E) The ss/p ratio, 10–90% onset rise time, and t/ss ratio were measured during a 5-s application of 500 μM glycine in cells expressing GluN1/GluN3B receptors; where indicated, the cells were pre-incubated with 200 μg/ml (C and D) or 20 μg/ml (E) ConA, WGA, or AAL (n ≥ 5 cells/group). **p < 0.01, ***p < 0.001 versus control-treated cells (one-way ANOVA).

Next, we examined whether the effect of lectins on GluN1/GluN3B receptors is conformation-dependent. We therefore measured glycine-induced currents before and after a 1-min application of 20 μg/ml ConA, WGA, or AAL and analyzed the p_2/p_1 ratio of GluN1/GluN3B receptors (Fig. 8A–B). Our analysis revealed that all three lectins significantly increased the p_2/p_1 ratio of GluN1/GluN3B receptors (Fig. 8B). Interestingly, we observed that compared to wild-type receptors the effect of AAL was significantly lower in receptors containing GluN3B–N465Q subunit (Fig. 8A, B), supporting the notion that N465 in the GluN3B subunit plays a role in the ability of AAL to modulate the functional properties of GluN1/GluN3B receptors. In contrast, when we applied the lectins in the continuous presence of 500 μM glycine, we found no or minor effect (Fig. 8C); thus, similar to our findings with respect to GluN1/GluN3A receptors, the

ability of lectins to modulate GluN1/GluN3B receptors appears to be dependent on the conformation.

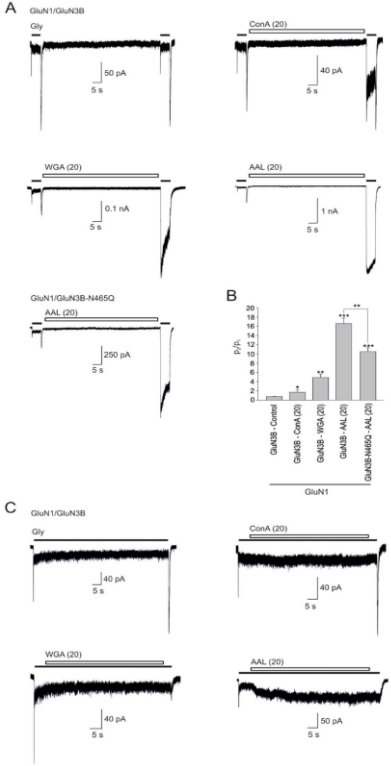

Fig. 8. Investigating the mechanism of action of selected lectins on GluN1/GluN3B receptors. (A) Whole-cell currents through GluN1/GluN3B receptors were elicited with a 5-sec pulse of 500 μM glycine (indicated by the black bar) before and after a 1-min application of 20 μg/ml ConA, WGA, or AAL. (B) Summary of p2/p1 measured in cells expressing either wild-type GluN1/GluN3B or GluN1/GluN3B–N465Q receptors; where indicated, 20 μg/ ml ConA, WGA, or AAL was applied between the two glycine pulses ($n \geq 5$ cells/group). (C) Representative whole-cell currents through GluN1/ GluN3B receptors elicited with an application of 500 μM glycine (indicated by the black bar); where indicated, 20 μg/ml ConA, WGA, or AAL was applied for 1 min in the continued presence of glycine. Only AAL had a slight potentiating effect, with a mean increase of the steady-state current amplitude of 310 ± 60% ($n = 5$) by the end of the 1-min application of AAL. *$p < 0.05$, **$p < 0.01$, ***$p < 0.001$ versus control-treated cells or between the in- dicated groups (ANOVA).

6. Discussion

6.1. Three pathogenic mutations in the M3 domain of the GluN1 subunit regulate the surface delivery and pharmacological sensitivity of NMDARs

We focused on three pathogenic mutations in the M3 domain of the GluN1 subunit - M641I, A645S, and Y647S - associated with intellectual disability, movement disorders, and seizures (Lemke et al., 2016). We showed that this mutations affect the surface delivery of NMDARs in HEK293 cells in subunit-dependent manner – specifically, GluN1-M641I mutation significantly reduces surface expression of GluN1/GluN2A receptors, but not GluN1/GluN2B or GluN1/GluN3A receptors, GluN1-Y647S mutation reduces

surface expression of GluN1/GluN2A and GluN1/GluN2B receptors, but not GluN1/GluN3A receptors and GluN1-A645S mutation did not affect the level of surface expression whether was co-expressed with GluN2A, GluN2B or GluN3A subunits. Moreover, our microscopy data obtained on using hippocampal neurons (DIV14) demonstrated the same changes in surface expression as observed in HEK293 cells when mutated GluN1 subunits were co-expressed with the GluN2A subunit. These results are consistent with the finding that hippocampal neurons have low expression of endogenous GluN3 subunit and high expression of GluN2A subunit (Hansen et al., 2021; Henson et al., 2010; Paoletti et al., 2013; Vieira et al., 2020). Similarly to this finding, it has been shown that *de novo* mutation GluN1-G620R – associated with developmental delay and behavioural abnormalities – reduces surface delivery of GluN1/GluN2B receptors, but not GluN1/GluN2A receptors (Chen et al., 2017).

Moreover, our group previously showed that specific amino acid residues in the M3 domain of GluN1 and GluN2 subunits (GluN1-W636, GluN2A-W634, GluN2B-W635) contribute to the regulation of trafficking of NMDARs to the cell surface (Kaniakova et al., 2012). Furthermore, pathogenic mutations GluN2B-W607C and GluN2B-S628F in the TMD - associated with intellectual disability and developmental delay - reduce surface delivery of NMDARs, as well as sensitivity of NMDARs to glutamate, glycine and Mg^{2+} block (Vyklicky et al., 2018). In our further experiment we also observed changes in the receptor's functional properties, specifically – we found that the EC_{50} value for glycine was increased for GluN1-

M641I/GluN3A receptors compared to WT GluN1/GluN3A, and we found that GluN1-A645S/GluN3A receptors had a slower τ_w of desensitization. The changes in desensitisation are consistent with evidences that mutations in the TMD, including SYTANLAAF motif, alter current kinetics of GluN1/GluN2A receptor (Hu and Zheng, 2005). Although we found that the GluN1-Y647S mutation does not alter expression of GluN1/GluN3A receptors, our electrophysiological experiments revealed no glycine-induced current unless CGP-78608 application was applied (Grand et al., 2018). Therefore, we hypothesise that GluN1-Y647S mutation presumably changes specific functional properties of GluN1/GluN3A receptors, such as P_o. However, we cannot test this assumption because, unlike the open-channel blocker of GluN1/GluN2 receptor MK-801, no specific open-channel blocker of GluN1/GluN3A receptor exists at present (Chatterton et al., 2002).

Reduction in agonist and/or antagonist sensitivity was also reported for other pathogenic mutations, such as N615I-GluN2B located at the beginning of the M2–M3 linker, and V618G-GluN2B, located in the M2–M3 linker – associated with West syndrome – reduce the sensitivity of NMDARs to Mg^{2+} and memantine (Fedele et al., 2018). The GluN1-G620R mutation, mentioned above, also reduces agonist sensitivity and Mg^{2+} block (Chen et al., 2017). However, in our study, we did not observe changes in the Mg^{2+} sensitivity of GluN1/GluN2 receptors with any of the examined mutation. Nevertheless, we observed that GluN1-A645S mutation reduces sensitivity of GluN1/GluN2 receptors to memantine

in the absence of extracellular Mg^{2+}, which is consistent with previous results obtained using *Xenopus* oocytes expressing GluN1/GluN2B receptors (Kashiwagi et al., 2002). Interestingly, we found that in the presence of physiological concentration of Mg^{2+}, IC_{50} value for memantine was decreased for GluN1-M641I/GluN2A receptors but increased for GluN1-A645S/GluN2A receptors, when compared to WT GluN1/GluN2A receptors. Similar results were obtained when we measured these GluN1 subunits expressed in hippocampal neurons, moreover, our analysis of NMDA-induced excitotoxicity in hippocampal neurons also supported this finding. Specifically, memantine significantly reduced excitotoxicity in neurons expressing GluN1-M641I subunit but was significantly less neuroprotective in neurons expressing GluN1-A645S subunit in comparison to neurons expressing WT GluN1 subunit.

In addition, we found that M641I-GluN1 and A645S-GluN1 mutations differentially affect the onset (τ_{on}) and offset (τ_{off}) kinetics of inhibition by memantine, as well as affect memantine's ability to induce SSI at NMDARs. Specifically, we found that τ_{off} of memantine inhibition was slower for GluN1-M641I/GluN2A receptors and faster for GluN1-A645S/GluN2A receptors in absent and present of Mg^{2+}, when compared to WT GluN1/GluN2A receptors. Previous studies found that the slow component of τ_{off} (τ_{slow}) represents memantine unbinding from its second low-affinity binding site, at the GluN1/GluN2 receptor (Glasgow et al., 2018). Thus, when we focused on τ_{slow}, we found increased values for GluN1-M641I/GluN2A receptors and decreased values for

GluN1-A645S/GluN2A receptors, when compared to WT GluN1/GluN2A receptors under all experimental condition tested. These findings indicate that these two pathogenic mutations in the M3 domain of GluN1 subunit differentially affect both the binding and unbinding kinetic of memantine, and may possibly affect the SSI of memantine or, based on the recent studies, affect the membrane-to-channel transfer of memantine (Wilcox et al., 2022). Taking together, our data indicate that specific pathogenic mutations in the M3 domain of the GluN1 subunit differentially affect the pharmacological sensitivity and surface delivery of NMDARs.

6.2. The presence of putative N-glycosylation sites and their interaction with specific lectins regulates the functional properties of GluN1/GluN3 receptors

We focused on studying the role of specific *N*-glycans of the GluN1, GluN3A and GluN3B subunits in the regulation of functional properties of NMDARs as well as the role of different lectins in the modulation of GluN1/GluN3A receptors. It has been previously reported that inhibition of glycosylation of NMDARs with tunicamycin decreases EC_{50} for glutamate of GluN1/GluN2B receptors (Everts et al., 1997), as well as EC_{50} for NMDA of native NMDARs (Lichnerova et al., 2015). It was also shown that *N*-glycosylation sites in the GluN1 subunit are required for the release of NMDARs from the ER (Skrenkova et al., 2018). Here we showed that disruption of putative *N*-glycosylation sites in GluN1 or GluN3A subunits do not affects the desensitisation of GluN1/GluN3A receptors independent of the glycine concentration. This observation is in agreement

with our previous finding that mutated *N*-glycosylation sites do not change weighted time constant (τ_w) of desensitization for GluN1/GluN3A receptors in response to 500 μM glycine (Skrenkova et al., 2018). In contrast, we found that mutated residues N440 and N674 in the GluN1 subunit and N786 in the GluN3B subunit altered functional properties of GluN1/GluN3B receptors. In our previous studies, we showed that 11 out of 12 *N*-glycosylation sites in the GluN1 subunit are modified by glycans but N674 residue is not glycosylated (Kaniakova et al., 2016). Thus, we suggest that glycosylation of N440 residue regulates desensitization properties of GluN1/GluN3B receptors, whereas the observed changes with the mutated N674 residue are caused by a structural change in the LBD of the GluN1 subunit. As for the N786 residue in the GluN3B subunit, it is currently unknown whether this site is glycosylated in the recombinant GluN3B subunit, however, since we observed changes in the "tail" current amplitude of GluN1/GluN3B receptors with the N786 mutated residue, we suggest that glycosylation at this residue alters the activation of GluN1/GluN3B receptors by altering the LBD in the GluN3B subunit, rather than affecting the desensitization kinetics via the LBD of the GluN1 subunit.

We have previously shown a strong association of GluN3A-containing NMDARs with numerous lectins such as ConA, WGA and AAL mainly selective for mannose residues, *N*-acetylglucosamine residues, and fucose residues respectively. Moreover, our previous biochemical data indicating that GluN3A-containing NMDARs comprise a wide variety of glycan structures (Kaniakova et al., 2016). Here, we

complemented these findings by showing that lectins modulate the functional properties of GluN1/GluN3 receptors. Considering that 14 out of 19 tested lectins significantly slowed τ_w of desensitization and altered peak amplitude, we hypothesized that this modulating effect is mediated by a decrease in desensitisation kinetics. Indeed, after introducing mutations into GluN1 subunit that makes it insensitive to glycine up to 30 mM (Kvist Trine, Greenwood Jeremy, 2013), we observed no changes after lectin application. These results confirmed our hypothesis that lectins modulate eceptor desensitisation, and are consistent with previous findings that the ConA lectin reduces desensitisation at AMPARs and KARs, though has no pronounced effect on GluN1/GluN2 receptors (Everts et al., 1997; M. L. Mayer and Vyklicky, 1989).

Interestingly, we observed the strongest modulating effect on GluN1/GluN3A and GluN1/GluN3B receptors with AAL, however, receptors, containing replacement in N565 site of GluN3A subunit and N465 site of GluN3B subunit showed s9milar sensitivity to AAL as WT GluN1/GluN3 to ConA and WGA. This observation suggests that the N565 residue in GluN3A subunit and its homologue residue N465 in GluN3B subunit re involved in potentiating the modulatory effect of AAL, which could be explained by the higher specificity or affinity of AAL for different glycans compared to WGA or ConA (Dam and Fred Brewer, 2009; Moremen et al., 2014). Furthermore, we observed that application of ConA, WGA or AAL in the persistent presence of glycine had virtually no effect on GluN1/GluN3A or GluN1/GluN3B receptors

desensitization; this finding is consistent with a previous report that ConA-induced reduction of KARs desensitization is conformation-dependent process (Everts et al., 1999). Taking together, our findings reveal new information on the role of *N*-glycans in regulating the functional properties of GluN1/GluN3 receptors in mammalian cells and provide new clues about lectins as a tool for modulating non-conventional NMDARs.

7. Conclusion

Proper regulation functioning and trafficking of NMDARs is crucial for normal synaptic transmission, learning, and memory and this regulation occurs at multiple levels. In this dissertation, we mainly focused on studying the role of NTD and TMD integrity in the regulation of the functional properties of different NMDARs. Using electrophysiological technique, we demonstrated the putative role of *N*-glycosylation sites and various lectins in the regulation of the functional properties of GluN1/GluN3 receptors. We showed that lectins affect functional properties of GluN1/GluN3 receptors, more likely by reducing desensitization. We also showed that integrity of LBD of GluN1 and GluN3A subunits is crucial for proper functioning and delivery of NMDARs to the cell surface. Finally, we provided new information about three previously identified pathogenic mutations in the M3 domain of the GluN1 subunit in terms of their impact on the functional and pharmacological properties of different subtypes of NMDARs. This information can be used for further understanding of the role of different

NMDARs both in normal conditions and in the development of various neurodegenerative diseases

8. References

Amin, J. B., Gochman, A., He, M., Certain, N., & Wollmuth, L. P. (2021). NMDA Receptors Require Multiple Pre-opening Gating Steps for Efficient Synaptic Activity. Neuron, 109(3): 488-501.

Ataman, Z. A., Gakhar, L., Sorensen, B. R., Hell, J. W., & Shea, M. A. (2007). The NMDA Receptor NR1 C1 Region Bound to Calmodulin: Structural Insights into Functional Differences between Homologous Domains. Structure, 15(12): 1603–1617.

Chatterton, J. E., Awobuluyi, M., Premkumar, L. S., Takahashi, H., Talantova, M., Shin, Y., Cul, J., Tu, S., Sevarino, K. A., Nakanishi, N., Tong, G., Lipton, S. A., & Zhang, D. (2002). Excitatory glycine receptors containing the NR3 family of NMDA receptor subunits. Nature, 415(6873): 793–798.

Chen, W., Shieh, C., Swanger, S. A., Tankovic, A., Au, M., McGuire, M., Tagliati, M., Graham, J. M., Madan-Khetarpal, S., Traynelis, S. F., Yuan, H., & Pierson, T. M. (2017). GRIN1 mutation associated with intellectual disability alters NMDA receptor trafficking and function. Journal of Human Genetics, 62(6): 589–597.

Dam, T. K., & Fred Brewer, C. (2009). Lectins as pattern recognition molecules: The effects of epitope density in innate immunity. Glycobiology, 20(3): 270–279.

Everts, I., Petroski, R., Kizelsztein, P., Teichberg, V. I., Heinemann, S. F., & Hollmann, M. (1999). Lectin-induced inhibition of desensitization of the kainate receptor GluR6 depends on the activation state and can be mediated by a single native or ectopic N-linked carbohydrate side chain. Journal of Neuroscience, 19(3): 916–927.

Everts, I., Villmann, C., Hollmann, M. (1997). N-glycosylation is not a prerequisite for glutamate

receptor function but is essential for lectin modulation. Molecular Pharmacology, 52(5): 861–873.

Fedele, L., Newcombe, J., Topf, M., Gibb, A., Harvey, R. J., & Smart, T. G. (2018). Disease-associated missense mutations in GluN2B subunit alter NMDA receptor ligand binding and ion channel properties. Nature Communications, 9(1). Furukawa, H., & Gouaux, E. (2003). Mechanisms of activation, inhibition and specificity: Crystal structures of the NMDA receptor NR1 ligand-binding core. EMBO Journal, 22(12): 2873–2885.

Furukawa, K. (2014). Crystal structure of a heterotetrameric NMDA receptor ion channel. Scienc, 344(6187): 992–997.

Glasgow, G. N., Madeleine, R. W., Johnsona, J.W., (2019). Effects of Mg^{2+} on recovery of NMDA receptors from inhibition by memantine and ketamine reveal properties of a second site. Physiology & Behavior, 176(3): 139–148.

Grand, T., Abi Gerges, S., David, M., Diana, M. A., Paoletti, P. (2018). Unmasking GluN1/GluN3A excitatory glycine NMDA receptors. Nature Communications, 9(1).

Hatton, C. J., & Paoletti, P. (2005). Modulation of triheteromeric NMDA receptors by N-terminal domain ligands. Neuron, 46(2): 261–274.

Henson, M. A., Roberts, A. C., Pérez-Otaño, I., & Philpot, B. D. (2010). Influence of the NR3A subunit on NMDA receptor functions. Progress in Neurobiology, 91(1): 23–37.

Hu, B., & Zheng, F. (2005). Differential effects on current kinetics by point mutations in the lurcher motif of NR1/NR2A receptors. Journal of Pharmacology and Experimental Therapeutics, 312(3), 899–904.

Huettner, J. E. (2015). Glutamate receptor pores. Journal of

Physiology, 593(1): 49–59.
Johansen Amin, Aaron Gochman, Miaomiao He, Certain, N., & Wollmuth, L. P. (2021). NMDA receptors require multiple pre-opening gating steps for efficient synaptic activity. Physiology & Behavior, 109(3): 488–501.
Johnson, J. W. (2019). Effects of Mg^{2+} on recovery of NMDA receptors from inhibition by memantine and ketamine reveal properties of a second site. *Physiology and Behavior* 176, 139–148.
Kaniakova, M., Krausova, B., Vyklicky, V., Korinek, M., Lichnerova, K., Vyklicky, L., & Horak, M. (2012). Key amino acid residues within the third membrane domains of NR1 and NR2 subunits contribute to the regulation of the surface delivery of N-methyl-D-aspartate receptors. Journal of Biological Chemistry, 287(31): 26423–26434.
Kaniakova, M., Lichnerova, K., Skrenkova, K., Vyklicky, L., & Horak, M. (2016). Biochemical and electrophysiological characterization of N-glycans on NMDA receptor subunits. Journal of Neurochemistry, 546–556.
Kashiwagi, K., Masuko, T., Nguyen, C. D., Kuno, T., Tanaka, I., Igarashi, K., & Williams, K. (2002). Channel blockers acting at N-methyl-D-aspartate receptors: Differential effects of mutations in the vestibule and ion channel pore. Molecular Pharmacology, 61(3): 533–545.
Kotermanski, Sh. E., Johnson, J. W. (2009). Mg^{2+} imparts NMDA receptor subtype selectivity to the Alzheimer's drug memantine. Journal of Neuroscience, 29(9):2774-9
Kvist Trine, Greenwood Jeremy, H. K. (2013). Structure-based discovery of antagonists for GluN3-containing N-methyl-D-aspartate receptors. Neuropharmacology, 23(1): 1–7.

Lee, C. H., Lü, W., Michel, J. C., Goehring, A., Du, J., Song, X., & Gouaux, E. (2014). NMDA receptor structures reveal subunit arrangement and pore architecture. Nature, 511(7508): 191–197.

Lemke, J. R., Geider, K., Helbig, K. L., Heyne, H. O., Schütz, H., Hentschel, J., Courage, C., Depienne, C., Nava, C., Heron, D., Møller, R. S., Hjalgrim, H., Lal, D., Neubauer, B. A., Nürnberg, P., Thiele, H., Kurlemann, G., Arnold, G. L., Bhambhani, V., Syrbe, S. (2016). Delineating the GRIN1 phenotypic spectrum: A distinct genetic NMDA receptor encephalopathy. Neurology, 86(23): 2171–2178.

Li, Z., Liang, D., & Chen, L. (2008). Receptor Ion Channels. Assay And Drug Development Technologies, 6(2): 298–487.

Lichnerova, K., Kaniakova, M., Park, S. P., Skrenkova, K., Wang, Y. X., Petralia, R. S., Suh, Y. H., & Horak, M. (2015). Two N-glycosylation sites in the GluN1 subunit are essential for releasing N-methyl-D-aspartate (NMDA) receptors from the endoplasmic reticulum. Journal of Biological Chemistry, 290(30), 18379–18390.

Mayer, M. L., & Vyklicky, L. (1989). Concanavalin A selectively reduces desensitization of mammalian neuronal quisqualate receptors. Proceedings of the National Academy of Sciences of the United States of America, 86(4): 1411–1415.

Meddows, E., Le Bourdellès, B., Grimwood, S., Wafford, K., Sandhu, S., Whiting, P., & McIlhinney, R. A. J. (2001). Identification of Molecular Determinants That Are Important in the Assembly of N-Methyl-D-aspartate Receptors. Journal of Biological Chemistry, 276(22): 18795–18803.

Moremen, K. W., Tiemeyer, M., Nairn, A. V. (2012)Vertebrate protein glycosylation: diversity,

synthesis and function. Nature Reviews Molecular Cell Biology, 13(7): 448-62.

Paoletti, P., Bellone, C., & Zhou, Q. (2013). NMDA receptor subunit diversity: Impact on receptor properties, synaptic plasticity and disease. Nature Reviews Neuroscience, 14(6): 383-400

Sanz-Clemente, A., Nicoll, R. A., & Roche, K. W. (2013). Diversity in NMDA receptor composition: Many regulators, many consequences. Neuroscientist, 19(1): 62-75.

Skrenkova, K., Lee, S., Lichnerova, K., Kaniakova, M., Hansikova, H., Zapotocky, M., Suh, Y. H., & Horak, M. (2018). N-glycosylation regulates the trafficking and surface mobility of GluN3A-containing NMDA receptors. Frontiers in Molecular Neuroscience,11: 188.

Smothers, C. T., Woodward, J. J., (2009). Expression of glycine-activated diheteromeric NR1/NR3 receptors in human embryonic kidney 293 cells Is NR1 splice variant-dependent. Journal of Pharmacology and Experimental Therapeutics, (3): 975-84.

Traynelis, S. F., Wollmuth, L. P., McBain, C. J., Menniti, F. S., Vance, K. M., Ogden, K. K., Hansen, K. B., Yuan, H., Myers, S. J., & Dingledine, R. (2010). Glutamate receptor ion channels: Structure, regulation, and function. Pharmacological Reviews, 62(3): 405–496

Vieira, M., Yong, X. L. H., Roche, K. W., Anggono, V. (2020). Regulation of NMDA glutamate receptor functions by the GluN2 subunits. Journal of Neurochemistry, 154(2): 121-143.

Vyklicky, V., Krausova, B., Cerny, J., Ladislav, M., Smejkalova, T., Kysilov, B., Korinek, M., Danacikova, S., Horak, M., Chodounska, H., Kudova, E., & Vyklicky, L. (2018). Surface expression, function, and pharmacology of disease-associated mutations in the

membrane domain of the human GluN2B subunit. Frontiers in Molecular Neuroscience, 11: 110.

Warnet, X. L., Bakke KroWarnet, X. L., Bakke Krog, H., Sevillano-Quispe, O. G., Poulsen, H., & Kjaergaard, M. (2020). The C-terminal domains of the NMDA receptor: How intrinsically disordered tails affect signalling, plasticity and disease. European Journal of Neuroscience, 54(8):6713-6739

Wilcox, M. R., Nigam, A., Glasgow, N. G., Narangoda, C., Phillips, M. B., Patel, D. S., Mesbahi-vasey, S., Turcu, A. L., Vázquez, S., Kurnikova, M. G., Johnson, J. W. (2022). Inhibition of NMDA receptors through a membrane-to-channel path. Nature Communications, 13(1): 4114

Wollmuth, L. P., & Sobolevsky, A. I. (2004). Structure and gating of the glutamate receptor ion channel. Trends in Neurosciences. 27: 321– 328

9. List of publications

9.1. Publications *in extenso*, related to this thesis

1. Marharyta Kolcheva, Stepan Kortus, Barbora Hrcka Krausova, Petra Barackova, Anna Misiachna, Sarka Danacikova, Martina Kaniakova, Katarina Hemelikova, Matej Hotovec, Kristyna Rehakova, Martin Horak (2021) Specific pathogenic mutations in the M3 domain of the GluN1 subunit regulate the surface delivery and pharmacological sensitivity of NMDA receptors. *Neuropharmacology*, 189:108528. IF= 5.25 (2021/2022).

2. Katarina Hemelikova*, **Marharyta Kolcheva***, Kristyna Skrenkova, Martina Kanikova, Martin Horak (2019) Lectins modulate the functional properties of GluN1/GluN3A – containg receptors. *Neuropharmacology*, 157:107671. IF= 5.25 (2021/2022).

3. Kristyna Skrenkova, Katarina Hemelikova, Marharyta Kolcheva, Stepan Kortus, Martina Kaniakova, Barbora Krausova, Martin Horak (2019) Structural features in the glycine-binding sites of the GluN1 and GluN3A subunits regulate the surface delivery of NMDA receptors. *Scientific Reports*, 9(1):12303. IF=4.996 (2021/2022).

4. Kristyna Skrenkova, Jae-man Song, Stepan Kortus, **Marharyta Kolcheva**, Jakub Netolicky, Katarina Hemelikova, Martina Kaniakova, Barbora Hrcka Krausova, Tomas Kucera, Jan Korabecny, Young Ho Suh, Martin Horak (2020) The pathogenic S688Y mutation in the ligand-binding domain of the GluN1 subunit regulates the properties of NMDA receptors. *Scientific Reports*, 10:18576. IF=4.996 (2021/2022).

** co-first authorship*

9.2. Publications *in extenso*, unrelated to this thesis

1. Jan Konecny, Anna Misiachna, Martina Hrabinova, Lenka Pulkrabkova, Marketa Benkova, Lukas Prchal, Tomas Kucera, Tereza Kobrlova, Vladimir Finger, **Marharyta Kolcheva**, Stepan Kortus, Daniel Jun, Marian Valko, Martin Horak, Ondrej Soukup, Jan Korabecny (2020) Pursuing the Complexity of Alzheimer's Disease: Discovery of Fluoren-9-Amines as Selective Butyrylcholinesterase Inhibitors and N-Methyl-d-Aspartate Receptor Antagonists. *Biomolecules*, 11(1):3. IF=4.569 (2021/2022).

2. Lukas Gorecki, Anna Misiachna, Jiri Damborsky, Rafael Dolezal, Jan Korabecny, Lada Cejkova, Kristina Hakenova, Marketa Chvojkova, Jana Zdarova Karasova, Lukas Prchal, Martin Novak, **Marharyta Kolcheva**, Stepan Kortus, Karel Vales, Martin Horak, Ondrej Soukup (2021) Structure-activity relationships of dually-acting acetylcholinesterase inhibitors derived from tacrine on N-methyl-d-Aspartate receptors. *European Journal of Medicinal Chemistry*, 219:113434. IF=6.514 (2021/2022).

10. Curriculum Vitae

Mgr. Marharyta Kolcheva

PERSONAL DATA

Date of birth: 30.12.1992
Citizenship: UKR
E-mail: marharyta.kolcheva@iem.cas.cz

EDUCATION

2017 – now: Ph.D. student of the Faculty of Science of the Charles Universit in Prague, department of *Animal Physiology*.

2013 – 2015: Master's degree in Biophysics Educational and Scientific Center „Institute of Biology“of the Taras Shevchenko National University of Kyiv

2009 – 2013: Bachelor's degree in Biology Educational and Scientific Center „Institute of Biology“ of the Taras Shevchenko National University of Kyiv

RESEARCH

2017 – now: Institute of Physiology CAS, Laboratory of Cellular Neurophysiology
2017 – now: Institute of the Experimental Medicine CAS, Department of Neurochemistry

LABORATORY SKILLS

- preparation and culture of human embryonic kidney 293 cells (HEK293) and embryonic hippocampal neurons
- transfection of cultivated HEK293 cells
- electrophysiological measurements using the patch-clamp technique in the whole-cell configuration
- site-directed, multi-site-directed mutagenesis
- NMDA-induced excitotoxicity
- immunofluorescence microscopy - surface and total staining, image acquisition, and analysis processing

CONFERENCES

FENS regional meeting 2019 Belgrade, Serbia

FENS Forum 2022 Paris, France